Modelling biological invasions: population cycles, waves and time delays

Thesis submitted for the degree of

Doctor of Philosophy

at the

University of Leicester

by

Masha Jankovic

Department of Mathematics

University of Leicester

November 2014

"We live on an island surrounded by a sea of ignorance. As our island of knowledge grows, so does the shore of our ignorance"

John Archibald Wheeler

Abstract

Biological invasions are rapidly gaining importance due to the ever-increasing number of introduced species. Alongside the plenitude of empirical data on invasive species there exists an equally broad range of mathematical models that might be of use in understanding biological invasions.

This thesis aims to address several issues related to modelling invasive species and provide insight into their dynamics. Part I (Chapter 2) documents a case study of the gypsy moth, *Lymantria dispar*, invasion in the US. We propose an alternative hypothesis to explain the patchiness of gypsy moth spread entailing the interplay between dispersal, predation or a viral infection and the Allee effect. Using a reaction-diffusion framework we test the two models (prey-predator and susceptible-infected) and predict qualitatively similar patterns as are observed in natural populations. As high density gypsy moth populations cause the most damage, estimating the spread rate would be of help in any suppression strategy. Correspondingly, using a diffusive SI model we are able to obtain estimates of the rate of spread comparable to historical data.

Part II (Chapters 3, 4 and 5) is more methodological in nature, and in a single species context we examine the effect of an ubiquitous phenomenon influencing population dynamics – time delay. In Chapter 3 we show that contrary to the general opinion, time delays are not always destabilising, using a delay differential equation with discrete time delay. The concept of distributed delay is introduced in Chapter 4 and studied through an integrodifferential model. Both Chapters 3 and 4 focus on temporal dynamics of populations, so we further this consideration to include spatial effects in Chapter 5. Using two different representations of movement, we show that the onset of spatiotemporal chaos in the wake of population fronts is possible in a single species model.

Acknowledgements

This PhD thesis is a result of an almost four year challenging, meandering and at times daunting journey. Along the way, I have received help and support from many people and would like to take the opportunity to acknowledge some.

Firstly, I would like to express my gratitude to my supervisor, Professor Sergei Petrovskii, for his utmost patience and support during my studies. Our meetings were not only of great importance for the development of my research, they were also essential in that they kept me inspired and, at times, helped me regain the confidence that it would all come to a good end.

I would like to thank the amazing staff in College House for their help and making so many things easier. I extend my appreciation to the guys and fellow research students in Michael Atiyah offices 126 and 108, Yadigar, Matt, Ali, Anwar, Laila and Misha. A special thanks goes to the irreplaceable Juxi for providing endless optimism, laughter and brightening up the office, making work more enjoyable.

My warmest thanks goes to my closest family and friends: Buba, Mami, Igor and Jovan. Thank you for always believing in me, for your unconditional support, strength and love. I will always be indebted to you.

Finally, for the one who has made the many hours spent in the office worthwhile after all, Dominic. Thank you for being there during the countless stresses and strains. You're next.

Contents

List of Figures

List of Tables

To my parents

Chapter 1

Biological Invasions

Biological invasion occurs when non-native organisms are introduced to a new area beyond their original (native) range. The topic of biological invasions has received much interest due to the rapidly accelerating number of introduced exotic species (*Hengeveld 1989, Lewis and Kareiva 1993, Williamson 1996, Shigesada and Kawasaki 1997, Parker et al. 1999, Sakai et al. 2001*). The rising awareness and interest in invasive species are mirrored in the growing number of contemporary publications, not only within the academic community, but with a wider audience as well (see Fig. 1.1). Prompted by increasing levels of trade and travel, biological invasions now pose a major threat to biodiversity of ecosystems and lead to vast economic losses worldwide (*Mooney et al. 2005*). Due to widespread and profound changes inflicted upon ecosystems, biological invasions have also been recognised as a significant part of global environmental change (*Vitousek et al. 1996*).

Many non-native species were intentionally introduced in the first instance, but since then have become harmful and major pests (*Elton 1958*). Invasion itself is regarded more a process rather than an event and therefore has a number of stages (*Kolar and Lodge 2001*). This stage-based approach has been adopted by many authors with a varying number of steps (*Williamson 1996, Blackburn et al. 2011, Davis 2009*), though the common standpoint is that invaders pass through at least three stages before they are able to inflict ecological and economic harm (*Lockwood et al. 2013*). As a rule, invasion begins with the introduction of a small number of individuals that are transported from their original range to a new habitat. These individuals must then establish, that is form self-sustained populations within their

new non-native range, and may then grow in abundance and expand their geographical range. Commonly, it is only when invasive species' populations become widespread and abundant that they will be noticed. Distinguishing the stages of the invasion process is important as it allows for the choice of appropriate measures to be undertaken, be it facilitating or inhibiting the spread of newly-founded populations (*Kolar and Lodge 2001*). Prior to introduction, and as an integral
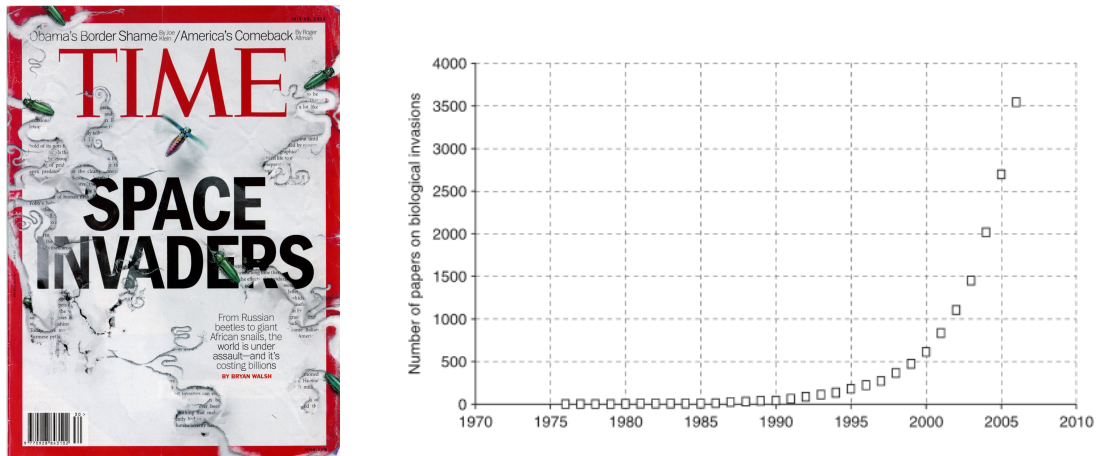
FIGURE 1.1: Front page of Time magazine (left) and the nearly exponential increase in number of scientific papers published on the topic of invasion ecology (right). Figures taken from Time magazine and *Richardson and Pyšek 2008*.

part of each stage of invasion, potential invasive species must overcome a series of inherent barriers (*Blackburn et al. 2011*). At first, the simple obstacle of overcoming the geography imposing physical barriers on the arrival and movement of invaders beyond their native range can clearly influence invasion success. Human entrainment, both intentional and accidental breaches bio-geographical boundaries and is the first step towards the introduction of exotic species. While not every invasion is a consequence of human activity, the vast majority have resulted from human-assisted transport (*Keller and Lodge 2007*). Subsequently, during establishment non-native species are faced with additional challenges: survival and reproduction. Coping with environmental stress, gaining access to resources, interacting with local species, mate finding and avoidance of pre-mating mortality are just a few of the ecological and environmental hurdles encountered by growing populations. Subject to successful establishment, non-native species tend to expand their geographical range through dispersal, and thereafter are faced with additional barriers to establish and further spread which may not necessarily be similar to the ones encountered previously. Initial invading populations tend to be small and are particularly vulnerable to Allee effects, which may even drive the population extinct (*Stephens et al. 1999*). Allee effects are found in a wide

range of taxa and ecosystems (*Courchamp et al. 2008*), but are particularly influential in the invasion process as they may significantly decrease the probability of establishment (*Taylor and Hastings 2005*).

Out of the ever-increasing number of introduced exotic species, how many manage to successfully establish? Interestingly, most introductions fail with only a limited number of taxa succeeding. Indeed, *Williamson (1996)* found that between 5 and 20% of species progress through the stages of invasion. On average, 10% of introduced invasive species establish, i.e. become self-sustained populations capable of reproducing, and a mere 10% of these species evolve into pests, yielding harmful consequences (tens rule). More recent estimates suggest this figure to be higher reaching even $20-30\%$ of the total number of introduced species (*Pimentel 2002*). Even though a small number of invaders succeed to establish, their cumulative effect has been and will continue to remain large. According to a summary report the cumulative losses incurred from harmful pest species were estimated at almost $100 billion by 1991 (*US Congress OTA 1993*), and are expected to rise in future years. Newer reports suggest that an outstanding $314 billion per year is spent on damage and control worldwide (*Pimentel 2002*). Costs not only include those associated with damage and losses caused by harmful non-indigenous species inflicted upon property and natural ecosystems, but also include expenditure related to various control mechanisms and programs. Enormous costs to agriculture, fisheries, forestry and other human enterprises are most noticeable. A more subtle and debatable issue arises from ecological consequences such as impacts on ecosystem biodiversity. Many authors agree that invasions do pose a major threat to biodiversity (*Williamson 1999, Richardson 2011, Lodge 1993, Lockwood et al. 2013*), as a result of competition from the invasives, as well as by predation. It is thought that the impact of invasive species is responsible for around 42% of the decline of native flora and fauna which are now listed as endangered or threatened (*Nature Conservancy*). More general ecological impacts include the effects pest species have on other species' dynamics and extinction (particularly interesting are the possible genetic modifications of invader and native species (*Sakai et al. 2001*)), effects on the food web, changes imposed on ecosystem processes and most evident of all are the changes in physical structure of the environment. Newly introduced species can also act as vectors of disease (*Vitousek et al. 1996*).

To date one of the largest programs tackling bio-invasion problems is the SCOPE program, a committee founded by the International Council for Science in 1969 with the aim to document problems caused by invasive species (*Mooney 2005*).

During 10 years of prolific research the resulting publications signalled the synthesis of the study of non-native species into a coherent field, calling for a more integrated, interdisciplinary approach (*Davis 2009*).

1.1   Classical examples of biological invasions

> "*Let it be remembered how powerful the*
> *influence of a single introduced tree*
> *or mammal has been shown to be*"[1]

In what follows, we will revisit some classical examples of biological invasion. The four examples include a mammalian species, the muskrat *Ondatra zibethica*, a sea-bird, the fulmar *Fulmarus glacialis*, the Japanese beetle *Popillia japonica*, and a plant, cheatgrass, *Bromus tectorum*. Whilst most invasions are driven by human action, the spread of the oceanic fulmar, *Fulmarus glacialis*, is one of several exceptions. Currently numbering at around $5 - 7$ million pairs it is one of the most abundant seabirds in the Northern hemisphere (*Mitchell et al. 2004*). Dating back to the 18th century there were reportedly only 2 known colonies in the temperate Atlantic: one off northern Iceland around the island of Grimsey and another at St Kilda, a small archipelago west of the Outer Hebrides of Scotland. From these humble beginnings, boreal populations have greatly expanded in the last 400 years (*Thompson 2006*). The fulmar has subsequently spread from Grimsey, across the Faroe Islands and Shetland, only to spread south throughout the UK and Ireland during the 20th century, even reaching Norway, parts of France and Germany. The expansion throughout Europe was well-documented and the finite rate of fulmar population increase was estimated to reach a maximum of 5% per year (*Fisher 1952, 1966*). Fulmars are slow-breeding populations, laying at most one egg per year, with an intrinsic rate of growth less than 0.05 per year (*Williamson 1996*). Despite the "fulmar wreck of 1962" (*Pashby and Cudworth 1962*), in which adverse weather conditions lead to the sudden and substantial decline in fulmar populations around the British Isles, fulmar populations have successfully recovered and resumed spread, with the rate of increase reaching even 20% in some parts (*Fisher 1966*). From thereafter the growth has considerably diminished, reaching a low of 4% during 1969-1986 (*Lloyd et al. 1991*). The fulmar is an ocean-living bird feeding on fish and plankton, coming to land only

---

[1]Darwin C (1859) "On the origin of species"

to breed (*Williamson 1996*). Thus, the spread of fulmar is commonly linked to fish trawling and whaling (*Fisher 1966, Phillips et al. 1999*). Although prey distribution is an important determinant in the distribution of seabirds at sea, and despite fulmars being regular and frequent ship-followers clearly profiting from the increased availability of fish offal and discarded fishes from commercial fisheries, fulmars are known to have an extremely varied diet. The distribution of fulmars has shown greater correlation with certain hydrographic features than with fisheries (*Camphuysen and Garthe 1997*). Preferred nesting sites include exposed tall sea cliffs, and hence it has been hypothesised that the direction and speed of the fulmar spread is influenced by the distribution of available cliffs (*Williamson 1996*). Other underlying causes of fulmar spread and distribution include climate warming (*Salomonsen 1965, Brown 1970, Thompson and Ollason 2001*) and genetically based changes in dispersal behaviour (*Wynne-Edwards 1962*). Albeit a more general explanation underlying fulmar spread is lacking, most likely possible driving mechanisms of the spread are a combination of these influential factors. Northern fulmars are known to have a slow invasion rate, and despite their huge numbers they have had a relatively small impact on other, native species. Competition for nesting sites has occasionally occurred, however the interaction with other sea birds is kept to a minimum (*Williamson 1996*).

Another example of invasion is the muskrat spread in Europe (Fig. 1.2, top right) which has been reproduced in almost all books written on the topic of biological invasions and was one of the examples used by *Elton (1958)* to emphasise the importance on why society should care about invasive species. Muskrats are a semi-aquatic rodent species native to North America, brought to Europe for fur-breeding. The spread over Europe started from only five individuals in Czechoslovakia in 1905 (*Elton 1958*), and today the populations number millions. As muskrats have a high reproductive rate with up to four litters per year, with four to six young per litter and disperse effectively, it is not surprising that they inhabited the entire European continent in the short period of 50 years with the muskrat range being additionally augmented by numerous subsidiary introductions. To date eradication attempts were only successful in Britain (in the 1930s) and Ireland, with control attempts in continental Europe being of rather limited success. Apart from illustrating an example of quasi-circular spread (*Skellam 1951*), muskrats are an example of a species which has been controlled and even eradicated in some areas, though elsewhere seem to be uncontrollable as feral populations now span from France through Central Europe, Russia, to China

(*Williamson 1996*). Muskrats have been shown to be destructive, particularly to embankments of rivers, lakes and even roads through their den building behaviour, which led to actively conducted suppression campaigns in many European countries. One of the first attempts to quantify the spread of muskrat was done by *Skellam (1951)*, in which it was concluded that up to 1927 range expansion occurred in approximately concentric circles centred at the original point of release (escape). Furthermore, the square root of the area occupied was shown to be a linear function when plotted against time, indicating that muskrats advanced at a constant speed of 11.3 km/year. From the distribution maps it is readily seen that not only did muskrat populations not expand in concentric circles, due to a natural preference towards swamp and wetland habitats, but also the speed along some radii seemed to be greater than estimated. Nonetheless, as an initial approximation, Skellam's estimate still remains a good average for spread in all directions. Taking into account the local topography, environmental conditions and complex shape of the range boundary, a subsequent study by *Andow et al. (1990)* estimated the spread of muskrats at 10.3 km/year towards the west and 25.4 km/year in the east-southeast direction. As a consequence of various trapping efforts muskrat expansion has subsided in the period after 1930 (*van den Bosch et al. 1992*), though complete eradication of muskrat populations in Europe seems to be far from achievable.

Most accidentally introduced insect species rarely reach high population densities, and are even seldom detected. However, a highly conspicuous minority of non-indigenous arthropod species cause immense economic, environmental and public health problems (*Hajek et al. 2009*), amongst which are populations of the Japanese beetle, *Popillia japonica*, in the US. As is the case with most biological invasions, the exact date and site of introduction are not known, though it is thought to have been brought into the US with irises or azaleas around 1911 from Japan. First detected in 1916, the population rapidly grew and despite concerted federal and state efforts to eradicate it and limit its spread the Japanese beetle has progressively spread outwards, extending its range. In less than 30 years, the Japanese beetle has successfully invaded over $50,000\ km^2$ and now encompasses the majority of the eastern US. The Japanese beetle is endemic to the main islands of the Japanese Archipelago, where it is regarded as a minor agricultural pest, possibly due to the unsuitable environmental conditions for development and the incidence of natural enemies keeping its populations low. In the US however, the Japanese beetle populations have found a favourable habitat and cause not only

damage to farm crops, but also defoliate over 250 tree species (*Williamson 1996*). Despite several biological control mechanisms including parasitic nematodes, the introduction of natural predators such as robins, grackles and predacious insects including praying mantids and wheel bugs, populations are still spreading. Following its introduction, the Japanese beetle spread was slow but then gradually increased, with population densities reaching very large values. The dynamics of invasion and geographical spread are given in Fig. 1.2 (top left). In the first decade of invasion, range expansion appeared to grow with accelerating speed, and indeed the rate of movement of the Japanese beetle increased dramatically each year during 1916-1926 (*Allsopp 1996, Petrovskii and Li 2006, Shigesada and Kawasaki 1997*). The combination of natural spread resulting from adult flight and inadvertent human activity has surely influenced the increase in invasion rate, and as an immigrant the Japanese beetle has proved to be spectacularly successful. Now representing one of the most widespread and destructive insect pests of turf and landscape in the eastern US, despite regulatory efforts the Japanese beetle remains a threat as an invasive species (*Potter and Held 2002*).

To quote *Heywood (1989)* "there are few ecosystems that have not been affected to a greater or lesser degree by invasions by terrestrial plants". In particular, introduced grass species now dominate the western US landscape, currently accounting for $50 - 80\%$ of vascular plant cover in over two thirds of the rangelands. Cheatgrass, *Bromus tectorum*, alone prevails on over a 100 million acres (*Belnap and Phillips 2001*) and is the dominant plant across at least $200,000 \ km^2$ in the Intermountain West region (*Novak and Mack 2001*). Its native range includes much of Europe, northern Africa and southwest Asia. Human activity has most likely facilitated the observed rapid range expansion of cheatgrass in the US, as the combination of long and short distance dispersal have drastically increased invasion rates. Evidence suggests that the accidental introduction of *Bromus tectorum* dates back to the early 1860s, from several widely separated sites. From these isolated foci the annual winter grass species has spread and occupied its current range, though at first was sparsely distributed, in about 40 years (*Novak and Mack 2001, Zouhar 2003*). Ecological consequences of cheatgrass invasion include serious impacts on biodiversity, an increased likelihood for fire ignition and spread and an increased susceptibility of landscapes to erosion. Indeed, the increase in fires in some invaded areas has even lead to the increased incidence of flooding (*Klemmendson and Smith 1964*). Furthermore, cheatgrass recovers rapidly following fires which in turn tends to favour its dominance by removing
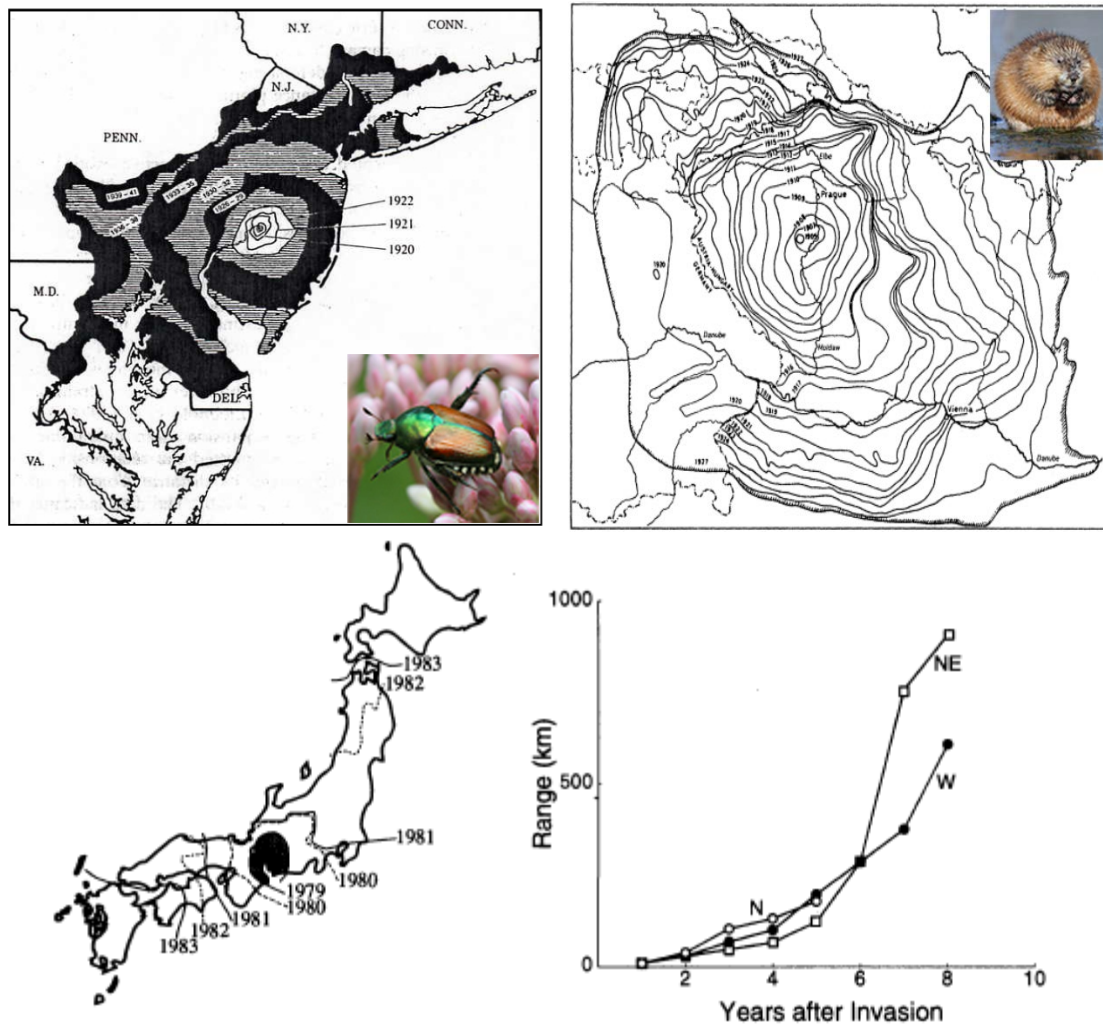
FIGURE 1.2: Geographical spread of the Japanese beetle in the US (top left), muskrat in Europe (top right) and cheatgrass in the US (bottom row). Taken from *Petrovskii and Li (2006)*, *Shigesada and Kawasaki (1997)*, `http://www.cdfa.ca.gov/plant/PDEP/target_pest_disease_profiles/` `images/JB_2106096_bugwood_DavidCappaert.jpg` and `http://environment.` `nationalgeographic.com/environment/photos/freshwater-mammals/`.

reproduction of competing native plants. Regardless of various suppression and eradication techniques ranging from chemical to biological control agents employed with the goal of limiting the spread, *Bromus tectorum* has been spreading to higher elevation sites and remains a quintessential invader.

1.2 Mathematical models: an overview

There is a great deal of empirical data available on invasive species, and there is also an equally broad range of models that might be of use in understanding biological invasions. One of the main difficulties lies in connecting the two, relating specific ecological mechanisms to testable predictions. Indeed, mathematical modelling is a powerful research tool in theoretical ecology. The approach to model building can be very different though. Depending on the purpose of the study, there have been two different streams *(Maynard Smith 1974)*. In case the intent of modelling is to predict the ecosystem's state, the model is expected to explicitly include many details of the ecosystem's structure. This approach is called predictive modelling. Though prediction of the success or otherwise of potential invaders and their corresponding population dynamics would be highly desirable, the more realism is included into modelling efforts the more unwieldy the model becomes and models arising in this way can become very complicated. Alternatively, the purpose of the study can be to understand some basic features of the ecosystem, e.g. to identify the factors potentially responsible for a population outbreak or population fluctuations, but not necessarily to predict their development quantitatively. In this case, the corresponding models can be pretty simple. This approach is conventionally called conceptual (educational) modelling (*Okubo and Levin 2001*). It is the latter that is used throughout this thesis as the aim here is to reveal some general tendencies rather than to provide any kind of detailed and/or predictive description. It has been pointed out *(Levins 1969)* that, when studying systems as complex as ecosystems, one should not look for inferences that are likely to be true for all cases. Instead, one should rather look for the causes of differences between different species or different systems. To address this sort of question, we need a model which is as simple as possible *(Maynard Smith 1974)*.[2]

In its simplest form population models assume spatial homogeneity, resulting in non-spatial models in which population density is now a function of time, but not space. Depending on whether the populations have overlapping generations or not, continuous- or discrete-time models are utilised. In the remainder of this thesis continuous-time models are used, and so correspondingly, ordinary differential equations give a relevant framework (*Murray 2002, Kot 2001*):

$$\frac{dU_i}{dt} = G_i(U_1, U_2, ...U_n), \quad i = 1, ..., n\,, \tag{1.1}$$

---

[2]Parts of this paragraph were taken from *Jankovic and Petrovskii (2014)*

where U_i is the population density of the ith species at time t, n is the number of species and functions G_i describe population change due to reproduction and mortality. In an ecological context, the functions G_i are usually nonlinear with respect to at least some of their arguments.

Even in the simplest of ecosystems there are many interacting species (numbering hundreds or even thousands), and thus the question facing modellers is the subtle decision on how many equations (species) should the system contain along with the suitable functional forms of G_i. Obviously, it is unrealistic to expect all species to be included, therefore a frequently used approach is to consider blocks of particular "functional groups" which correspond to different trophic levels (e.g. predator and prey) (*Malchow et al. 2008*). Granted a rough simplification, such an approach has yielded successful results in both empirical and theoretical studies. Another option is to merely minimise the number of included species and focus on the dynamics of a particular one. This results in single- or few-species models, whereby the impact of other species can be accounted for indirectly (e.g. additional mortality accounting for predation). As expected, the predictive power of such conceptual models is rather limited, but even so they offer an opportunity to comprehensively study the implications of basic inter- and intra-specific interactions in a wider theoretical context.

The properties of model (1.1) will depend on the particular parametrisation of function(s) G_i, or rather the factors affecting population growth. In general, dynamics of a single species population can be described by (*Petrovskii and Li 2006*):

$$\frac{dU}{dt} = G(U) = U f(U) \,, \tag{1.2}$$

where $f(U)$ is the per capita growth rate. One of the earliest population models (*Malthus 1798*) assumed a density independent form of $f(U) = r$ leading to unbounded, exponential growth for a positive value of the constant, $r > 0$. In the short run near exponential growth can be observed for some natural populations, however in the long run there must be some adjustment made to account for density-dependent mechanisms. Indeed, as the population density increases, intraspecific competition gains greater significance, which results in a decrease of the per capita growth rate. Without choosing any particular parametrisation, mathematically the function $G(U)$ should therefore satisfy the following conditions (Fig. 1.3):
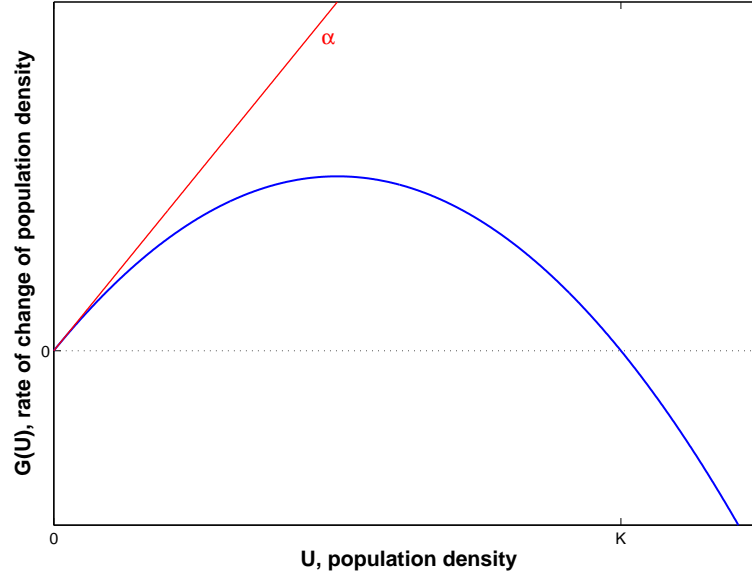
FIGURE 1.3: Sketch of logistic growth function.

$$G(0) = G(K) = 0\,, \tag{1.3}$$

$$G(U) > 0 \quad \text{for} \quad 0 < U < K\,, \quad G(U) < 0 \quad \text{for} \quad U > K\,, \tag{1.4}$$

$$G'(0) = \alpha > 0, \quad G'(U) < \alpha \quad \text{for} \quad U > 0 \tag{1.5}$$

where α can be considered as the per capita growth rate at low population densities and K is the carrying capacity. Possibly the most famous model accounting for intraspecific competition is the Verhulst-Pearl logistic model (*Verhulst 1845*; see Chapter 5). According to the model of logistic growth, the per capita growth rate decreases monotonously, which is not always the case as many populations suffer from a reduction in the per capita growth rate at low population densities (Allee effect). At particularly low densities the per capita growth can become negative, and a rather generic description of the growth function $G(U)$ in the case of the strong Allee effect can be given as (Fig. 1.4):

$$G(U) < 0 \quad \text{for} \quad 0 < U < \beta \quad \text{and} \quad U > K\,, \tag{1.6}$$

$$G(U) > 0 \quad \text{for} \quad \beta < U < K\,, \tag{1.7}$$

where β is a certain threshold density and an unstable equilibrum (*Lewis and Kareiva 1993*, *Dennis 1989*; for more details see Chapter 3).

The next level of model complexity would imply the inclusion of interactions with other species, resulting in a multi-species model. In general, the dynamics of a
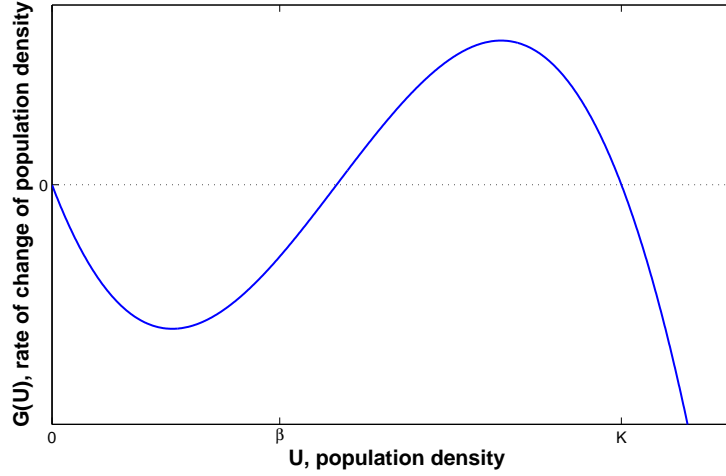
FIGURE 1.4: Sketch of the growth function $G(U)$ in case of the strong Allee effect.

two-species community can be described by two coupled ODEs:

$$\frac{dU_1}{dt} = G(U_1) + \kappa_{12}R_1(U_1, U_2) \tag{1.8}$$

$$\frac{dU_2}{dt} = G(U_2) + \kappa_{21}R_2(U_1, U_2)\,, \tag{1.9}$$

where functions $G(U_1)$ and $G(U_2)$ describe population growth of species 1 and 2, functions R_1 and R_2 are positive and describe interspecific competition and κ_{12} and κ_{21} are constants. Depending on the signs of the coefficients, the above model (Eqs. (1.8) and (1.9)) can describe either a competitive framework ($\kappa_{12} = \kappa_{21} = -1$) or a mutualistic community ($\kappa_{12} = \kappa_{21} = 1$). The case in which the coefficients are of opposite sign correponds to the well-known predator prey system:

$$\frac{dU_1}{dt} = U_1 f(U_1) - R(U_1)U_1 U_2 \tag{1.10}$$

$$\frac{dU_2}{dt} = \kappa_{21}R(U_1)U_1 U_2 - M(U_2)U_2\,, \tag{1.11}$$

where U_1 and U_2 are the prey and predator densities, M is a positive function describing predator mortality and $0 < \kappa_{21} < 1$ is the food utilisation constant accounting for the conversion of prey into predator biomass. The function $R(U_1)$ is the functional response of predator to prey and can take many forms, however the most common are Holling II or Holling III (*Holling 1959a, b, 1965, 1966*).

One of the simplest epidemic models takes a similar form, with distinctly classing a population into two compartments, susceptible and infected (*Kermack-McKendrick 1927*):

$$\frac{dS}{dt} = -\beta SI \tag{1.12}$$

$$\frac{dI}{dt} = \beta SI - \gamma I\,, \tag{1.13}$$

where β is the transmission rate and γ is the mortality rate of infected individuals. The disease is assumed to be transmitted directly (i.e. not through any vector[3]) and despite its simplicity the model clearly captures the essence of initial disease establishment. The underlying assumptions of the classic Kermack-McKendrik model (Eqs. (1.12) and (1.13)) include:

- Disease transmission occurs in direct contact between susceptible and infected individuals

- All susceptible individuals are susceptible to the disease in the same way, therefore there is no transmission preference

- All infected individuals are equally infectious

- There is no incubation period of the disease, therefore the infection occurs instantaneously

- The population size is fixed, i.e. no births or migration occur and all the deaths are taken into account

Spatial counterparts of variants of both models (Eqs. (1.10-1.11) and (1.12-1.13)) will be analysed in more detail in Chapter 2.

To a greater or lesser extent, movement is one of the defining features of many organisms. The reality that the world is unavoidably spatial has long been ignored by most ecologists and therefore one might not be particularly surprised that historically, movement has played a rather peripheral role in most of the mathematical ecology literature, with spatial considerations in general being largely discarded. In a collection of 40 seminal ecological papers (*Real and Brown 1991*) only one addresses the issue of movement explicitly (*Skellam 1951*). Possibly this was a

---

[3]The use of the word vector here refers to a biological vector i.e. a carrier of disease.

combined consequence of the lack of appropriate data needed to stimulate theoretical development and the difficulty of mathematical expression. Since then, stemming from the pioneering works of *Fisher (1937)*, *Kolmogorov et al. (1937)* *Skellam (1951)* and *Turing (1952)*, spatially explicit reaction-diffusion equations have been receiving growing attention and have set the foundation for mathematical modelling of biological invasions (*Okubo and Levin 2001*).

The generic form of reaction-diffusion equations is formulated as follows:

$$\frac{\partial U}{\partial t} = D \triangle U + U f(U) \,, \tag{1.14}$$

where D is the diffusion coefficient, $f(U)$ is the per capita growth rate and $\triangle$ is the Laplace operator. Travelling wave solutions predicted by such models are of considerable ecological relevance and are in good agreement with empirical studies on invasion (*Petrovskii and Li 2006*, *Shigesada and Kawasaki 1997*, *Volpert and Petrovskii 2009*). One of the fundamental questions regarding biological invasions is how fast will the invasive species progress. Can mathematical models be of help in predicting the advance of invasive species? In the absence of the Allee effect (*Skellam 1951*, *Fisher 1937*, *Kolmogorov et al. 1937*) travelling fronts propagate with an asymptotic rate of spread equal to $c = 2\sqrt{f'(0)D}$, whereas the inclusion of the Allee effect has shown to reduce the speed of invasion (*Lewis and Kareiva 1993*). To what extent does this "passive" diffusion approach adopted by reaction-diffusion systems approximate the local movement of animals sparked numerous experimental investigations of animal dispersal. Typically, estimates of the diffusion coefficient, D, are obtained from mark recapture data. Both early quantitative laboratory attempts and more recent mark recapture experiments indicate the ability of simple diffusion models to reasonably approximate animal dispersal (*Dobzhansky and Wright 1943*, *Watanabe et al. 1952*, *Kareiva 1983*). With parameters obtained from historical and field data, reaction-diffusion models have been successfully applied to a wide variety of taxa (*Skellam 1951*, *Andow et al. 1990*, *Shigesada and Kawasaki 1997*). Despite capturing the basic idea behind range expansion, the coupling of dispersal and population growth, diffusion models are often criticised for being an oversimplification of animal movement (*Skellam 1973*, *Turchin 1988*). As the simplest conceptual description of dispersal, diffusion assumes a random, uncorrelated motion and clearly, animals do not move in a purely random manner. However, with the choice of an appropriate spatial scale, in which the mean length of individual moves is not large, the dispute on random movement can be somewhat overcome (*Malchow et al. 2008*, *Shigesada et al. 1995*,

Murray 2002). Furthermore, *Holmes (1993)* has shown that if the direction of motion is to some extent correlated (telegraph model) the results have no significant qualitative difference, as the solutions are still travelling waves propagating with speeds that differ from the original Fisher equation by a small percentage, $< 8\%$. Reaction-diffusion equations assume that movement is isotropic, i.e. that individuals move at equal speeds in all directions, with no preference, and this is far from reality for many species. In particular, marine and freshwater species disperse via water currents, and plants through seed dispersal largely governed by wind currents. Such directed motion can easily be incorporated into the standard diffusion framework as advection or taxis (*Kareiva and Odell 1987, Shigesada and Kawasaki 1997, Cantrell and Cosner 2003*).

Of course, the spread rate of invasive species is not the only prediction of interest when modelling biological invasions. A prominent feature of biological invasions is the distinct spatiotemporal patterns observed in natural populations (*Caughley 1970*). Though the underlying driving factors of such a pattern formation are yet to be fully understood, there are a number of proposed mechanisms. Indeed, complex spatial patterns in reaction-diffusion systems can arise as a result of Turing and diffusive-like instabilities (*Turing 1952, Segel and Jackson 1972*). The controversy surrounding Turing type patterns is their tendency to be spatially periodic, and though some ecological examples are readily observed (*Klausmeier 1999*), in general spatial periodicity in natural populations seems to be more of an exception than a rule. Therefore, the generality of Turing-like patterns acting as a generic mechanism for pattern formation still remains highly debatable. If periodic patterns are known to be only part of the rich spectrum of observed spatiotemporal dynamics, a question arises as to the other type(s) of pattern formation resulting from the propagation of travelling fronts, if any. In fact, continuous propagating fronts with homogeneous distributions of population density in the wake are not the only possible outcome. For a diffusive Lotka-Volterra system it has been shown that spatiotemporal patterns may appear in the wake of travelling fronts, first observed by *Dunbar (1983)* as damped regular oscillations. Moreover, subsequent studies have shown that the propagating travelling fronts can lead to emerging chaotic patterns (*Sherratt 1994, Sherratt et al. 1995, Sherratt 2001, Petrovskii et al. 2001*). Though, in all cases, a clear continuous boundary separates invaded from non-invaded areas and this is often in disagreement with field observations (see Fig. 1.5). Qualitatively similar dynamics of patchy distribution have also been observed in reaction-diffusion systems
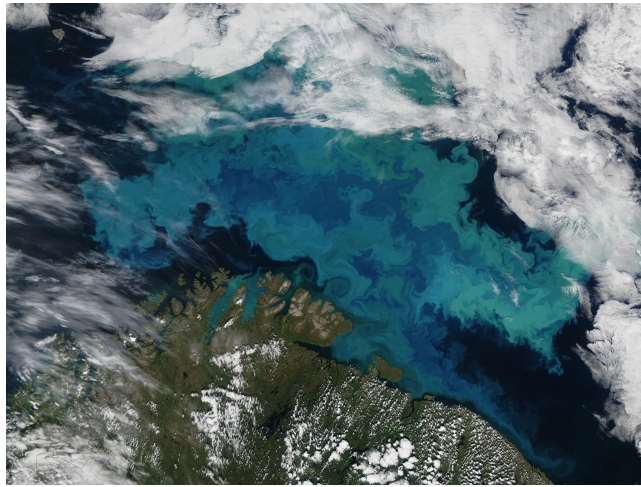
FIGURE 1.5: Patchy distribution of plankton in the Barents Sea. Different shades of blue and green correspond to different densities of phytoplankton species. Image is taken from `http://eoimages.gsfc.nasa.gov/images/imagerecords/51000/51765/BarentsSea_amo_2011226_lrg.jpg`

subject to population growth being damped by the strong Allee effect (*Petrovskii et al. 2001, Petrovskii et al. 2002, Morozov et al. 2006*), and will be the focus of Chapter 2.

The distribution of dispersal distances may not necessarily conform to a normal distribution as assumed by reaction-diffusion systems (*Lonsdale 1993*) and the main drawback of diffusion models is their inability to account for different forms of dispersal. In some cases, dispersal is often skewed to further distances than described by a normal distribution, thus an alternative approach would entail the use of various probability functions accounting for this fact (*Neubert and Caswell 2000, Kot and Schaffer 1986*). Also, for processes where the spatial scale is large compared to the temporal scale, both integrodifferential and integrodifference models offer better approximation and insights into population dynamics (*Lee et al. 2001*).

Species with nonoverlapping generations can therefore be modelled by time-discrete models allowing for a broad range of dispersal kernels known as integrodifference equations. The topic of such models goes beyond the scope of this study, but I would like to just briefly mention their form and applicability. In general, the form of integrodifference models used to describe biological invasions includes both population growth and dispersal:

$$U_{t+1}(x) = \int_{\Omega} k(x,y)G(U_t(y))dy \,, \tag{1.15}$$

where $k(x, y)$ is the probability density function describing individual dispersal, Ω is the domain and $G(U)$ accounts for population growth. Life characteristics, landscape structures and many other factors influence the exact choice of dispersal kernel (*Greene and Calogeropoulos 2001*), yet based on any specific choice made, integrodifference models allow for the estimation of spread rate (*Kot 1992*). Leptokurtic (broad-tailed) dispersal kernels are commonly observed in ecological populations (*Okubo and Levin 2001, Wallace 1966*), and as a result of their use in integrodifference models accelerating rates of spread are observed (*Kot et al. 1996*).

1.3   Time delay and population dynamics

Whether invasive species will exhibit sporadic outbreaks, or undergo regular, periodic cycles is of interest in planning control and management strategies. Therefore, temporal dynamics of invaders are of equal importance to the study of biological invasions as are the corresponding spatial structures. Population densities of many species tend to fluctuate nearly periodically over time (*Turchin 1990, 2003*). Such cyclic dynamics has long fascinated ecologists, though despite the plenitude of research and considerable progress made in unravelling such complex dynamics, underlying mechanisms still remain debatable (*Elton 1924, Hutchinson 1948, Krebs 1996*). Although a fairly intuitive concept itself, at the core of understanding population variability lays the issue of population regulation. A common approach for revealing dominant ecological mechanisms is time series analysis, and it seems there is consent amongst the ecological community that delayed density dependence plays an important role (*Turchin et al. 1999, Berryman and Turchin 2001*). Populations are influenced both by factors that are functions of current and past population densities. In fact, the latter case of delayed density dependence is thought to make populations more prone to cycle. Though the origin of delay is not clearly known, some most commonly considered factors include predator-prey interactions, the effect of parasitoids and pathogens, competition for resources, maternal effects, etc. Indeed, possible causes of delayed density dependence are numerous and it is highly unlikely that a single causal factor can be isolated, as different exogenous and endogenous factors are tightly intertwined (*Krebs 1996, Royama 1981*).

Nevertheless, time delays remain a ubiquitous phenomenon and integral part of ecology (and of nature, in general), and thus should be included in any modelling

efforts. Although the motivation to include time delays is easily perceivable, the way to do it is not so clear. One possibility is to incorporate a discrete time delay which would result in a simple delay differential equation, which can be modelled as:

$$\frac{dU}{dt} = G(U(t), U(t - \tau)),$$ (1.16)

where $\tau > 0$ is the delay parameter. A more accurate description would strive to average the delay over all past populations, which in turn results in an integrod-ifferential equation and in case of logistic growth takes the form:

$$\frac{dU}{dt} = rU \left(1 - \frac{1}{K} \int_{-\infty}^{t} \omega(t - s) U(s) ds \right),$$ (1.17)

where ω is a weighting factor, known as a kernel, that describes the relative strength of importance given to populations at earlier times. A generally accepted idea is that time delays are a potent source of instabilities in population models (*Nunney 1985*). Time delays in feedback mechanisms destabilise positive, otherwise stable, equilibria and lead to oscillatory behaviour (*Maynard Smith 1974*, *Kuang 1993*, *Ruan 1995*), though this is not always the case (*Hastings 1984*, *Jankovic and Petrovskii 2014*). Hence, time delay models are capable of generating more complex and rich dynamics, closely resembling observed population patterns. However, there are a few questions that remain unaddressed, such as when are time delays destabilising, what form should the time delay take, how fast should the kernel decay and what are the driving factors and consequences of such dynamics?

1.4   Thesis outline

This dissertation is roughly divided into two parts. Part I (Chapter 2) documents a case study of biological invasion of gypsy moth, *Lymantria dispar*, in North America. By using the introduced framework of reaction-diffusion systems, we test whether prey-predator interactions or the influence of a naturally occurring viral infection (nuclear polyhedrosis virus – NPV) are able to reproduce qualitatively similar patterns of spread of gypsy moth populations as observed in nature. The patchy distribution of gypsy moth is widely explained by accidental human-assisted dispersal, e.g. when egg masses are transported by cars and vehicles. To some extent this theory disagrees with the existence of the strong Allee effect

which tends to wipe out small new colonies. Therefore, we propose an alternative hypothesis, that the patchiness may be a result of the interplay between two natural factors: dispersal and NPV/prey-predator interactions. We also estimate the spread of gypsy moth populations using a diffusive Susceptible-Infected (SI) model and obtain spread rates comparable to historical data.

Part II (Chapters 3, 4 and 5) focuses on another aspect affecting population dynamics – time delay. Both ecological and mathematical implications of time delays in population dynamics are discussed. In Chapter 3 we consider single species population dynamics affected by the Allee effect and coupled with discrete time delay. Contrary to the general opinion that time delays are always destabilising, we show that that is not always the case. The results included are both analytical and numerical, followed by a discussion of possible ecological applications.

Chapter 4 continues the study of time delays through an integrodifferential model. We revisit some known results on exponential memory kernels and introduce a power law memory dependence to model single species population dynamics.

In Chapter 5 we examine the properties of the diffusive logistic equation with a discrete time delay, and extend the study to incorporate a biologically more relevant concept of spatial averaging. This results in an integrodifferential delay model which surprisingly exhibits a wider than expected variety of spatiotemporal patterns.

I conclude in Chapter 6 giving a summary of the work done and possible future directions.

Chapter 2

Gypsy moth invasion in North America:
A simulation study of the spatial pattern and the rate of spread

2.1   Introduction

Another prime example of biological invasion is the gypsy moth invasion, *Lymantria dispar*, in the US. [1] Since its introduction in the late 1860s the gypsy moth has spread throughout North America, causing significant damage to forests in all or parts of nineteen northeastern states (*Maloney et al. 2010*). Currently occupying only a third of its potential habitat, various management strategies are utilised to control gypsy moth spread. To date, the eradication of gypsy moth populations in northeastern US has not been successful, as it is still spreading. The gypsy moth is known to be an invasive pest in its native range as well, including countries such as Romania, former Yugoslavia, France and Japan (*Gerardi and Grimm 1979*). However, the most devastating consequences are observed in North America where since its introduction it has invaded over 10^6 km^2 (*Liebhold et al. 1992*). Apart from widespread defoliation, the gypsy moth indirectly affects native population dynamics (*Jones et al. 1998*), carbon sequestration and nutrient cycling, alters biogeochemical conditions and changes the acid–base status of

---

[1]The majority of this chapter has been published in *Jankovic and Petrovskii (2013)*

affected catchments (*Webb et al. 1995*) and also has a negative effect on radial growth of tree hosts (*Naidoo and Lechowicz 2001*). Rightfully, the gypsy moth has earned the title as one of a hundred world's worst invasive species by the ISSG (*Invasive Species Specialist Group*).

The goal of this study is to re-examine the biological factors and the corresponding mechanisms that can affect the pattern and rate of spread of gypsy moth populations in North America. For this purpose, we first carefully examine available evidence and perform an extensive literature review of gypsy moth biological traits and the possible impact of environmental forcing; see Section 2.2. From this examination, we infer that the two main factors controlling high density gypsy moth abundance are likely to be the Allee effect and the nuclear polyhedrosis virus (NPV); see Section 2.5. On the other hand, low density gypsy moth populations are regulated by the interplay between the Allee effect and prey-predator interactions. Correspondingly, we then consider spatially explicit prey-predator and SI models (see Section 2.6) and show that the qualitative features of gypsy moth spread can be well explained by the interplay between short-distance dispersal, local disease dynamics or predatory effects and the Allee effect. Based on parameter estimates available from the literature, we show (see Section 2.7) that the SI model prediction of the rate of spread is in good agreement with field data.

2.2 Gypsy moth: biology, population dynamics, dispersal

Gypsy moth is univoltine, meaning it produces one generation per year. Different stages of metamorphosis include the egg phase, larval (caterpillar), pupal (cocoon) and adult phase. Each egg mass oviposited by females contains roughly around 500 to 1,000 eggs, which overwinter usually in sheltered areas: attached to trees, stones or logs. Oviposition occurs roughly 1–2 m from the site of adult emergence (*Odell and Mastro 1980*) and hatching of egg masses usually coincides with budbreak (April and May), even though the process of larvae formation is completed within a month. Gypsy moth larvae shut down their metabolic activities and enter diapause. This mechanism allows them to become insensitive to cold, as low temperatures have been shown to influence mortality. By chewing through their egg shells, larvae emerge and mature through five to six instars, over a period of about four to six weeks. After locating a preferable place, pupation occurs, mainly on

trunks of trees. The pupal stage is brief, lasting around two weeks, in which feeding does not occur, and in the majority of this period pupae are immobile. Mature adults emerge in midsummer (late June, early July) and usually live a week or less (*Tobin and Liebhold 2011*). Males tend to develop slightly before females and this time lag is known as protandry. Females are typically larger than males, baring a whitish cream colour with some black markings on their wings, and are flightless (in North America, though some Asian strains are capable of sustained, directed flight). Males are usually brown or dusky coloured with darker markings on their wings, and capable of flight. Following emergence, mating occurs, and success is hugely dependent on the distance between males and females.

Due to the female's incapability of flight, range distribution and expansion is largely reliant on spread mechanisms such as larval crawling, windborne dispersal of first instars, and increasingly dependent on artificial dispersal originating from inadvertent human transport. This combination of different dispersal scales induced by long-distance "jumps" originating from artificial dispersal and local colony growth due to short-distance ballooning of early instars is known as stratified diffusion (*Liebhold and Tobin 2010*). Upon hatching, first instar gypsy moth larvae crawl to branch twigs and suspend on silken threads awaiting passive dispersal by wind. This ballooning of early instars yields short range dispersal. Whilst natural dispersal is limited to early instars, artificial dispersal affects all life stages but most frequently involves egg masses. Long distance dispersal leads to the formation of isolated colonies ahead of the initially infested area, which may grow and coalesce thereby increasing the rate of spread.

Counts of male moths in pheromone baited traps are a widely used tool for monitoring low density populations and detecting new isolated colonies. Other methods of monitoring gypsy moth populations are the examination of forest defoliation aerial maps and counts of overwintering egg masses. Though a tedious process, egg mass counts are frequently utilised for monitoring medium to high density populations and are used to make decisions of various suppression techniques. However, egg mass sampling programs tend to have low spatial resolution and often produce inconclusive data, hence male moth counts are the preferred measure of population abundance.

Compared to other invasive species, the rate of spread of gypsy moth is relatively slow largely due to the female's incapacity of flight. Spread rates have shown

considerable variation throughout the years of gypsy moth invasion. To date, explanations of this variation in spread speed have been numerous, such as, on the one hand, the continuous growing of forests which increase proportions of suitable hosts for this pest insect and, on the other hand, the enactment of quarantine measures limiting and suppressing further population spread. In particular, it has been proven that the large-scale "Slow the Spread" program since its employment in 1995 has successfully reduced the spread by at least 50% (*Sharov et al. 2002*); see Section 2.4. Analysing available historical county level quarantine data on gypsy moth invasion *Liebhold et al. (1992)* concluded that the spread rates differed, throughout the past century, from a mere 2.82 km/year to a worrying 20.78 km/year. More recently, *Tobin et al. (2007a)*, using various spread rate estimation techniques, came up with even a broader range of spread rates as 2.6–28.6 km/year. Increased rates of range expansion are usually linked to increased inadvertent transport of gypsy moth by humans. Also the geographic variation affects the spread rate as spread to the north was significantly slower than to the south and west regions, probably due to severe weather conditions (cold temperatures in particular) which tend to cause heavy mortality in overwintering egg masses.

Another factor shown to affect the gypsy moth spread is the Allee effect (*Liebhold and Bascompte 2003, Tobin et al. 2009, Vercken et al. 2011*). In essence, the Allee effect describes a positive relationship between individual fitness and population density (*Dennis 1989, Courchamp et al. 1999*); therefore, the lower the density the more prominent the impact of the Allee effect can be. As a particular consequence, low density populations can be, and often are, driven to extinction. In the formation of new isolated colonies of gypsy moth, successful establishment and the subsequent growth largely depend on factors affecting sparse populations. Gypsy moth isolated colonies are of low abundance and highly prone to Allee effects and extinction (*Liebhold and Bascompte 2003, Sharov et al. 1995, Whitmire and Tobin 2006*). Mating success is the most important density dependent factor affecting sexually reproducing sparse populations. *Sharov et al. (1995)* found that successful mating is more likely to occur in high density than in low density populations, highlighting the possibility of extinction through the Allee effect in sparse populations.

Allee effects exhibit region specific behaviour, thus indirectly influencing the rate of range expansion (*Tobin et al. 2007b*). Although mate-finding failure is thought to be a universal cause of Allee dynamics, reasons underlying spatial and temporal variation of Allee effect strength remain obscure. Numerous studies have shown an

inverse relationship between Allee effect strength and invasion speed (*Lewis and Kareiva 1993, Tobin et al. 2009, 2007b, Whitmire and Tobin 2006*). However, quantifying Allee effects and establishing thresholds is by no means a simple task. The estimates of Allee thresholds obtained in several studies are largely based on monitoring techniques, such as pheromone baited trap catch data, and expressed in units of male moth counts per trap. These counts provide only relative information and should not be treated as absolute population density measures but rather as measures of relative gypsy moth abundance (*Sharov et al. 1995*).
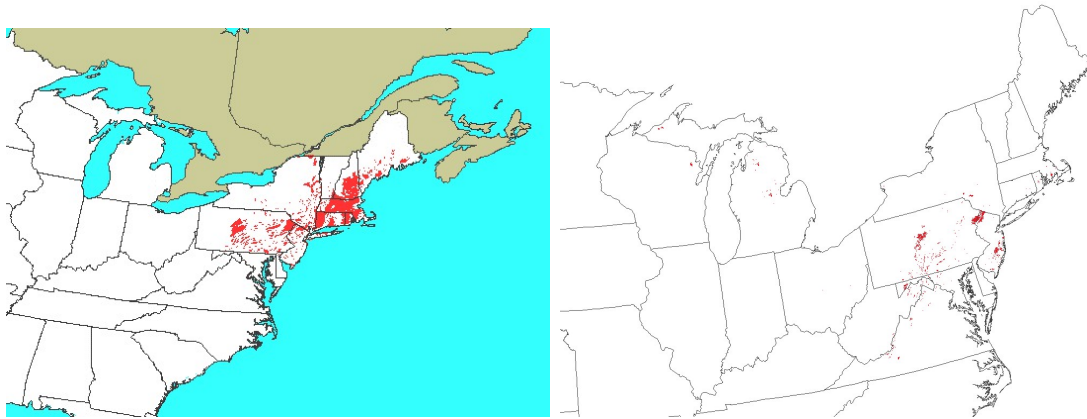
FIGURE 2.1: Gypsy moth defoliation maps of US states for 1981 (left) and 2007 (right). Red colour shows defoliated areas. From `http://www.fs.fed.us/ne/morgantown/4557/gmoth/atlas/#defoliation`, by curtesy of Sandy Liebhold.

Dispersal of individual insects results in the gypsy moth population spread over space. In North America, this spatial spread results in the formation of a highly heterogeneous spatial distribution or 'pattern' (see Fig. 2.1) where areas with high level of infestation alternate with areas where gypsy moth is either absent or present at a low density. Having mentioned spatial variability of the strength of the Allee effect, an immediate intuitive attempt would be to relate the observed pattern to environmental heterogeneity. Gypsy moth is a polyphagous herbivore and currently feeds on a total of around 300 tree species, including both deciduous and coniferous species; however, some tree species are more preferable than others. In areas with more preferred tree species, higher numbers of gypsy moths are more likely (*Liebhold et al. 1994, Witter et al. 1992*). Interestingly, the evidence suggests spatial heterogeneity is not as significant a factor in distribution as one might expect. *Sharov et al. (1997)* looked at pheromone trap data from 1988 to 1994 in northern Virginia and southern West Virginia to find correlations between landscape characteristics (land use, slope, elevation, aspect and two forest classifications) and gypsy moth density that could be used to improve understanding of the spread. However, only elevation was found to be statistically significant, and

only strongly significant in the transition zone. *Whitmire and Tobin (2006)* looked at new outbreaks across the US and concluded that "the abundance of preferred host tree species and land use category did not appear to influence persistence". Overall, environmental forcing through spatial heterogeneity does not appear to be enough to explain the pattern of gypsy moth distribution.

Having the effect of environmental heterogeneity excluded, one therefore may hypothesise that the pattern formation in the gypsy moth spatial distribution is an inherent property of biological interactions. Indeed, a well-developed theory predicts self-organised formation of irregular spatial structure in the wake of the propagating invasion front (*Sherratt et al. 1995, 1997*) in case the alien species is affected either by predators or pathogens. Interestingly, a closer look at the defoliation maps reveals that in case of gypsy moth spread there is no apparent continuous front separating infested from non-infested regions (Fig. 2.1). This scenario of alien species spread has been referred to as patchy invasion (*Petrovskii et al. 2002, Morozov et al. 2006, Mistro et al. 2012*). In what follows, we will explore this hypothesis further and show that the patchy spread of gypsy moth can appear as a result of the interplay between short-distance dispersal, the Allee effect and prey-predator interactions or a certain viral infection (NPV) which is common in gypsy moth.

2.3   History of gypsy moth introduction

Precise details regarding the accidental release of gypsy moth in North America are not known, and there are many speculations surrounding the issue of this non-native species. A widely accepted hypothesis involves import of gypsy moth to Medford, Massachusetts, by French amateur entomologist, Etienne Leopold Trouvelot. The gypsy moth introduction is a "remarkable example of an experiment gone wrong" (*Dunlap 1980*). In the late 1860s, Trouvelot's prime hobby research comprised of silkworm breeding, and of particular interest was breeding a disease resistant hybrid for use in commercial production (*Spear 2005*). In 1868 (or 1869 according to some authors) during the course of his experiments disaster struck: some eggs got lost, and larvae escaped captivity. Knowing the potential damage these forest pests could cause, Trouvelot began destroying the egg masses, and alerted government officials. Not much attention was paid to the accident at the time, as only agricultural entomologists, lacking sufficient influence, understood

the severity of this event. The gypsy moth remained unnoticed and was considered to be little more than a curiosity for quite some time, with populations remaining at innocuous levels. Populations expanded slowly and covered forest lands including 30 towns and cities in the greater Boston area (*McFadden and McManus 1991*). Only following severe defoliation incurred during the first outbreak observed in 1889, were eradication programs initiated. Various insecticides played a key role in this program, such as paris green designed to destroy all life stages of the gypsy moth. However due to high doses of insecticides damaging foliage, and primitive mechanical methods of dispersal (horse-drawn ground sprayers), eradication failed. This triggered a series of management efforts attempting eradication and suppression, marking the beginning of "the great gypsy moth war" (*Spear 2005*). Paris green was substituted with lead arsenite, and improvements to spray technology were made. Eradication of the gypsy moth seemed to be successful, and was for that reason halted, which has to date been shown as an irreversible mistake. Following this crucial mistake, populations began to grow once again and in 1905 the federal government was involved to comprise a reasonable strategy.

In general, there are two extremes of biological control that were attempted in eradication, and later in suppression of this insect. The former, classical approach implies introduction of natural enemies, parasitoids (egg parasitoids *Ooencyrtus kuvanae* and *Anastatus japonicas*), predators (dermestid beetles, *Trogoderma tarsale Melsheimer* and *Anthrenus verbasci*) and pathogens (*Bacillus thuringiensis* and *Streptococcus faecalis*) (*Leonard 1974*). To date, more than 60 species have been introduced since 1906 (*Hoy 1976*), but despite all possible efforts, many of them have not been able to establish, for various reasons. This still appears to be a work in progress, with most promising results expected of two tachinid parasitoids, *Blepharipa schineri* and *Ceranthia samarensis* (*Kenis and Vaamonde 1998*). The latter case of biological control involves using a biological agent, as if it were a chemical; examples include the use of microbial insecticides Bt (*Bacillus thuringiensis*) and Gypchek (*LdNPV*). In the long run biological control has proved as an efficient eradication/suppression tool, however at that particular moment the development of bioinsecticides, and research on potential natural enemies of gypsy moth was progressing, but at a slow pace, while immediate action was needed.

In 1912 a federal domestic quarantine was put in place and in 1922 a barrier zone

was placed along the Hudson River, in the hope of containing the moth population in New England. These attempts have proven to reduce the rate of invasion by gypsy moth (*McFadden and McManus 1991, Liebhold et al. 1992*). Throughout the 1920s the dominant control mechanism lay with insecticides, however improved application techniques have proved to be ineffective in forests. During the upcoming years, aerial spray application was perfected and vast quantities of the synthetic pesticide DDT (dichlorodiphenyltrichloroethane) were employed. DDT was regarded as a rising star in gypsy moth population regulation, applied everywhere, even in residential areas ("DDT is good for me"). The side effects of such uncontrolled use of DDT were beginning to be noticeable, natural gypsy moth predators were severely affected and gypsy moth populations started to grow, once again. During the late 1950s gross concerns were arising regarding the negative effects of the chemical on crops, wildlife and human health. Gradually DDT was dropped from use, and substituted by Carbaryl (Sevin®). The evolution of gypsy moth pesticides had begun, and was substantially progressing. In the 1960s, Carbaryl, due to its adverse effects on honeybees, was replaced by trichlorfon (Dylox®). A recurrent issue in pesticide production was the need to establish a target specific chemical agent, which was posing a significant problem. Eventually trichlorfon was replaced by pesticides such as acephate (Orthene®) and diflurobenzuron (Dimilin®), also exhibiting adverse effects on a large number of non target species. With the 1980s came the idea of utilising Bt, unfortunately also causing damage to other species, however a fair amount of effort has been and is being put in to produce more effective strains.

Following numerous failed attempts to eradicate gypsy moth populations, objectives started to shift to suppression and limiting the damage incurred by such pests. These efforts were at first implemented locally and restricted to residential areas, however following the most severe defoliation observed in 1981, efforts of integrated pest management (IPM) were employed. Two pilot projects were overseen by the USDA Forest Service: Maryland IPM Pilot Project (1985-1988) and Appalachian IPM Demonstration Project (1988-1992). Both management programs relied on detection of low density gypsy moth populations by deploying grids of pheromone-baited traps ahead of the expanding population front. This enabled delineation of isolated colonies, followed by eradication treatments to eliminate them or retard their population growth. Following the success of these programs one of the largest programs devoted to gypsy moth population control in North America named "Slow the Spread" was adopted by the USDA Forest Service and

Animal and Plant Health Inspection Service (APHIS). In essence, seasonal controlled release of (+)disparlure (gypsy moth sex hormone) interferes with normal mate-searching behaviour and communication of male moths, thus decreasing the probability of mating. The favoured noninsecticidal treatment used is Disrupt II, containing a synthetic version of disparlure.

Corresponding to each phase of invasion appropriate measures are undertaken. Quarantines, in particular international, and rigorous inspections are used to prevent the arrival of exotic species, such as the gypsy moth. If these fail detection and eradication processes are undertaken to prevent and reverse, if possible, population establishment. However, if the species persists and accomplishes successful establishment various types of barrier zones and domestic quarantines are used to limit range expansion.

Techniques aiding gypsy moth outbreak prevention also include cultural and silvicultural controls which tend to manage stand characteristics (species, composition, age and density) and help site maintenance in avoiding disturbance of sites, making them less prone to invasion (*Coulson and Witter 1984*).

Management and control strategies should also heavily exploit the so-called Achilles heel of invasions, and attempt to strengthen Allee effects in gypsy moth populations, and reduce the population size below the Allee threshold consequently leading to extinction. Examples of such exploitations are mating disruption, mass-trapping and the release of sterile insects (*Liebhold and Tobin 2010*).

Prospects of new research and potential success lies in the improvement of existing strategies, and perhaps uncovering new methods. Hopes of re-introduction of natural enemies that have failed to establish in the past, introduction of new species (tachinid fly *Blepharipa schineri*, dermestid beetles,etc) and introduction of new bio-types of already established natural enemies, seem to yield plausible evidence of success (*Kenis and Vaamonde 1998*).

2.4 "Slow The Spread"

Instigated by successes of previous management programs, the USDA Forest Service initiated a pilot project known as "Slow the Spread" (initially called the gypsy moth Containment Program) in 1993. The program was designed to examine the

feasibility of reducing the spread of gypsy moth over large regions, through extending the use of area-wide integrated management tactics. The strategy implemented implies the detection and eradication (if possible) of isolated, individual gypsy moth colonies occurring in the transition zone. In the case eradication is unachievable, suppression methods are employed to reduce growth and coalescence of newly founded colonies, thereby decreasing the rate of spread. The reduction of gypsy moth spread rate is a common objective of many integrated pest management programs, the novel feature in Slow the Spread is the lesser use of pesticides. Barrier zones were established along the advancing front of gypsy moth populations, and encompassed the Appalachian region in Virginia and West Virginia, northeastern North Carolina and the Upper Peninsula of Michigan. Following the success of the pilot project, Slow the Spread has been integrated into USDA's national program for managing gypsy moth since 1999. This national program boasts three strategies: suppression, eradication and slow the spread. Whilst eradication efforts tend to be used to eliminate isolated infestations in areas where the gypsy moth has not yet fully established, suppression programs are implemented in areas where the gypsy moth has established with the goal of reducing the damage incurred by outbreaks. As a combined federal and state government effort to slow gypsy moth spread, Slow the Spread (STS) is one of the largest and most comprehensive programs to date in the management of forest pest species.

In contrast with other management programs STS is preventive, and its implementation is not only expected to decrease the rate of spread of gypsy moth, but is also expected to spare ca. 20,202 km^2 of new territory from invasion each year (*Sharov et al. 2002*). While large funds are allocated to such a program, sceptics would be right to question the efficiency of STS. However, it has been shown that the benefits outweigh the cost at least 3:1 (*Leuschner et al. 1996, Mayo et al. 2003*). Largely reliant on pheromone trap catch data, STS focuses on populations situated in the transition zone, which are not targeted by traditional eradication/suppression efforts. Once isolated gypsy moth populations are detected, colonies are delimited and treated to eliminate, or merely suppress further growth. The use of pheromone baited traps has been proven to be an efficient and inexpensive method for identifying and recording gypsy moth populations, as other life stages are more difficult to locate and other methods (e.g. egg mass counts) tend to exceed budget constraints.

One of the elements attributed to the success of STS has been mating disruption. The transition zone within STS containing relatively few individual colonies is

often aerially treated to disrupt mating by plastic laminated flakes, impregnated with synthetic gypsy moth sex pheromone, attached to a sticker. This target specific method of managing invasive species is by far the most crucial in preserving unique, endangered and rare habitats and species, and should serve as an exemplar in controlling other pests. The barriers implemented are in no way static, i.e. their location moves over time and is estimated relative to population boundaries interpolated from gypsy moth counts (*Tobin et al. 2004*). For this purpose a 10 *moth/trap* threshold is utilised as it exhibited satisfying spatiotemporal stability (*Sharov et al. 1997*). The STS project area is situated on both sides of this 10 *moth/trap* boundary, and spreads ca. 170 km in width. Isolated gypsy moth colonies are present in areas beyond STS, however their frequency drastically declines with increasing distance. The project area alone consists of two zones: the action and monitoring zones, with the action zone implying active management, i.e. detection and eradication of isolated colonies, and the monitoring zone serving to delineate colonies and estimate population boundaries. The effect of the project on spread rate and the yearly adjustment of population boundaries is all handled within the monitoring zone. Traps are placed at particular distances: intertrap distances vary from 2 km, in the action zone, to 8 km, in the monitoring zone. Surveyors are responsible for trap catch placements, removal and obtaining spatial information on traps. This data is then uploaded to a database and thoroughly processed by the Decision Algorithm, which evaluates the effectiveness of the STS program as well as calculates the spread rate of gypsy moth populations.

Numerous analyses have been undertaken, and seem to yield on average a 50% decrease in spread rate since the implementation of STS. *Sharov and Liebhold* (*1998*) estimated the spread rate, with the use of barrier zones, and compared to corresponding historical "pre barrier" data resulting in a 54% reduction, close to the actual reduction of 59% since 1990.

2.5   Regulatory mechanisms

The dynamics of gypsy moth populations are governed by both density dependent and density independent factors. Density independent factors include environmental factors which exert a direct or indirect effect on the pest population regardless of the population size or structure. Examples of such are temperature, rain, moisture, evaporation and light, to name a few. Overwintering gypsy moth egg masses

are vulnerable to low winter temperatures: it has been shown that some egg masses are killed when exposed to $-30\,°C$, and overall mortality occurs with exposure to $-35\,°C$ (*Summers 1922*). It is assumed that these cold winter temperatures serve as a limiting factor in gypsy moth spread to the north. Gypsy moth egg masses also exhibit snow insulating properties, shielding the egg masses from the destructive consequences of low winter temperatures. Thin layers of ice and setae covering also act as insulators to overwintering egg masses. In contrast, high temperatures do not influence larval survival, but do accelerate short term growth and marginally increase final pupal weights (*Lindroth et al. 1997*). Periods of high humidity are associated with increased mortality rates of gypsy moth larvae, mostly due to the increased incidence of pathogens such as NPV and *E.maimaiga*.

On the other hand, density dependent factors are those tightly linked to the population itself, primarily depending on its size (density), e.g. disease and starvation. Two reasonably host specific entomopathogens are responsible for the collapse of outbreak populations: *Entomophaga maimaiga* (fungal pathogen) and the naturally occurring viral disease *Nucleopolyhedrosis virus* (multicapsid LdNPV). Most studies are based on the NPV pathogen, which often produces spectacular epizootics ceasing gypsy moth outbreaks.

2.5.1 Nuclear Polyhedrosis Virus

NPV is commonly known as "wilt disease" due to the soft and limp appearance of infected larvae. This naturally occurring viral infection induces a bimodal pattern of mortality. Early instars become infected with lethal doses of NPV on the surface of egg masses and a shiny oily appearance is typical for infected larvae. Mortality occurs usually a week or two after hatch; virus killed larvae hang in an inverted V position and cadavers are usually a brownish black colour. The DNA of NPVs is enclosed in a polyhedral protein matrix, known as a polyhedral occlusion body (*Dwyer 1992*). Cadavers of the killed larvae serve as inoculums of infection to older instars, feeding on contaminated foliage, causing a second wave of mortality (*Elkinton et al. 1990, Elkinton and Liebhold 1990, Dwyer and Elkinton 1993*); see Fig. 2.5. Cadavers rupture and subsequently release large numbers of polyhedral occlusion/inclusion bodies (also known as PIBs) that can survive outside hosts and remain in the soil and surrounding areas for up to one year (*Elkinton and Liebhold 1990, Reardon et al. 2009*), hence the ubiquity of the virus. The corresponding gypsy moth mortality rate is estimated to be about

90% (*Reardon et al. 2009*). There are several NPV transmission mechanisms in gypsy moth populations. Horizontal transmission of the virus is thought to be the principal means of transmission between generations, as egg masses contract the disease from contaminated surfaces. The viral infection can also be passed on from female parent to offspring known as vertical (or maternal) transmission and is thought to occur less often than horizontal transmission, however this still remains a debatable issue. Some studies have shown that the majority of larval mortality occurs by means of surface contamination (transovum), rather than within the egg (transovarial) (*Elkinton et al. 1990*). Other studies have shown that transmission may originate from male gypsy moths during mating, and even from egg parasitoids such as *Ooencyrtus kuvanae*. Other mechanisms of NPV transmission within gypsy moth populations are vectoring of the disease by various predators (*Lautenschlager et al. 1980*). NPV epizootics are associated with high density populations; however, the virus can be found in low density populations as well.

2.5.2 Entomophaga maimaiga

Entomophaga maimaiga is a natural occurring virulent fungal pathogen, native to Asia, possessing the same ability as NPVs – to suppress gypsy moth outbreaks. Increasing interest that *Entomophaga maimaiga* has received is largely due to its promising use as a biological control mechanism. As it is reasonably host specific, i.e. does not affect other non-target organisms, in particular other *Lepidoptera*, easily introduced and has shown to induce high mortality levels in gypsy moth larvae, it essentially satisfies the criteria. By reducing gypsy moth populations to levels lower than NPVs alone, it is regarded as a highly valuable control mechanism (*Smitley et al. 1995*).

E.maimaiga has three life stages, two of which are spore forms: conidia, which are produced on cadavers (externally), azygospores (resting spores) which are produced within the cadavers and hyphal bodies (a vegetative growth stage occurring within infected organism) (*Hayek 1999, Pilarska et al. 2006*). Gypsy moths are infected from conidia produced either from azygospores or discharged by cadavers. After being discharged, conidia are ready to spud under appropriate environmental conditions, but are short-lived. *E.maimaiga* overwinters in the form of resting

spores, usually present in the soil or on tree bark. In early spring azygospores germinate producing germ conidia just above the soil surface. The general mean of infection is entry through host cuticle, as gypsy moth larvae encounter spores in their search for suitable foliage. Following this penetration, *E.maimaiga* grows inside the host body producing hyphal bodies. Unlike NPV infected larvae that exhibit a wide variety of behavioural and physical changes, larvae infected by *E.maimaiga* have not shown such prominent symptoms, only that larvae reduce feeding a couple of days before death (*Hayek 1999*). Following infection larvae tend to die within a couple of days. The appearance of cadavers differs from NPV-killed larvae: *E.maimaiga*-killed larvae remain attached to tree stems and branches, with a stiff and straight appearance (*Buss et al. 2001*).

The period of activity of *E.maimaiga* coincides with the larval stage of gypsy moth populations, and is known to target only this stage of gypsy moth. *E.maimaiga* is prone to windborne dispersal of conidia reflecting short range spread, but also exposed to dispersal of infected larvae (ballooning of first instars, larval crawling). Humans also tend to facilitate the spread of *E.maimaiga*, whilst the role of other vertebrates in pathogen spread is questionable.

Ultimately, both NPV and *E.Maimaiga* have shown the ability to suppress gypsy moth populations and can effectively serve as biological means of control, however are not preferable controlling factors in low density populations, as they only cause minor mortality.

2.5.3 Predation

In contrast to pathogens, predation appears to provide a regulatory mechanism for low density gypsy moth populations (*Elkinton et al. 1996, Liebhold et al. 2000*). As the majority of gypsy moth predators are generalists, it is noticed that this regulation of sparse gypsy moth populations is not density dependent (*Liebhold et al. 2000*). Whilst pathogens are limited to larvae, predation affects nearly all gypsy moth life stages. Predation by small mammals is the most prominent gypsy moth regulator and acts as the major cause of mortality in sparse gypsy moth populations (*Campbell and Sloan 1977*). In some cases, predation accounts for up to 20% of pupal mortality per sparse population (*Campbell 1969*). There are many known vertebrates and insect predators that feed on gypsy moth populations and around a dozen parasites that attack various gypsy moth life stages. The list

of gypsy moth predators includes several species of the carabid genus *Calosoma* (genus of large ground beetle), small mammals such as the short-tailed shrew (*Blarina brevicauda*), the grey squirrel (*Sciurus cardinensis*), and a number of avian species (over 40, with only 14 of them actually controlling gypsy moth populations), such as the red-winged blackbirds (*Agelanius phoeniceus phoeniceus*), grackles (*Quiscalis spp.*), cuckoos (*Coccyzus spp.*, red-billed and black-billed), and the sparrow *Passer montanus*, which has been found to be an important regulatory factor in sparse populations on the Japanese island of Hokkaido (*Leonard 1974*). The most prominent and important small mammal predator is the white-footed deer mouse (*Peromyscus leucopus*), accounting for the largest mortality caused to gypsy moth late instar larvae and pupae. An interesting link between mast production, white-footed mice and gypsy moth populations was proposed by *Elkinton et al. (1996)* providing an alternative approach to modelling gypsy moth population dynamics. Predation levels on gypsy moth depend on the abundance of the white-footed mouse, which is in turn linked to the mast production by host oak trees, therefore temporal and spatial patterns of mast production may influence and provide underlying reasons for gypsy moth outbreaks in North America.

Although many bird species act as gypsy moth predators, feeding on gypsy moth larvae and adults, it seems that gypsy moth larvae are not the preferred food item. Studies have shown that birds prefer hairless caterpillars to gypsy moth (*Elkinton and Liebhold 1990*). Vertebrate predators on gypsy moth eggs are in 6 families of birds and 3 families of mammals (*Brown and Cameron 1982*).

Less is known about the influence of insect or insect-related gypsy moth predators. Ground beetle larvae and adults actively seek their prey, by climbing up trees, and feed mainly on late gypsy moth larvae and pupae. Beetles are also abundant in high density gypsy moth populations. In particular *Calosoma sycophanta*, a large carabid, is thought to be an important predator in high density gypsy moth populations (*Gould et al. 1990*). Among invertebrate predators, ants (*Formicidae*) also play an important role, mostly preying on young larvae. Ant predation on female adult gypsy moths ranged from 30-94% per day (*Sharov et al. 1995*). In general, invertebrate predators unambiguously have a lesser impact on gypsy moth populations compared to vertebrate predators.

Elkinton and Liebhold (1990) gave strong evidence that parasitoids also have a significant impact on gypsy moth populations, and coupled with predation may cause more than 99% mortality within a generation. The introduction of parasitoids to

North America was just one of the strategies of biological control (eradication/suppression) of the gypsy moth population in North America. The most prominent effect was achieved by the introduction of *Ooencyrtus kuwanai*, an egg parasitoid, especially in the time succeeding outbreak culmination when egg masses are small and more eggs become available to ovipositing females. It has shown a good degree of efficiency in low host densities. Another egg parasitoid introduced for the same purpose is the *Anastatus japonicus*, providing a limited control mechanism, as it only parasitises superficial layers of eggs in egg masses. Other important parasitoids include larval parasitoids such as *Cotesia Melanoscela* and *Parasetigena sylvestris* and the pupal parasitoid *Brachymera intermedia* (*Tobin and Liebhold 2011*).

2.6   Model formulation and results

Based on the evidence revealed in previous sections, there are three specific features of the pattern of gypsy moth spread: (i) at any time, the large-scale spatial distribution of the population density is distinctly heterogeneous, the heterogeneity being self-organised and not directly related to environmental forcing, (ii) there is no continuous front separating infested and non-infested areas, and (iii) the rate of spread may show considerable variation (up to one order of magnitude).

The existing literature provides various explanations for each of these features. In particular, the patchy structure is usually related to the effect of human-assisted dispersal when the egg masses inadvertently transported to a new location ahead of the main range eventually develop into a new gypsy moth colony. However, here we argue that the importance of human-assisted dispersal may be significantly over-estimated. The impact of the strong Allee effect, which is typical for gypsy moth population dynamics, turns the successful establishment of new colonies into a rare event as theory predicts (e.g. *Lewis and Kareiva 1993*) that a new colony can only survive if its initial size is sufficiently large. Indeed, *Liebhold and Bascompte (2003)* studied the development of 194 new isolated colonies and found that none of them survived. Of these, eradication treatments were applied to only 32 colonies, whilst the rest died without intervention and 123 of them within a year of detection. We also mention here that the main infested range by itself rarely shows homogeneous population distribution but, on the contrary, often consists of separate patches (cf. Fig. 2.1). The goal of this study is to demonstrate that

features (i) and (ii) of the gypsy moth spread can, in fact, be explained by purely natural factors, namely, by the interplay between (short-distance) wind-assisted dispersal, the Allee effect and the effect of predators or pathogens such as NPV. Moreover, we are going to show that even the rate of spread predicted by the SI model appears to be in good agreement with observations.

2.6.1 Prey-Predator Model

We treat the wind-assisted dispersal as diffusion and model the multi-annual spatiotemporal dynamics of low density gypsy moth populations, regulated through predation. The spatially explicit predator-prey model then becomes a diffusion-reaction system consisting of two coupled diffusion-reaction PDEs:

$$\frac{\partial U(\mathbf{r},T)}{\partial T} = D_1 \nabla^2 U(\mathbf{r},T) + F(U) - f(U,V) \ , \tag{2.1}$$

$$\frac{\partial V(\mathbf{r},T)}{\partial T} = D_2 \nabla^2 V(\mathbf{r},T) + \kappa f(U,V) - MV \ , \tag{2.2}$$

where $U(\mathbf{r},T)$ and $V(\mathbf{r},T)$ are the prey and predator population densities at time T and position $\mathbf{r} = (X,Y)$. D_1 and D_2 are the corresponding diffusion coefficients and κ is the food utilisation coefficient. The function $F(U)$ describes growth of the prey population, whilst $f(U,V)$ is the term describing predation and M is the predator mortality rate. The particular choice of functions $F(U)$ and $f(U,V)$ may vary depending on the species properties. In our case we choose a Holling type II trophical response with the following parametrisation (*Petrovskii et al. 2005a, b*) for the function $f(U,V)$:

$$f(U,V) = \frac{AUV}{U+B} \ , \tag{2.3}$$

where A stands for the predation intensity and B is the half-saturation prey density. As evidence suggests (*Liebhold and Bascompte 2003, Sharov et al. 1995, Whitmire and Tobin 2006*), gypsy moth population dynamics are affected by a strong Allee effect, hence $F(U)$ is chosen accordingly:

$$F(U) = \left(\frac{4\eta}{(K-U_0)^2} \right) U(U-U_0)(K-U) \ , \tag{2.4}$$

(cf. *Lewis and Kareiva 1993*) where K is the carrying capacity of the susceptible population, η is the maximum per capita growth rate and U_0 is the Allee threshold. For $0 < U_0 < K$ the Allee effect is strong, for $-K < U_0 < 0$ the Allee effect is weak, and in the case of $U_0 \leq -K$ the Allee effect is absent.

An inherent property of diffusion-reaction systems is the existence of travelling waves that have a clear biological meaning and a broad variety of biological applications (e.g. see a recent review by *Volpert and Petrovskii 2009*). Particularly in biological invasions, the rate of spread of invasive species appears to be in good agreement with the predicted speed of travelling fronts (*Shigesada and Kawasaki 1997*). However, a common prejudice against diffusion-reaction equations as a model of biological invasion is that they are thought to predict a continuous propagating front with a homogeneous population distribution in the wake, which is often at odds with observations (e.g. see Fig. 2.1). This prejudice was partially dispelled by *Sherratt et al. (1995)* who showed that, when affected by predators or pathogens, the spread of invasive species can be followed by chaotic spatiotemporal pattern formation in the wake of the travelling front. Yet a clear continuous population front boundary separating invaded from non-invaded areas had still been regarded as an immanent factor of diffusion-reaction equations. This is obviously not the case of gypsy moth spread; this apparent disagreement brings forward the question whether diffusion-reaction equations make an adequate model after all. However, a new property of diffusion-reaction systems known as "patchy invasion" has been discovered in *Petrovskii et al. (2002)*, provided the population growth rate is affected by a strong Allee effect. The corresponding scenario describes the spread of invasive species through the dynamical formation and irregular movement of separate population patches (*Petrovskii et al. 2005, Morozov et al. 2006*) not linked to the propagation of a continuous population front. In what follows, we examine the model's dynamics and show that the simulated patchy distribution is qualitatively similar to what is observed in gypsy moth populations.

In order to simplify numerical calculations, we scale the model to dimensionless variables (*Petrovskii et al. 2005a, b*):

$$\frac{\partial u(x,y,t)}{\partial t} = \left(\frac{\partial^2 u}{\partial x^2} + \frac{\partial^2 u}{\partial y^2}\right) + \gamma u(u-b)(1-u) - \frac{uv}{1+\lambda u} , \qquad (2.5)$$

$$\frac{\partial v(x,y,t)}{\partial t} = \epsilon\left(\frac{\partial^2 v}{\partial x^2} + \frac{\partial^2 v}{\partial y^2}\right) + \frac{uv}{1+\lambda u} - \mu v , \qquad (2.6)$$

where $u = U/K$, $v = V/K$, $a = A\kappa K/B$, $x = X(a/D_1)^{1/2}$, $y = Y(a/D_1)^{1/2}$, $t = aT$, $\lambda = K/B$, $b = U_0/K$, $\gamma = 4\nu BK/(A\kappa(K-U_0)^2)$, $\mu = M/a$ and $\epsilon = D_2/D_1$. The domain of the system (2.5 2.6) is square-shaped, such that $0 < x, y < L$, with no-flux boundary conditions used at the domain boundaries.

For the initial conditions, we consider functions of compact support:

$$u(x, y, 0) = u_0 \; if \; x_{11} < x < x_{12} \; and \; y_{11} < y < y_{12} \; otherwise \; u(x, y, 0) = 0 \;, (2.7)$$

$$v(x, y, 0) = v_0 \; if \; x_{21} < x < x_{22} \; and \; y_{21} < y < y_{22} \; otherwise \; v(x, y, 0) = 0 \;, (2.8)$$

where u_0 and v_0 are the initial prey and predator densities, and parameters x_{ij} and y_{ij} $(i, j = 1, 2)$ determine the initially occupied area. These initial conditions are an obvious simplification of species distribution, as in nature the initial distribution of species can be, and often is, more complex. However, *Petrovskii et al. (2005)* have shown that this does not pose a drawback since system dynamics depend more on the radius of the initially occupied domain, than on the particular population density profile.

We investigate the system (2.5 –2.6) of two nonlinear PDEs through extensive computer simulations. The equations were solved by forward finite-differences (see Appendix A), with mesh steps $\Delta x = \Delta y = 1$ and $\Delta t = 0.1$. The domain size was chosen to be sufficiently large throughout simulations (indicated in figure captions), therefore minimising the impact of boundaries, and mesh step sizes were tested to provide a good approximation. We assume that $\epsilon = 1$. In order to discover and define the succession of regimes of the system's dynamics, over two hundred simulations were run. The nondimensional predator mortality, μ, is considered as a controlling parameter, along with the prey growth rate γ. All other parameters were kept constant throughout simulations: $\lambda = 0.1$, $b = 0.2$, $u_0 = 1$, $v_0 = 0.5$, $x_{11} = y_{11} = 390$, $x_{12} = y_{12} = 410$, $x_{21} = y_{21} = 395$, $x_{22} = y_{22} = 405$, $u_0 = 1$ and $v_0 = 0.5$. The system's response to the change in μ or γ resulted in a distinct succession of different dynamical scenarios, which are shown in the parameter plane map (γ, μ), see Figure 2.2.

Examples of particular scenarios are shown in Figs. 2.3 and 2.4 with more details provided in the text below. Dynamics of predator and prey populations are qualitatively similar, thus for the sake of brevity simulation results are shown for the prey population only.

For sufficiently large values of the dimensionless predator mortality, μ, spread of gypsy moth populations occurs through the propagation of continuous circular travelling fronts. For a reduction in μ the propagation of continuous fronts ceases with spread occurring through the formation and interaction of separate patches; see Figs. 2.3 and 2.4. At any moment in time, the individual patches can split, interact and merge into new patches. The apparent symmetry observed in the
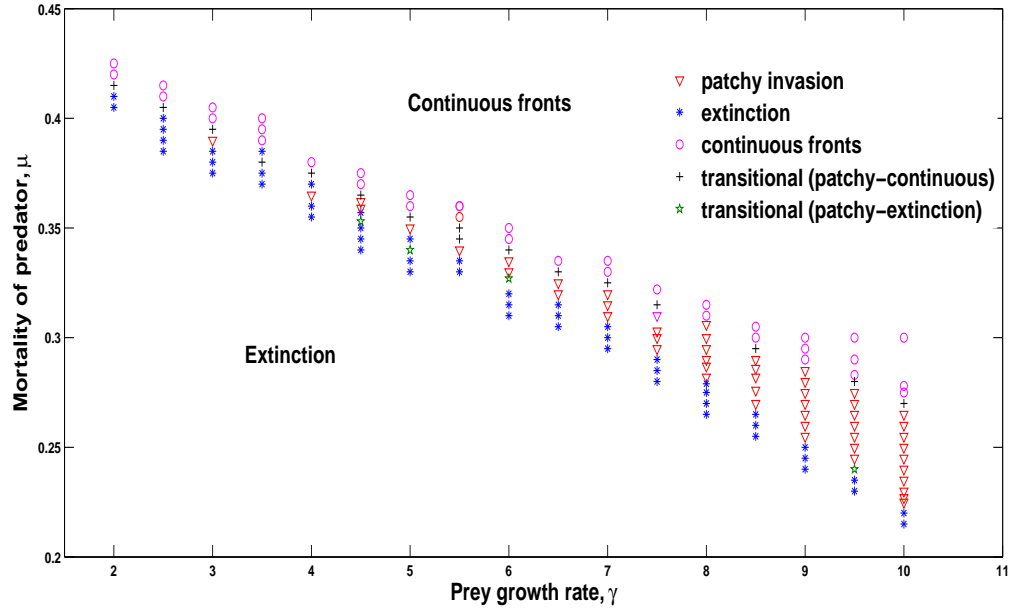
FIGURE 2.2: Plot of dimensionless mortality of predator population against local growth rate of prey population. Different scenarios are indicated by the figure legend.

spatial pattern is the consequence of the chosen (symmetric) initial conditions. This regime shift from continuous to patchy dynamics does not occur abruptly as in many cases there is a transitional region, in which invasion at an early stage is patchy, but at later stages becomes continuous. A similar scenario is observed in the SI model also, see subsection 2.6.2. With an increase in the prey population growth rate, γ, the patchy region becomes more prominent and is observed for a wider range of μ. However, for small values of γ, the range for patchy invasion becomes very narrow and is difficult to locate (e.g. for $\gamma = 2$, 2.5 and 3.5 we could not find it at all).

For a fixed γ, a further decrease in μ leads to patchy invasion alternating with extinction, shown as 'transitional patchy to extinction' in Fig. 2.2. For an even smaller μ the population goes extinct. This succession of dynamical scenarios, following a decrease in μ is biologically well-founded. Recalling the scaling of the model, the dimensionless predator mortality is directly proportional to the actual predator mortality. Therefore, lower values of μ correspond to a stronger predator able to bring down its prey and exerting more pressure on the prey population, leading to a patchy distribution of gypsy moth populations.

The patchy spread of gypsy moth populations is usually attributed to the effect of
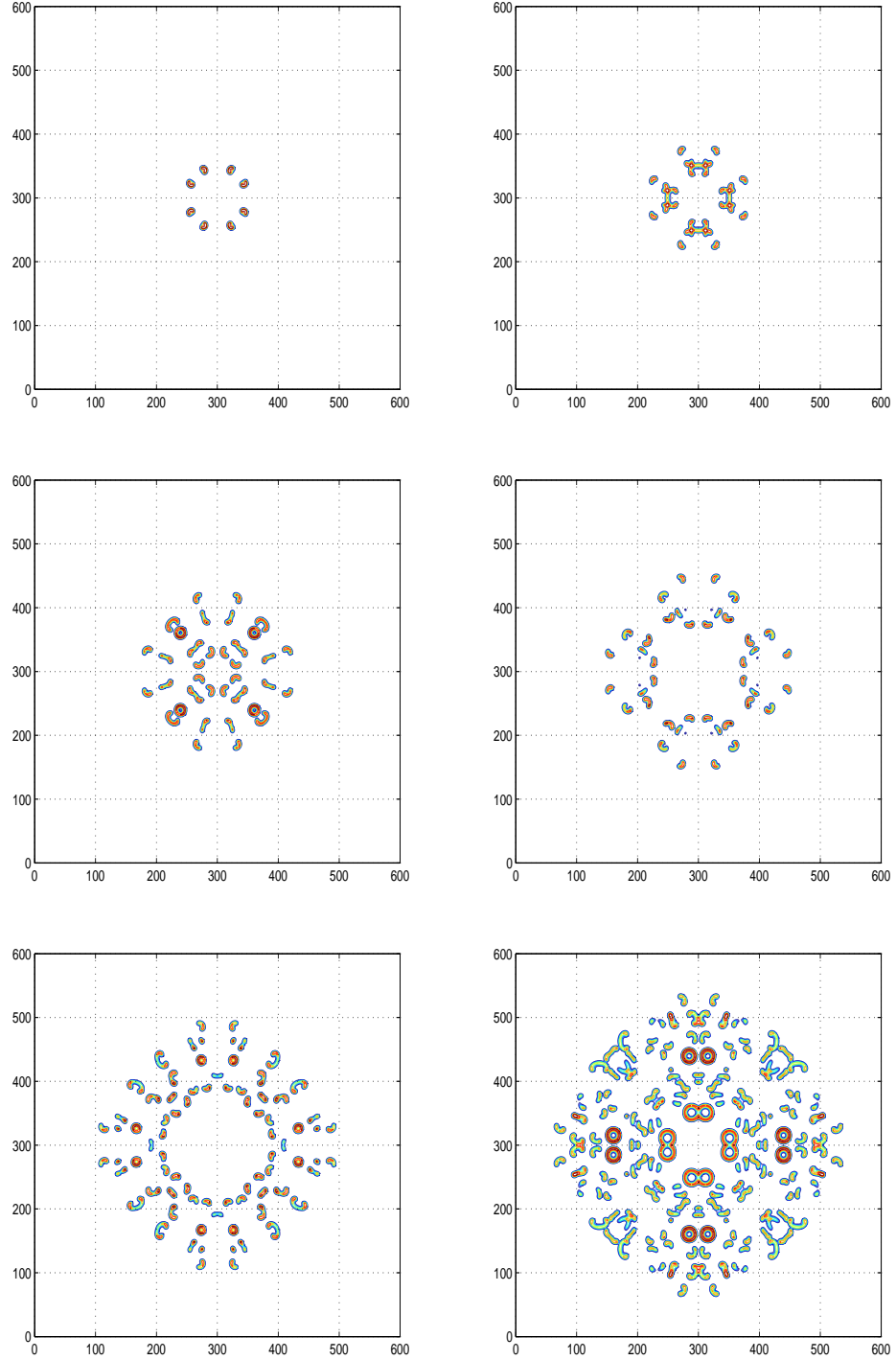
FIGURE 2.3: Patchy invasion in prey predator model. Snapshots show prey density at $t = 100$, $t = 200$, $t = 350$, $t = 450$, $t = 600$ and $t = 750$, with the parameter set: $\gamma = 5$, $\mu = 0.347$ and $L = 600$.

artificial, human assisted dispersal. However, we have shown that purely natural factors such as prey-predator interactions coupled with the Allee effect can produce qualitatively similar patterns to the observed gypsy moth distribution. Be that
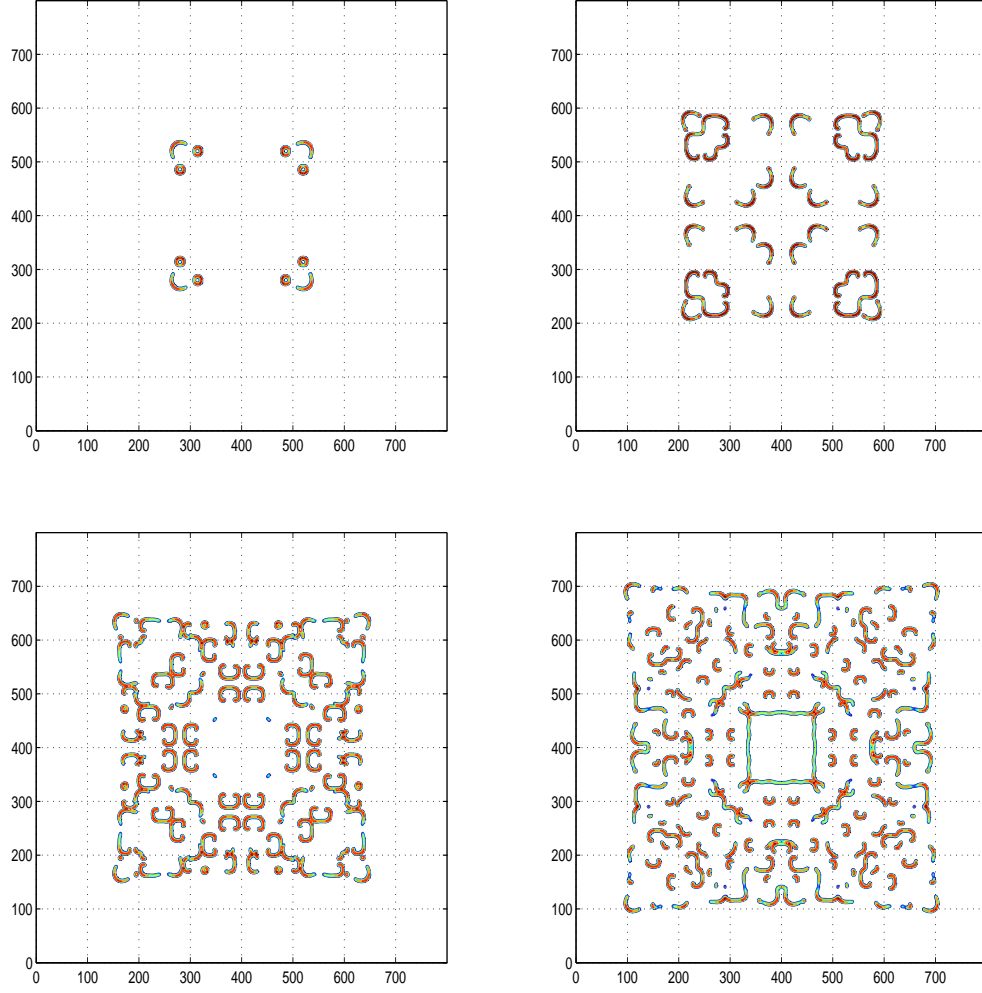
FIGURE 2.4: Patchy invasion in prey predator model. Snapshots show prey density at $t = 200$, $t = 300$, $t = 400$ and $t = 500$, with the parameter set: $\gamma = 8$, $\mu = 0.292$ and $L = 800$.

as it may, predation is a significant regulatory mechanisms only in low density populations, thus in the following sections we explore an alternative hypothesis to model high density gypsy moth populations. As these populations incur the most damage, and largely influence the spread of gypsy moth we also calculate the rate of spread of such populations.

2.6.2 Susceptible-Infected (SI) Model

The naturally occurring viral infection – nuclear polyhedrosis virus (NPV) is one of the main controlling factors of high density gypsy moth populations, and with
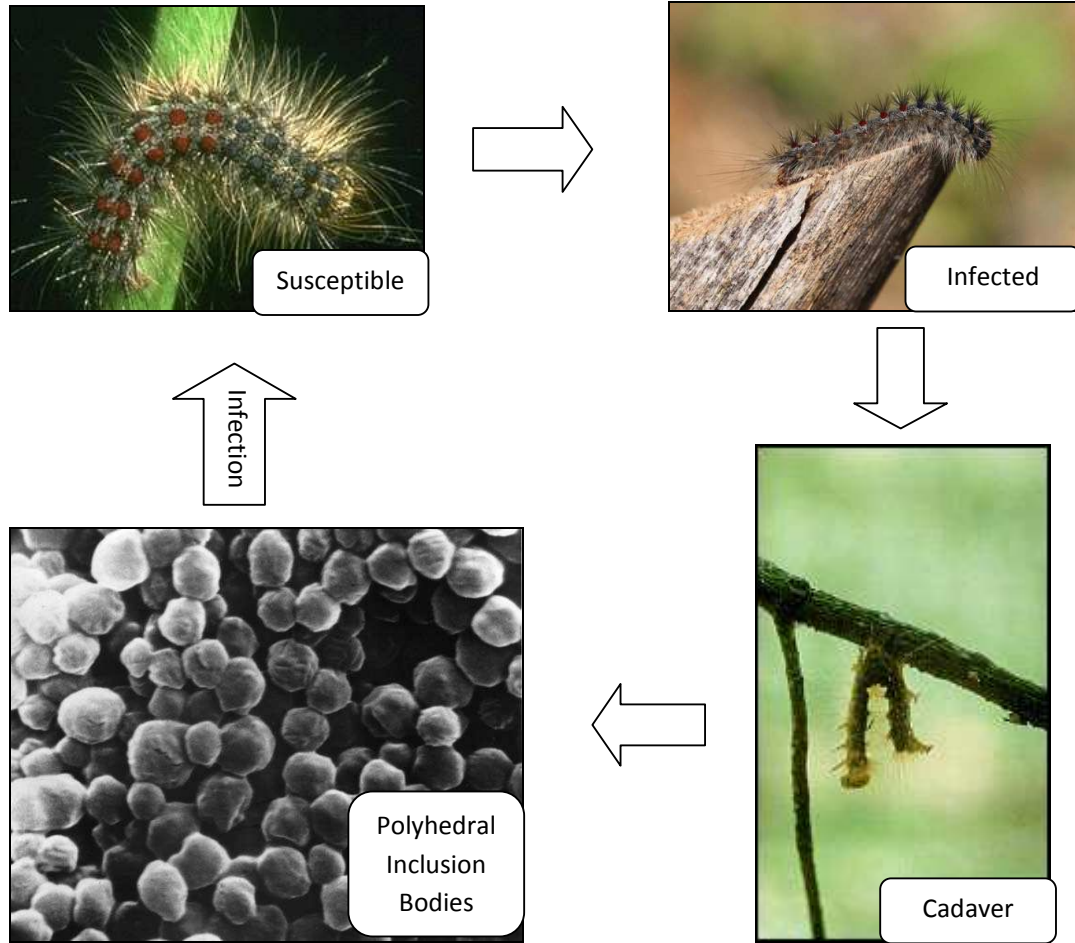
FIGURE 2.5: A sketch of the infection occurrence between the gypsy moth and nuclear polyhedrosis virus. Arrows indicate the transition between different stages of the infection occurrence cycle. For more details see section 2.5.1.

recovery from NPV being extremely rare, the SI model seems to be an appropriate framework. Note that the classical SI model assumes that disease transmission occurs in direct contact between susceptible and infected individuals (see Chapter 1). However, gypsy moths become infected with NPV through contact with occlusion bodies resulting from the rupture of cadavers, rather than from direct contact with infected individuals. Therefore, for our purposes, we indirectly treat infected individuals as infective particles, i.e. NPV occlusion bodies. Since the aim of this work is to improve the understanding rather than develop a predictive model, we neglect the second wave of mortality and focus on larvae infection through consumption of contaminated foliage. Correspondingly, the infection cycle begins with infected individuals and evolves to infection of susceptible population through consumption of occlusion bodies, hence enabling us to retain the form of the SI model over the whole infection cycle (see Fig. 2.5).

As above, wind dispersal is treated as diffusion, therefore our model becomes a reaction-diffusion system:

$$\frac{\partial S(\mathbf{R},T)}{\partial T} = D_1 \nabla^2 S(\mathbf{R},T) + P(S) - E(S,I) \ , \qquad (2.9)$$

$$\frac{\partial I(\mathbf{R},T)}{\partial T} = D_2 \nabla^2 I(\mathbf{R},T) + E(S,I) - MI \ , \qquad (2.10)$$

where $S(\mathbf{R},T)$ and $I(\mathbf{R},T)$ are the densities of susceptible and infected populations, $\mathbf{R} = (X,Y)$ is the position in space, T is time, and D_1 and D_2 are diffusion coefficients of susceptible and infected populations, respectively. We neglect long-distance (human-assisted) dispersal and assume that short-distance (wind-assisted) dispersal can be mathematically regarded as diffusion and described with the usual diffusion terms. Since both susceptible and infected larvae (including viral occlusion bodies) disperse with the wind, we consider $D_1 = D_2 = D$. The function $E(S,I)$ describes disease transmission and parameter M accounts for the mortality rate of infected individuals. $P(S)$ describes the local population growth; note that, since NPV is a terminal disease for gypsy moth, infected individuals do not contribute to the growth rate. Gypsy moth population's growth rate is damped by the strong Allee effect, hence $P(S)$ is chosen, as previously, accordingly:

$$P(S) = \left(\frac{4\eta}{(K - S_0)^2} \right) S(S - S_0)(K - S) \ . \qquad (2.11)$$

As for the transmission function E, based on available evidence (*Elkinton et al. 1995,Dwyer and Elkinton 1993, Barlow et al. 2000*), we consider it in the form of the mass-action law:

$$E(S,I) = ASI, \qquad (2.12)$$

where A is the rate of infection transmission.

Note that the biological literature tends to consider differently the dynamics of high-density populations where the impact of NPV is thought to be important but the Allee effect does not apply and the dynamics of low-density, e.g. newly-invaded populations where the Allee effect plays a crucial role but the effect of NPV is less important. Interestingly, the diffusion-reaction modelling framework predicts that those two apparently different cases in fact cannot be separated. Contrary to the case of the population growth without Allee effect where the speed of the propagating front is fully determined by the system's properties in the low density

range, in the presence of the strong Allee effect the speed of the travelling front is determined by the dynamics of the high density population behind the front (cf. "pulled" and "pushed" travelling fronts, e.g. *Lewis and Kareiva 1993*).

We also want to mention that at low population densities stochasticity becomes important. In particular, extinction of new colonies can be attributed to the effects of environmental and, possibly, demographic stochasticity. A question therefore may arise as to whether the deterministic diffusion-reaction framework is relevant. However, here we recall that diffusion-reaction equations only claim to describe the population dynamics 'on average', i.e. implicitly assuming averaging over many stochastic realisations (*Turchin 1988, Renshaw 1991, Okubo and Levin 2001*). The link between the two mathematical frameworks can be easily established; in particular, it means that the stronger the Allee effect in Eqs. (2.9) and (2.10), the less is the probability for the survival of a new colony in the corresponding probabilistic system. In that capacity, diffusion-reaction equations are applicable to low population densities as well as to high ones. In what follows we give an overview of the model properties and show that the parameter values corresponding to gypsy moth population dynamics and dispersal correspond well to the parameter range of the diffusive SI system where patchy invasion occurs.

For convenience (e.g. in order to decrease the number of parameters, thereby simplifying numerical simulations), we scale the SI model (2.9–2.12) to dimensionless variables:

$$\frac{\partial s(x,y,t)}{\partial t} = \left(\frac{\partial^2 s}{\partial x^2} + \frac{\partial^2 s}{\partial y^2} \right) + \gamma s \left(s - \beta \right) \left(1 - s \right) - si \ , \qquad (2.13)$$

$$\frac{\partial i(x,y,t)}{\partial t} = \left(\frac{\partial^2 i}{\partial x^2} + \frac{\partial^2 i}{\partial y^2} \right) + si - mi \qquad (2.14)$$

where $s = S/K$, $i = I/K$, $a = AK$, $x = X(a/D)^{1/2}$, $y = Y(a/D)^{1/2}$, $t = aT$, $\beta = S_0/K$, $\gamma = 4\eta K / \left(A(K - S_0)^2 \right)$, $m = M/a$. The system (2.13–2.14) is considered in a square domain of size L so that $0 < x, y < L$. At the domain boundaries, no-flux boundary conditions are used.

For the initial conditions, the population is considered to be homogeneously distributed at its carrying capacity within a square area of size ψ placed at the center of the domain, so that

$$s + i = 1 \ \ \text{for} \ \left| x - \frac{L}{2} \right| < \psi \ \text{and} \ \left| y - \frac{L}{2} \right| < \psi, \ \ \text{and} \ s + i = 0 \ \text{otherwise}, \ (2.15)$$

where $0 < \psi < L/2$. This initial population is assumed to largely consist of susceptibles, so that the infected individuals are concentrated in a smaller square-shaped domain inside:

$$i(x,y,0) = \kappa \text{ for } \left| x - \frac{L}{2} \right| < \omega \text{ and } \left| y - \frac{L}{2} \right| < \omega \text{ and } i(x,y,0) = 0 \text{ otherwise,}$$

where $0 < \omega < \psi$ and $\kappa \leq 1$.

Since a 2D system of two nonlinear PDEs can rarely be studied analytically, our primary analysis of the system (2.13–2.14) is through extensive computer simulations. For numerical approximation we used the explicit forward Euler scheme with mesh steps $\Delta t = 0.1$ and $\Delta x = \Delta y = 1$. It was checked that these values are sufficiently small to provide good approximation and to avoid numerical artifacts. Also, the domain size L was set to be large enough in order to minimise the impact of boundaries during simulation time ($L = 600$).

We consider the dimensionless mortality m of infected individuals and the growth rate γ of susceptible individuals as the controlling parameters and keep all other parameters constant. The simulation results shown below were obtained for $\beta = 0.2$, $\psi = 10$, $\omega = 5$ and $\kappa = 0.5$. The system exhibits, as a response to changes in m or γ, a distinct succession of invasion scenarios including patchy invasion,
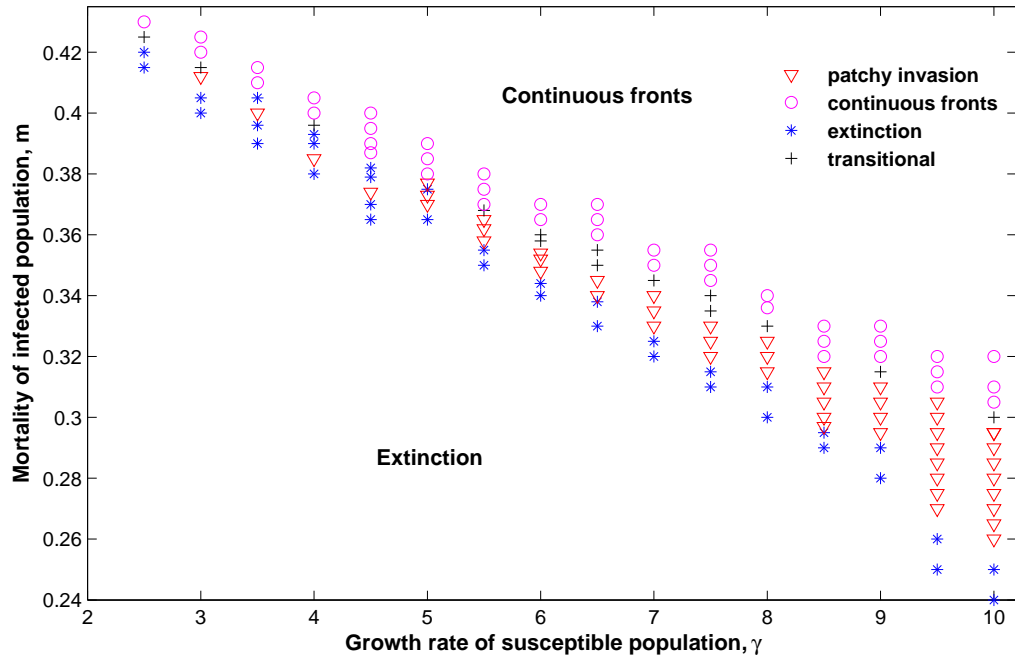
FIGURE 2.6: Map of different invasion scenarios as explained by the figure legend.
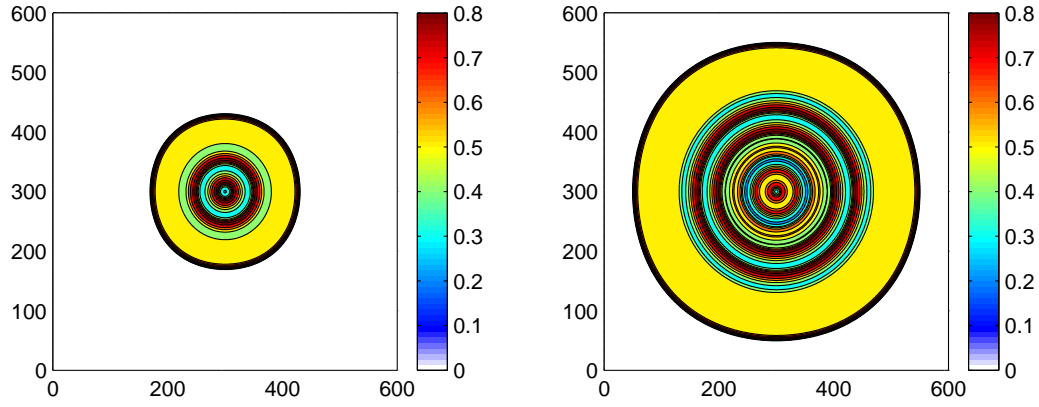
FIGURE 2.7: Snapshots of the susceptible population density taken at times $t = 200$ (left) and $t = 400$ (right). Propagation occurs through circular expanding fronts. Parameters are $\gamma = 3$ and $m = 0.57$.

propagation through continuous population fronts and extinction. The results are summarised as a map in the parameter plane (γ, m), see Fig. 2.6, where different symbols correspond to different scenarios.

Examples of different scenarios are shown in Figs. 2.7–2.11 and commented in the text below. As the dynamics are qualitatively similar for the infected and susceptible populations, for the sake of brevity simulation results are shown for the susceptible population only.

For all checked values of γ in the range from $\gamma = 2.5$ to $\gamma = 10$, for sufficiently large values of mortality m population spread occurs through propagation of continuous travelling fronts. While for small values of γ the front always has the intuitively expected circular shape (Fig. 2.7), an increase in γ may result in fronts of a more exotic shape, e.g. butterfly-like (Fig. 2.8). For a given γ, the shape eventually turns back to circular with an increase in m. If, on the contrary, m decreases,
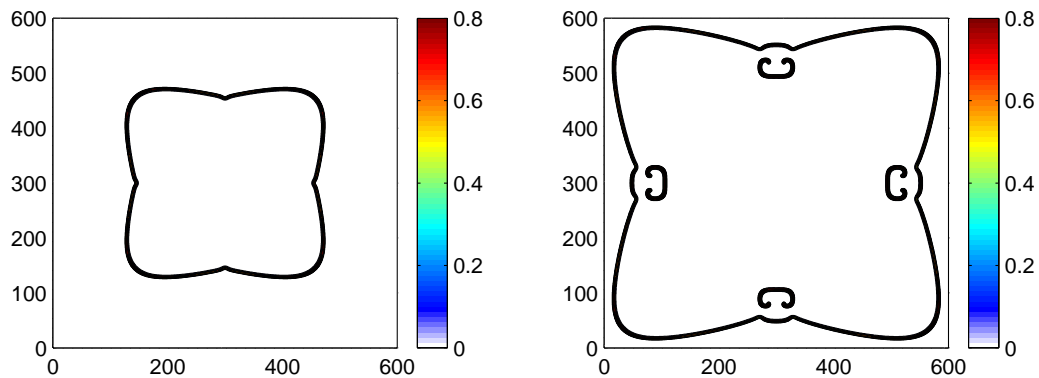
FIGURE 2.8: Snapshots of susceptible population taken at times $t = 200$ (left) and $t = 350$ (right). Parameters are $\gamma = 9.5$ and $m = 0.31$. Invasion occurs through the propagation of fronts of non-circular 'butterfly-like' shape.

the irregularity of the front shape increases sharply, promptly resulting in the front discontinuity and patchy invasion; see Fig. 2.9. In this case, a continuous propagating front does not exist and invasion takes place through the formation and dynamics of separate patches. We mention here that the apparent symmetry of the spatial pattern shown in Fig. 2.9 is a consequence of the symmetric initial conditions (2.15–2.16). For asymmetric initial conditions (e.g. for non-concentric initial domains) the emerging patchy structure would hardly bear any trace of symmetry (*Petrovskii et al. 2002, 2005, Morozov et al. 2006*); see also Section 2.8.

The change from invasion through propagating continuous front to patchy invasion does not happen abruptly, though. With a decrease in m, the system's dynamics go through a transitional scenario when the spread is predominantly patchy at an early stage of invasion, say for $t \leq t_*$, but can turn into the continuous-front spread at later time (for $t > t_*$); see Fig. 2.10. The duration t_* of the patchy spread is not known in advance; simulations show that it depends on parameter

FIGURE 2.9: Patchy invasion: snapshots of susceptible population density taken at times $t = 100$, $t = 400$, $t = 700$, and $t = 1000$ (left to right, top to bottom). Parameters are $\gamma = 4.5$ and $m = 0.375$. Note that the symmetry of the simulations can be easily broken (bottom right) due to the chaotic nature of the solution.

FIGURE 2.10: Transitional dynamics. Snapshots of susceptible population density at times $t = 100$, $t = 150$, $t = 400$ and $t = 600$ (left to right, top to bottom). Snapshots reveal the transitional dynamics when the patchy spread at an early stage of invasion (cf. the top row) turns into the continuous-front spread at later times (the bottom row). Parameters are $\gamma = 5$ and $m = 0.378$.

values and, for the parameter sets used in this study, varies between 100-300 (in dimensionless units).

With an increase in γ, patchy spread becomes even more distinct as the individual patches tend, on average, to become smaller and separated with wider empty areas, cf. Figs. 2.9 and 2.11. Also the range of values of m where patchy invasion is observed grows significantly for large γ; see the right-hand side of the diagram in Fig. 2.6. For small values of γ, the parameter range for patchy invasion shrinks and is difficult to locate. For $\gamma = 2.5$ we could not find it at all, although being based on simulation results only it is not possible to tell whether the parameter range disappears completely or just becomes very narrow.

Interestingly, for a given value of γ patchy invasion can alternate with extinction, e.g. see the diagram of Fig. 2.6 for $\gamma = 3.5$ and $\gamma = 4.5$.

By further decreasing mortality and surpassing the patchy region, extinction occurs inevitably. Note that this succession of invasion scenarios following a decrease
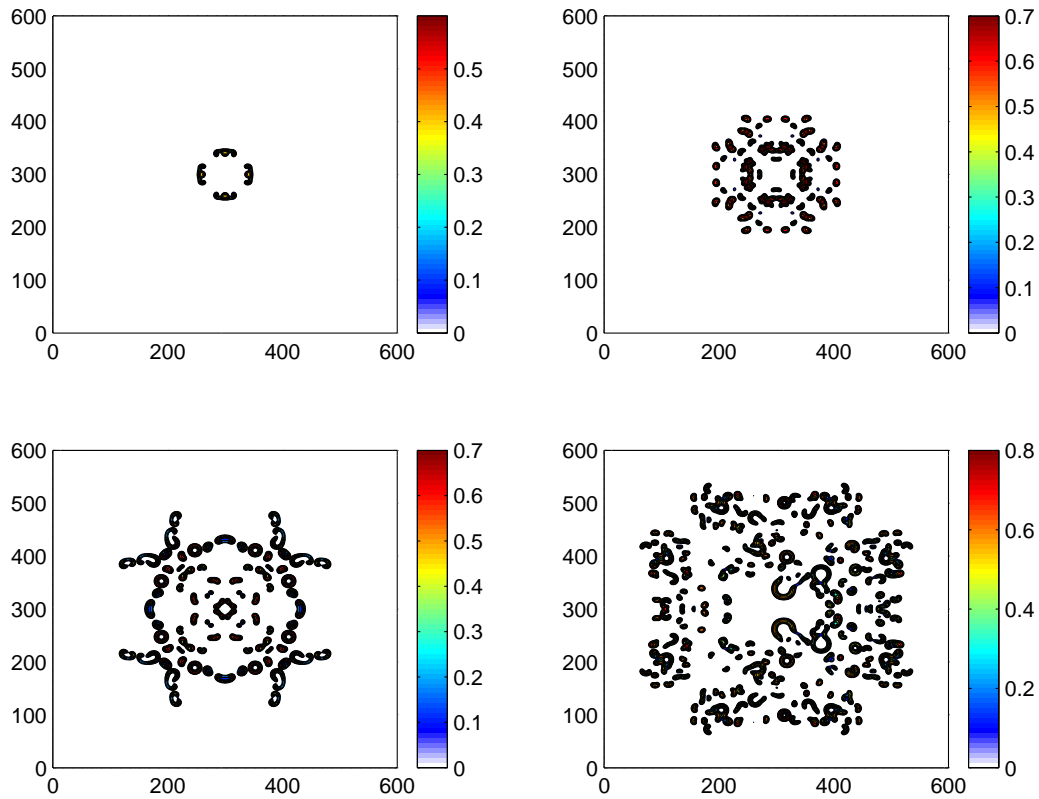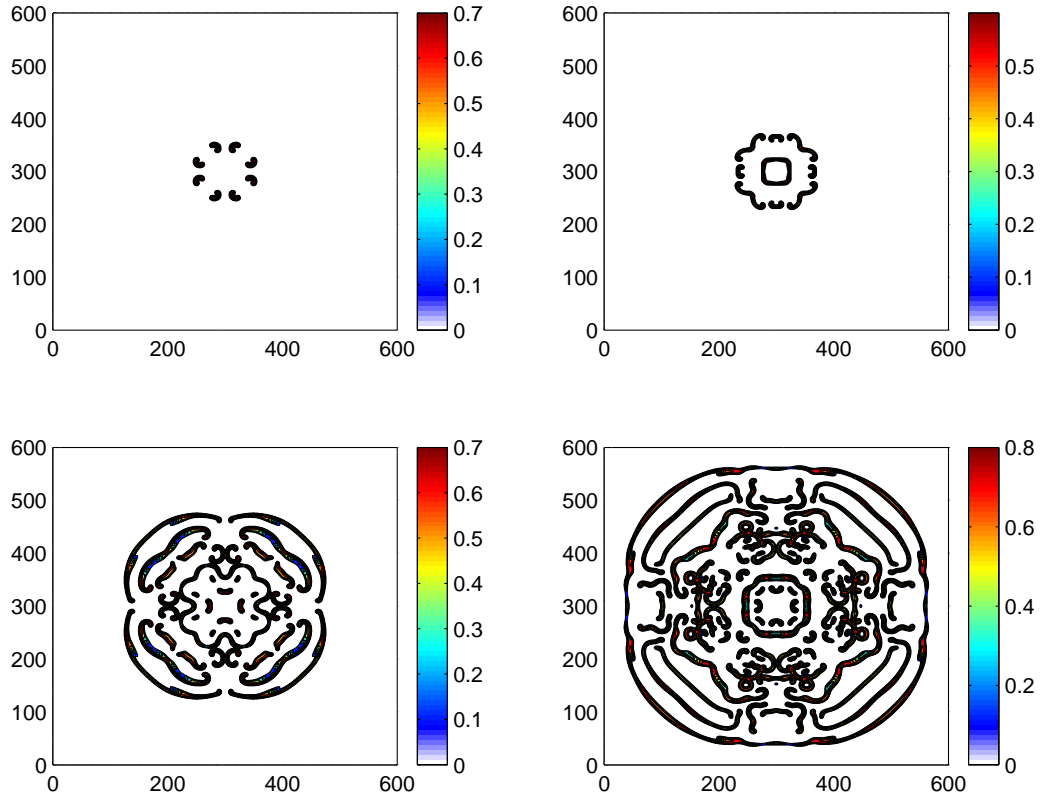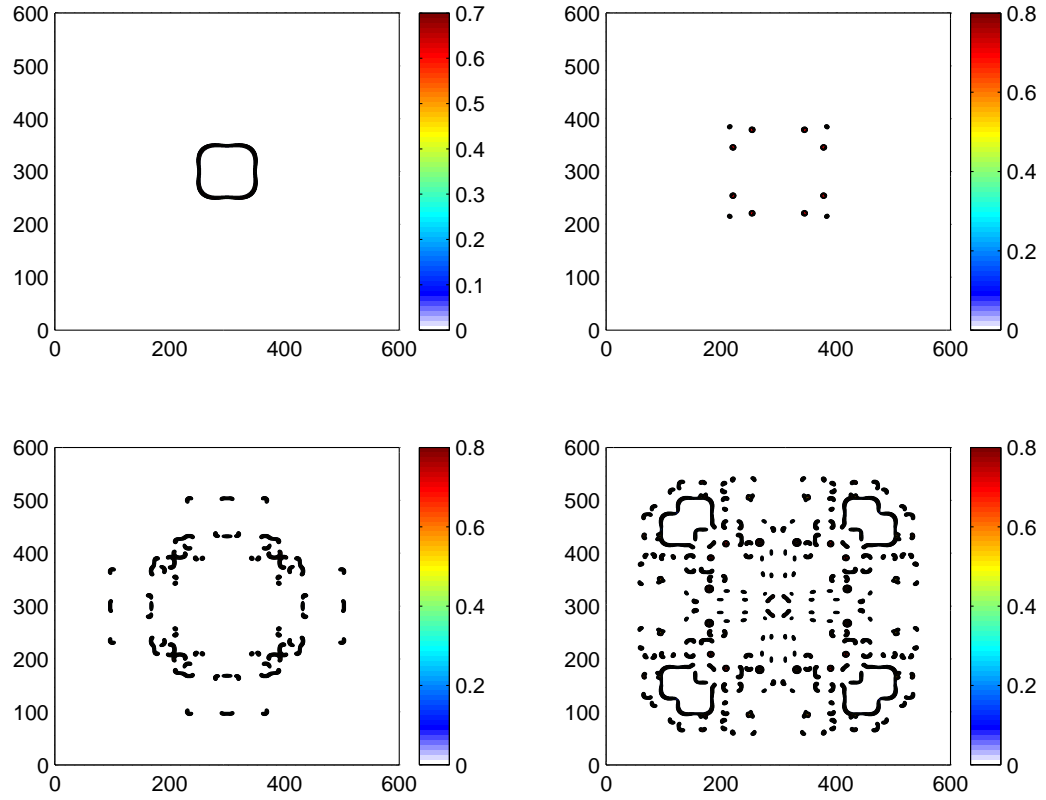
FIGURE 2.11: Patchy dynamics. Snapshots of susceptible population density at times $t = 50$, $t = 150$, $t = 450$, and $t = 700$ (left to right, top to bottom). The parameter set used: $\gamma = 8.5$ and $m = 0.298$.

in mortality m is consistent with biological arguments. Namely, the dimensionless mortality m yields the ratio of dimensional mortality of infected individuals M and the infection transmission rate A. An increase in the dimensionless mortality parameter m may therefore correspond to a disease with a lower transmission rate which puts less pressure on the species and allows the susceptible population to spread uninterrupted through expansion of population fronts. Lower values of mortality m would then correspond to a more severe disease with a higher transmission rate, which exerts more pressure on the species and hence may bring it to the brink of extinction.

2.7 Parameter estimation and the rate of spread

In the previous section, we showed that the invasion pattern predicted by the spatial SI model is qualitatively similar to what is seen in field observations (e.g. compare Fig. 2.1 with Figs. 2.9 and 2.11), that is, exhibiting patchy spread without

any continuous population front. Now our goal is to reveal whether the rate of spread observed in simulations is in agreement with field data.

For this purpose, we first recall the relation between the dimensionless and dimensional variables. As $x = X(a/D)^{0.5}$ and $t = aT$ where $a = AK$ (see the text after Eqs. (2.13–2.14)), we obtain the following expression for the rate of spread:

$$\frac{\Delta X}{\Delta T} = \frac{\delta x}{\delta t} \cdot \sqrt{ADK} \; , \tag{2.16}$$

where $\delta x/\delta t$ presents the dimensionless rate of spread obtained from simulations and $\sqrt{ADK}$ is the scaling factor with the dimension of speed.

The next step is to understand what is the biologically relevant range for parameter values. This appears to be a difficult task. Close inspection of available literature sources reveals that different studies often give very different estimates, sometimes varying over two orders of magnitude; see Table 2.1.

We begin with the disease transmission rate A. As mentioned earlier, in our model the transmission parameter is scaled to the number N of PIBs (polyhedral inclusion bodies; see subsection 2.5.1) produced per larval cadaver, so that $A = A_1 N$ where A_1 is the transmission rate per PIB. With maturation of gypsy moth larvae, NPV yield increases. It is generally accepted that first instars produce the least amount of NPV, whilst pathogen production increases with larval age and size at the time of death. *Shapiro (1981)* estimated the number of PIBs per gypsy moth cadaver as $N = 4.0 \cdot 10^8$ per small larva, and $N = 3.0 \cdot 10^9$ per large larva. According to data from *Dwyer and Elkinton (1993)*, fourth instar larvae are estimated to produce $N = 2 \cdot 10^9$ virus particles per cadaver. However, studies on a similar species, Douglas fir tussock moth *Orgyia pseudotsugata*, indicate a smaller order of magnitude of PIB production, i.e. $N = 10^7$ PIB/larva (*Dwyer 1991*), $N = 10^7$ PIB/early instar larva and $N = 4 \cdot 10^8$ PIB/late instar larva (*Vezina and Peterman 1985*). As our model does not distinguish larval instars, we describe the release of polyhedral virus particles by their average number. Indeed, despite the apparent fluctuation in PIB production rates, *Barlow et al. (2000)* obtained promising modelling results under the assumption of a constant rate of virus particle production as $N = 2 \cdot 10^9$ PIB/larva.

The estimates for A_1 range from $1.7 \cdot 10^{-12}$ to $1.45 \cdot 10^{-10}$ m^2/day per PIB (*Barlow et al. 2000, Elkinton et al. 1995, 1996, Dwyer and Elkinton 1993*). Studies largely relied on the extrapolation of collected small scale or laboratory data to field scale.

TABLE 2.1: Summary of parameter estimates. Estimates for the transmission coefficient are given in m^2/PIB day units.

Parameter	Species	Parameter Estimate	Reference
Transmission coefficient, A_1	Lymantria dispar	1.7×10^{-12}	Barlow et al. (2000)
	Orgyia pseudotsata	$0.01 - 6.82 \times 10^{-9}$	Dwyer (1991)
	Lymantria dispar	$2.12 - 13.1 \times 10^{-12}$	D'Amico et al. (1996)
	Lymantria dispar	1.45×10^{-12}	Dwyer and Elkinton (1993)
	Lymantria dispar	1.45×10^{-10}	Elkinton et al. (1995)
	Orgyia pseudotsata	1×10^{-9}	Vezina and Peterman (1985)
	Spodoptera exempta	$3.38 - 6.65 \times 10^{-12}$	Reeson et al. (2000)
	Mamestra brassicae	2.16×10^{-12}	Goulson et al. (1995)
Diffusion coefficient, D	Lymantria dispar	$0.003 \ km^2$/generation	Liebhold and Tobin (2006), Robinet et al. (2008)
	Battus philenor	$239 \ m^2$/day	Kareiva (1983)
	Lymantria dispar	0.1 ha/year ($0.274 \ m^2$/day)	Wilder et al. (1995)
	Orgyia pseudotsata	$0.0274 \ m^2$/day	Dwyer (1992)
	Lymantria dispar	332 m/generation	Liebhold et al. (1992)
Disease decay rate, M	NPV	$0.003 \ day^{-1}$	Barlow et al.(2000), Dwyer and Elkinton (1993)
	NPV	$0.002 \ day^{-1}$	Dwyer (1992)
	NPV	$4.8 \ year^{-1}$	Vezina and Peterman (1985)
Carrying capacity, K	Lymantria dispar	283 moth/trap	Tobin et al. (2007 a,b)
	Lymantria dispar	673 moth/trap	Tobin et al. (2007 a,b)
	Lymantria dispar	687 moth/trap	Johnson et al. (2006)
	Lymantria dispar	$200\,000$ egg masses/km^2	Sharov and Liebhold (1998)
	Lymantria dispar	500 larva/m^2	Dwyer et al. (1993)
Allee threshold, S_0	Lymantria dispar	2.2 moth/trap	Tobin et al. (2007b)
	Lymantria dispar	20.7 moth/trap	Tobin et al. (2007b)
	Lymantria dispar	17 moth/trap	Johnson et al. (2006)
	Lymantria dispar	106 male moth/colony	Liebhold and Bascompte (2003)
Number of virus particles produced per larval cadaver	Lymantria dispar	2×10^9	Barlow et al. (2000)
	Orgyia pseudotsata	10^7	Dwyer (1991)
	Lymantria dispar	2×10^9	Dwyer and Elkinton (1993)
	Lymantria dispar	4×10^8	Elkinton et al. (1995)
	Orgyia pseudotsata	$1 \times 10^7 - 4 \times 10^8$	Vezina and Peterman (1985)

In order to ensure the plausibility of the estimate, comparison to NPV transmission rates in similar insect species was also undertaken involving species such as the cabbage moth *Mamestra brassicae*, the Douglas-fir tussock moth *Orgyia pseudotsugata* and the African armyworm *Spodoptera exempta*, all of which belong to the same *Lepidoptera* order, and a general consistency between the estimates was observed (*Vezina and Peterman 1985, Reeson et al. 2000, Goulson et al. 1995, Dwyer 1991*). In some studies, particularly in *Dwyer and Elkinton (1993)* and *Elkinton et al. (1995)*, the estimate of the transmission rate was made using different units such as foliage area instead of the ground area. However, the required conversion is minor (a median of $1.4m^2$ of foliage per $1m^2$ ground, see *Liebhold et al. 1989, Dwyer et al. 1997*) and hence is not expected to further increase the uncertainty.

The diffusion coefficient D acts as a measure of dispersal and is expressed in units of distance^2/time (*Kareiva 1983, Shigesada and Kawasaki 1997*). Since females are flightless, the primary mechanism of dispersal originates from windborne movement of first instar larvae hanging on silken threads. Attempts have been made to estimate distances covered through this passive mechanism by means of experimental release-recapture efforts (*Kareiva 1983, Mason and McManus 1981*). Unfortunately, the results found in literature are not fully consistent with each other. For instance, the value of $D = 0.003$ km^2/year $= 3 \cdot 10^3$ m^2/year was referred to by several authors (e.g. *Liebhold and Tobin 2006, Robinet et al. 2008*). Estimates of D for other related insect species, such as the Pinevine Swallowtail (*Battus philenor*), produced a somewhat larger value $D = 239$ m^2/day $\approx 10^4$ m^2/year (*Kareiva 1983*). *Wilder et al. (1995)* used the value $D = 1$ ha/year $= 10^4$ m^2/year for modelling gypsy moth spread and obtained reasonable results. However, *Liebhold et al. (1992)* estimated the diffusion coefficient of gypsy moth to be $D = 332$ m/generation, thus sparking an inconsistency in terms of the units.

With regard to the carrying capacity K and the Allee threshold S_0, they both have the meaning of density and hence should normally be measured in density units such as number of insects per unit area. In practice, the most extensive information on gypsy moth abundance is obtained and monitored by using pheromone baited traps. However, interpretation of trap counts in terms of the population density is a challenging and largely open issue [see *Petrovskii et al. (2012)* for a discussion of the problem]. For this reason, in the literature estimates of the gypsy moth carrying capacity and the Allee threshold density are often given in trap counts, i.e. in moths per trap.

Estimates of K and S_0 can be found in *Johnson et al. (2006)* and *Tobin et al. (2007b)*. Data were collected from spatially-referenced pheromone trap catches and used to generate a continuous interpolated surface of gypsy male moth abundance. Grids of 5×5 km cells encompassed states of Ohio, Illinois, Indiana, Virginia, West Virginia, North Carolina and Wisconsin. The estimated number of male moth counts per trap was extracted from the centre of the grid, for each year during the full period of the study (1996-2004).

The Allee threshold was defined as the lowest abundance at which a local population is likely to replace itself in the following year, below which the population is more likely to decrease and above which it is more likely to increase (*Tobin et al. 2007b, Johnson et al. 2006*). To deduce the Allee effect, pairs of counts per trap were compared in subsequent years. The carrying capacity was defined as the highest abundance at which the replacement probability decreases below 0.5 (*Tobin et al. 2007b*). Data for Ohio, Indiana and Illinois were inconclusive, due to low replacement rates, ergo no estimates were obtained. Allee threshold and carrying capacity in Wisconsin were estimated at 2.2 moths/trap and 283 moths/trap, respectively (*Tobin et al. 2007b*). A much higher value of the Allee threshold of 20.7 moths/trap was established in West Virginia, Virginia and North Carolina, with a carrying capacity of 673 moths/trap (*Tobin et al. 2007b*). *Johnson et al. (2006)* provided overall estimates as 17 moths/trap for the Allee threshold and 687 moths/trap for the carrying capacity.

In a similar study, having analysed pheromone trapping data from a large-scale field study in Washington, *Liebhold and Bascompte (2003)* estimated the Allee threshold as 106.7 moths/colony, which is much higher than the estimate by *Johnson et al. (2006)*.

In an earlier study (done on a much smaller spatial scale), *Dwyer and Elkinton (1993)* estimated the carrying capacity as 500 larvae/m^2. We mention here that this value is difficult to compare with the estimates mentioned above as it refers to a different life-stage. It seems to indicate a different order of magnitude for the carrying capacity. Indeed, the pheromone trap catchment area for the flying insects is known to be tens of square meters (*Yamanaka et al. 2003, Hicks and Blackshaw 2008*); therefore, the value of the carrying capacity at 687 moths/trap obtained by *Johnson et al. (2006)* gives a rough estimate of the population density as, at most, 20-30 moths/m^2. However, the latter is obviously inconsistent with

the estimate of the Allee threshold made by *Liebhold and Bascompte (2003)* or otherwise assumes a very low survival rate for larvae before they become moths.

Having the information about A, D and K at hand, we can now calculate the scaling factor in Eq. (2.16). Since all three parameters vary over a wide range, apparently, numerous combinations of parameter sets may be used. Therefore, here we only endeavour to give an illustrative example of possible range bounds. We choose $D = 3 \cdot 10^3$ m^2/year according to *Liebhold and Tobin (2006)*. Since disease transmission usually occurs during the larval stage, we use $K = 500$ larvae/m^2 according to *Dwyer and Elkinton (1993)*. For the average number of PIBs released by a larval cadaver, we accept the value $N = 2 \cdot 10^9$ as in *Barlow et al. (2000)*. Also, in our estimation we use a maximum length of the larval period as 10 weeks $= 70$ days (*Dwyer et al. 2000*). Correspondingly, for the lower and upper estimates of the transmission rate A_1, we obtain the following values of the scaling factor:

$$
\begin{aligned}
(\sqrt{ADK})_{min} &= \left[70 \cdot 1.7 \cdot 10^{-12} \text{ m}^2/(\text{PIB} \cdot \text{year}) \cdot 2 \cdot 10^9 \text{ PIB/larva} \right. \quad (2.17) \\
&\quad \left. \cdot 500 \text{ larva}/m^2 \ \cdot 3 \cdot 10^3 \ m^2/\text{year} \right]^{1/2} \approx 600 \text{ m/year} \\
&= 0.6 \text{ km/year},
\end{aligned}
$$

$$
\begin{aligned}
(\sqrt{ADK})_{max} &= \left[70 \cdot 1.45 \cdot 10^{-10} \text{ m}^2/(\text{PIB} \cdot \text{year}) \cdot 2 \cdot 10^9 \text{ PIB/larva} \right. \quad (2.18) \\
&\quad \left. \cdot 500 \text{ larva}/m^2 \ \cdot 3 \cdot 10^3 \ m^2/\text{year} \right]^{1/2} \approx 5500 \text{ m/year} \\
&= 5.5 \text{ km/year}.
\end{aligned}
$$

The next step is to estimate the parameters that determine the simulation results, i.e. β, γ and m. Based on the available range of estimates for the carrying capacity K and Allee threshold S_0, we accept the value $\beta = S_0/K = 0.2$.

Gypsy moth populations, as many insect species, may undergo fluctuations of several orders of magnitude. The estimation of per capita growth rate therefore involves considerable uncertainty. It is also often based on specific assumptions. Most gypsy moth studies assume exponential growth, the exponent being found to vary between $1.65 - 4.6$ per year, which results in the range of actual replacement rates η (see Eq. (2.11)) as $5 - 100$-fold increase in population density between two subsequent generations (*Liebhold and Tobin 2006, Liebhold et al. 1992, Sharov et al. 1995a, Sharov and Liebhold 1998*). Recall that $\gamma = 4\eta K \left[A(K - S_0)^2\right]^{-1} \approx 6.25\eta(AK)^{-1}$ where the scaling factor AK varies over two orders of magnitude, i.e. from 120 to 10^4; see Eqs. (2.17–2.18). Correspondingly, parameter γ can have any value from approximately 5 and down to 0.003. We however note that,

according to our model, for any given value of mortality a decrease in γ almost certainly results in population extinction; see Fig. 2.6. It may indicate that small values of γ are in fact not feasible[2]. We therefore restrict our attention to the values of γ on the order of one or larger.

Due to our interpretation of the SI model, it appears more appropriate to interpret the 'mortality rate' M as the rate of decay of PIBs (occlusion bodies), i.e. the virus particles. This issue was addressed in a few studies and a consistent estimate of $0.003 \; day^{-1}$ was obtained (*Dwyer and Elkinton 1993, Barlow et al. 2000, Elkinton et al. 1995*). This value is in agreement with studies on a similar species, the Douglas fir tussock moth (*Dwyer 1992*). It is readily seen that this estimate corresponds to the dimensionless decay rate of, at most, $m = M(AK)^{-1} \approx 0.01$. However, here we argue that this estimate should more likely be regarded as a lower bound of the decay rate rather than its actual value. The matter is that the above estimate only takes into account the effect on the virus particles produced by weather conditions (such as high/low temperature, sunlight etc.) but not the 'geometry' of the disease transmission. While the virus particles may still remain active inoculums for infection, they may be carried away by the wind or washed-out by the rain to places where they could not be accessed by larvae, thus making any contact between occlusion bodies and susceptible larvae impossible. The decay rate of the virus particles as used in our SI model should take the wash-out rates into account. Unfortunately, we are not aware of any study concerned with estimating the wash-out rates. Therefore, here we use it essentially as a tuning parameter which determines the type of spread; see Fig. 2.6. In particular, we choose the value(s) of m that corresponds to patchy spread.

In order to estimate the rate of spread, we now choose two different parameter sets, i.e. (a) $\gamma = 4.5$ and $m = 0.3755$ and (b) $\gamma = 8.5$ and $m = 0.98$. In case (a), the dimensionless spread rate $\delta x/\delta t \approx 0.3$ and in case (b) $\delta x/\delta t \approx 0.6$. For different values of the scaling factor, see Eqs. (2.17–2.18), we therefore obtain:

$$\left(\frac{\Delta X}{\Delta T}\right)^{(a)}_{min} = 0.18 \text{ km/year}, \qquad \left(\frac{\Delta X}{\Delta T}\right)^{(a)}_{max} = 1.65 \text{ km/year}, \quad (2.19)$$

$$\left(\frac{\Delta X}{\Delta T}\right)^{(b)}_{min} = 0.36 \text{ km/year}, \qquad \left(\frac{\Delta X}{\Delta T}\right)^{(b)}_{max} = 3.3 \text{ km/year}. \quad (2.20)$$

---

[2]or that for small γ our model is inappropriate.

The range of gypsy moth spread rates observed in nature is known to vary from about 2.5 to almost 29 km/year (*Liebhold et al. 1992, Tobin et al. 2007a*). It is readily seen that our theoretical estimate has an overlap with this empirical range. The impact of pathogens and wind dispersal, that are essential components of our model, are thus capable of explaining the lower values of the observed rates of gypsy moth spread, which we regard as a success of our approach.

2.8   Discussion and Concluding remarks

In this study, we tried to identify the factors that control the spatial pattern and the rate of spread of the gypsy moth population in North America. By now, a common tendency has been to relate the peculiarities of gypsy moth invasion to human-assisted dispersal (*Elkinton and Liebhold 1990, Tobin and Blackburn 2008*). However, we argue that this point of view disagrees to some extent with the proved existence of the strong Allee effect in gypsy moth populations (*Vercken et al. 2011*), which is known to usually wipe out small new colonies (*Liebhold and Bascompte 2003*). Correspondingly, here our goal is to check whether natural factors such as wind dispersal and impact of predators or pathogens might be sufficient to explain, at least partially, the features of the gypsy moth spread.

Our approach is based on mathematical modelling and computer simulations. Depending on the density of gypsy moth populations the dynamics of gypsy moth is known to be strongly affected by either predation or the nuclear polyhedrosis virus (NPV). Correspondingly, we have used spatially explicit predator-prey and SI models of reaction-diffusion type where dispersal is thus described by the standard diffusion term. We then performed extensive computer simulations and found that, within a certain parameter range, both models exhibit a pattern of spread surprisingly similar to what is seen in field observations, i.e. a distinct patchy spatial structure. Note that the patchy pattern obtained in simulations is completely self-organised, it is not related to any pre-defined heterogeneity and it does not require any asymmetry in the initial conditions. We have checked in simulations (see Fig. 2.12) that use of asymmetric initial conditions does not affect the patchy spread as such but breaks the symmetry of the emerging patchy structure, hence making it look 'more realistic.'

In order to choose biologically relevant parameter values to evaluate the spread rate of high density gypsy moth populations we made an extensive literature search.
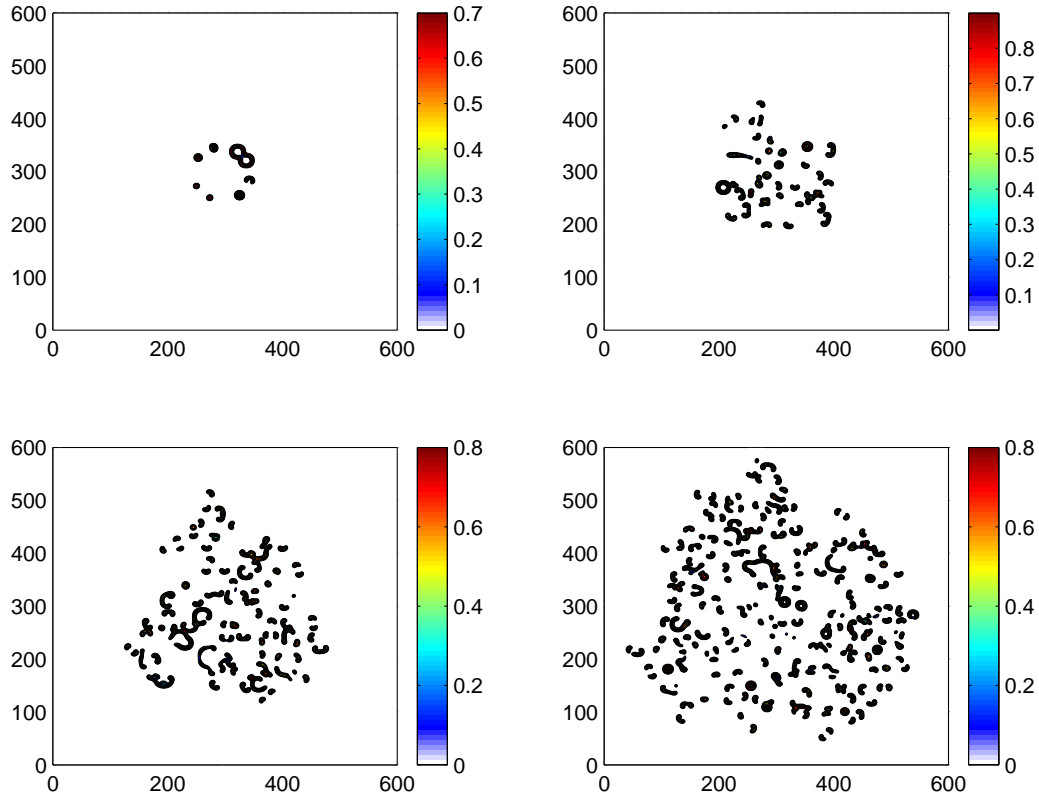
FIGURE 2.12: Patchy invasion simulated with slightly asymmetric initial conditions. Snapshots of susceptible population density at times $t = 100$, $t = 400$, $t = 700$ and $t = 1000$ (left to right, top to bottom). The parameter set used: $\gamma = 6$ and $m = 0.348$.

The search revealed a considerable amount of uncertainty (and sometimes even inconsistency) in parameter estimation made in different studies; see Table 2.1. We then showed that the parameter values that we used in numerical simulations of the epidemiological model were generally in agreement with the estimated parameter range. Based on the parameter values taken from the literature, we showed that the rates of gypsy moth spread predicted by our SI model are in very good agreement with the lower range of the rates of spread observed in field data.

An interesting theoretical question is what are the temporal dynamics of the population density corresponding to different invasion scenarios. Note that pattern formation as such is not sufficient to draw any conclusions about this as irregular patterns sometimes correspond to periodical temporal dynamics but some simple regular patterns may exhibit multi-periodicity and chaos (cf. *Morozov et al. 2004*). Figure 2.13 shows the population density of susceptibles averaged over the spatial domain as obtained in the course of the system's dynamics. Apparently, the population variation over time exhibits distinct irregularity. Although a detailed consideration of this issue should include calculation of the dominant
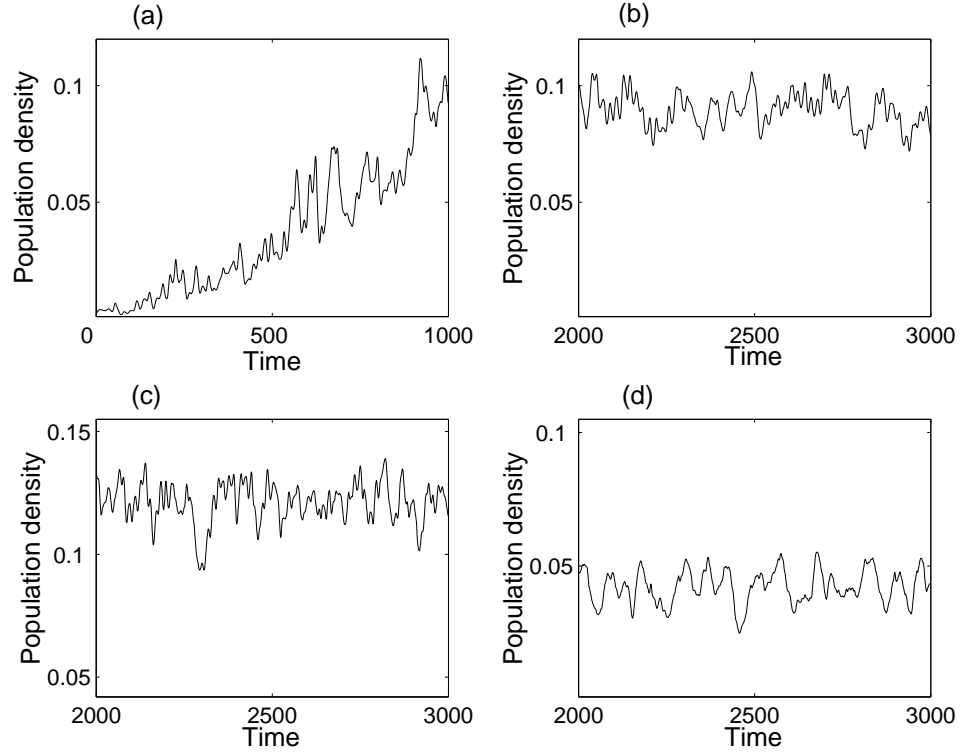
FIGURE 2.13: Spatial average of the population density vs. time obtained in numerical simulations for different invasion scenarios: (a-b) for the patchy spread for parameters the same as in Fig. 2.9 and for two different intervals, (a) for $0 < t < 1000$, (b) for $2000 < t < 3000$; (c) for the transitional regime shown in Fig. 2.10, (d) for the patchy spread as in Fig. 2.11.

Lyapunov exponent, the apparent irregularity in the time dependence indicates that the corresponding temporal dynamics are chaotic.

We want to emphasise that, in this study, it was not our goal to develop a comprehensive model of the gypsy moth invasion. Rather, we aimed to demonstrate that the human-assisted dispersal is not necessarily a primary mechanism of the gypsy moth spread. In particular, there is clearly an alternative explanation of the typical patchy structure in the gypsy moth spatial distribution (cf. Fig. 2.1); indeed, it can appear as a result of the interplay between wind dispersal, the Allee effect and the impact of NPV or predators see Figs. 2.9 and 2.11, 2.3 and 2.4.

A more general model of gypsy moth spread should include both modes of dispersal along with other specifics, such as weather conditions and the effect of elevation, which would make the model parameters space-dependent. Interaction between the short-range (wind-assisted) dispersal and the long-range (human-assisted) dispersal then may be capable of explaining the observed variability in the rate of spread (*Tobin et al. 2007a,b, Tobin and Blackburn 2008*). Parametrisation of such a model is however going to be a difficult problem as there is currently not enough

information available about relevant human movement. Distinguishing between different dispersal modes and/or between different types of movement is a challenging issue and may have hidden pitfalls, especially if statistical analysis of the movement data is involved (e.g. *see Jansen et al. 2012*).

Chapter 3

Are time delays always destabilising?

3.1 Introduction

With this chapter, we begin Part II of this thesis, which focuses on the effects of time delays on population dynamics.[1] One of the main challenges in ecology is to determine the cause of population fluctuations. Both theoretical and empirical studies suggest that delayed density dependence instigates cyclic behaviour in many populations; however, underlying mechanisms through which this occurs are often difficult to determine and may vary within species. In this chapter, we consider temporal dynamics of a single species population affected by the Allee effect coupled with discrete time delay. We use two different mathematical formulations of the Allee effect and analyse (both analytically and numerically) the role of time delay in different feedback mechanisms such as competition and cooperation. The bifurcation value of the delay (that results in the Hopf bifurcation) as a function of the strength of the Allee effect is obtained analytically. Interestingly, depending on the chosen delay mechanism, even a large time delay may not necessarily lead to instability. We also show that, in case the time delay affects positive feedback (such as cooperation), the population dynamics can lead to self-organised formation of intermediate quasi-stationary states. Finally, we discuss ecological implications of our findings.

---

[1]This chapter has been published as *Jankovic and Petrovskii (2014)*

60

The classical theory of population dynamics predicts that the smaller the population (or the lower its density), the less individuals will suffer from constraints of intraspecific competition. The fewer individuals there are, the more resources would be available, and steadily the population would increase in size. Though this enhanced resource availability would ostensibly benefit the population, such a population would lack conspecifics (advantages of which include predator saturation or dilution, cooperative predation or resource defense and social thermoregulation, e.g. see *Stephens et al. 1999*) which may lead to a decrease in the population's fitness. This phenomenon, termed the Allee effect, was first described in the 1930*s*, and has become a topic of much interest over the last 25 years, largely in light of the concerns over conservation and the problems of already endangered or rare species (*Dennis 1989, Courchamp et al. 2008*). The Allee effect refers to a positive relationship between (any component of) individual fitness and population density (*Stephens et al. 1999*). The per capita growth rate is nonmonotonic and can even become negative at particularly low values of population density (termed as the strong Allee effect), resulting in a critical density known as the Allee threshold below which population extinction is likely.

Mechanisms through which the Allee effect appears are abundant, and to name just a few, include inbreeding depression, absence of cooperative feeding, failure to satiate natural enemies, failure in mate finding and temporal asynchrony in reproductive maturing between sexes (known as protandry); see *Courchamp et al. (1999), Stephens et al. (1999)*. One way in which individuals gain protection from predators is through cooperative strategies such as aggregation. By grouping, the population reduces predation risk through dilution effects; the larger the group size the less chance that an individual may be harmed. At the same time, aggregation can be costly and overshadowed by deleterious consequences such as a paradoxical increase in exposure to predators, as larger groups are easily detected. Furthermore, it can lead to overcrowding and an increase in intraspecific competition (*Griffiths et al. 2003*). These negative effects can be counteracted through behaviour such as parental care, which restores the positive aspects and need for animal grouping (*Nakaoka et al. 2009*). A less appreciated and frequently overlooked mechanism through which Allee effects emerge are predator-prey interactions. It has been shown, that size-selective predation on prey regulated through density-dependence leads to a positive relationship between predator density and population growth, through intraspecific competition in the prey population (*De Roos and Persson 2002, De Roos et al. 2003, van Kooten et al. 2005*). Such

an Allee effect is known as "emergent", as it results from the predator induced changes in prey size distribution and is essentially a consequence of the feedback of predator feeding on its own performance.

Despite Allee effects usually being difficult to detect and quantify in natural populations (but see *Vercken et al. 2011*), the variety of mechanisms and affected ecological processes suggest their prevalence. Moreover, the current state of research indicates ample empirical evidence (albeit often indirect) of the ubiquity of Allee effects in a diverse range of taxa and ecosystems (*Courchamp et al. 2008, Courchamp et al. 1999*). Along with stochasticity, the Allee effect is particularly influential in biological invasions (*Fagan et al. 2002, Petrovskii et al. 2002, 2005a*), as it may cause longer lag times (*Petrovskii et al. 2005b*), slower spread (*Lewis and Kareiva 1993*) and decrease the probability of establishment which may lead to underestimation of invasion risk posed (*Taylor and Hastings 2005*). Further consequences include impacts on distribution of invasive species *(Morozov et al. 2006)*, metapopulation fluctuations, predator-prey interactions, parasite transmission (*Kramer et al. 2009*), exploitation management and biodiversity preservation (*Taylor and Hastings 2005, Courchamp et al. 1999*). It is thought that the collapse of cod, *Gadus morhua*, in the Northwest Atlantic might be an unfortunate consequence of emergent Allee effects, as these populations are not known to exhibit mechanisms commonly associated with positive density dependence (*De Roos and Persson 2002*). Allee effects also form a crucial aspect of biological control (e.g. through release of sterile insects, cf. *Lewis and van den Driessche 1993*) and are increasingly exploited as the "Achilles heel" of biological invasions (*Liebhold and Tobin 2010, Dennis 1989*).

The ways to include the Allee effect into mathematical models of population dynamics are well understood. The resulting models are often described by differential equations *(Murray 2002, Kot 2001)* hence assuming that the processes shaping the dynamics are taking place at the same time. However, processes in ecology (as well as in nature in general) are rarely instantaneous *(Hutchinson 1948, Maynard Smith 1974)*. As it was pointed out by *Kuang (1993)*, "time delays occur so often (in almost every situation) that to ignore them is to ignore reality". Aiming to create a somewhat more realistic description, one should include a time delay into the model, which results in a delay differential equation. Delay differential equations have been of sufficient importance in modelling real life phenomena, and arise in various practical applications such as population dynamics (most often

accounting for maturation/gestation periods), immunology (incubation/latent periods) and physiological and pharmaceutical kinetics (Cheyne-Stokes respiration, glucose-insulin regulation, blood pressure oscillations), etc. Time delays in feedback mechanisms tend to destabilise positive, otherwise stable, equilibria and lead to oscillatory behaviour. Thus, delay differential equations are capable of generating more complex and rich dynamics compared to ordinary differential equations *(Ruan 1995, Cooke and Grossman 1982)*. Indeed, population densities of many species are known to fluctuate nearly periodically over time *(cf. Turchin 2003)*, a phenomenon to which delayed density dependence may provide an explanation.

Consequently, the conditions under which time delay can lead to an instability are studied in much detail. Interestingly, there is some evidence that the Allee effect can have an effect on the system's dynamics opposite to that of the time-delays, i.e. increasing stability of the positive equilibrium rather than decreasing it. In particular, *Gopalsamy and Ladas (1990)* proposed a single species model in which population growth is damped by the Allee effect and per capita growth is subject to time delays. Under certain conditions that included the case of a weak Allee effect (but not the strong Allee effect), they showed the positive equilibrium was globally attractive. Subsequent studies by *Cao and Gard (1995)* and *Liz et al. (2003)* provided conditions of global asymptotic stability; however, if a delay exceeds a critical value, the solutions oscillate around the positive equilibrium. *Freedman and Gopalsamy (1986)* obtain conditions for local stability for a class of models including the delayed weak Allee effect. Recently, it was shown that a mere inclusion of a (non-delayed) Allee effect can have a stabilising effect on the positive equilibrium compared to Hutchinson's model (*Merdan et al. 2009*), in the sense that the steady state is stable under less restrictive conditions. Moreover, the conditions become less and less restrictive – hence the stabilising effect becomes more prominent – with increasing strength of the Allee effect (*Merdan et al. 2009*).

Regarding the effect of various factors on the system's stability, we also mention here the work by *Beddington and May (1975)* who showed that the effect of time delay can be delicate. We however point out here, that their context of stability differs principally from other studies, including ours. Namely, they showed that, although an increase in the value of time delay causes the solution to start oscillating around the upper equilibrium, simultaneously it spends more time in the vicinity of the lower, trivial, otherwise unstable equilibrium. Thus, time delays can slow the growth of instabilities and can therefore be interpreted as having a "stabilising" effect on unstable stationary points (*Beddington and May 1975*).

In spite of several papers having been published about the interplay between the time delay and the Allee effect, there are a few questions that have never been addressed. Note that most of the previous research focuses on the weak Allee effect. On the contrary, here we consider both cases of weak and strong Allee effects. *Merdan et al. (2009)* obtain results for a general class of Allee functions, however our chosen parametrisations are different and do not satisfy their imposed restrictions. That raises an issue of the structural sensitivity *(Fussmann and Blasius 2005)* of models with regard to parametrisation of the time-delayed Allee effect. In this study, we show that the interplay between the Allee effect and time delay can be non-trivial and counterintuitive depending on the choice of delayed process(es). The remainder of the chapter is organised as follows. In Section 3.2 we introduce our modelling frameworks and consider the effects of different time delay terms. Results presented include both numerical simulations and analytical results. Then, in Section 3.3 we address possible ecological applications of our models and outline what ecological implications our findings may leave.

3.2 Models and results

Under the assumption of spatial homogeneity, the dynamics of a single species population is described by the following equation:

$$\frac{dU(t)}{dt} = G\left(U(t)\right) = U(t)F\left(U(t)\right),\tag{3.1}$$

where $U(t)$ is the population density at time t, $G(U)$ the rate of change of population density due to reproduction and mortality and $F(U)$ is the per capita growth rate. If population growth is damped by the Allee effect, the per capita growth rate is dome-shaped and can be described by a square polynomial (*Lewis and Kareiva 1993*, *Amarasekare 1998a*, *Amarasekare 1998b*, *Courchamp et al. 2008*):

$$F(U) = \gamma(K - U)(U - \beta),\tag{3.2}$$

where K is the carrying capacity and γ the coefficient proportional to the maximum per capita growth rate *(cf. Lewis and Kareiva 1993)* which we call, for convenience, the characteristic growth rate. Parameter β is the so-called Allee threshold or threshold density and can be regarded as a measure of the strength of the Allee effect, so that the Allee effect is called strong if $\beta > 0$ and weak if $-1 < \beta < 0$.

Accordingly, our baseline non-delayed model is as follows:

$$\frac{dU}{dt} = \gamma U(K - U)(U - \beta). \tag{3.3}$$

Equation (3.3), albeit very simple, accounts for the two dominant feedback mechanisms: positive, arising from cooperation at low population densities, and negative occurring at high densities due to competition; see Fig. 3.1. Therefore, in the chosen parametrisation (3.2) we can loosely associate cooperation and competition with factors $(U - \beta)$ and $(K - U)$, respectively.

Once the delay τ is taken into account, the generic Eq. (3.1) turns into

$$\frac{dU(t)}{dt} = G(U(t), U(t - \tau)) = U(t)F(U(t), U(t - \tau)), \tag{3.4}$$

where, similarly to the above, G is a cubic polynomial but the delay can enter different terms depending on the type of the feedback.

In population ecology, typical biological regulating mechanisms are competition for food and territories, amongst others (*Berryman et al. 1987*), thus we begin by including time delay into the competition term, obtaining a model comparable to
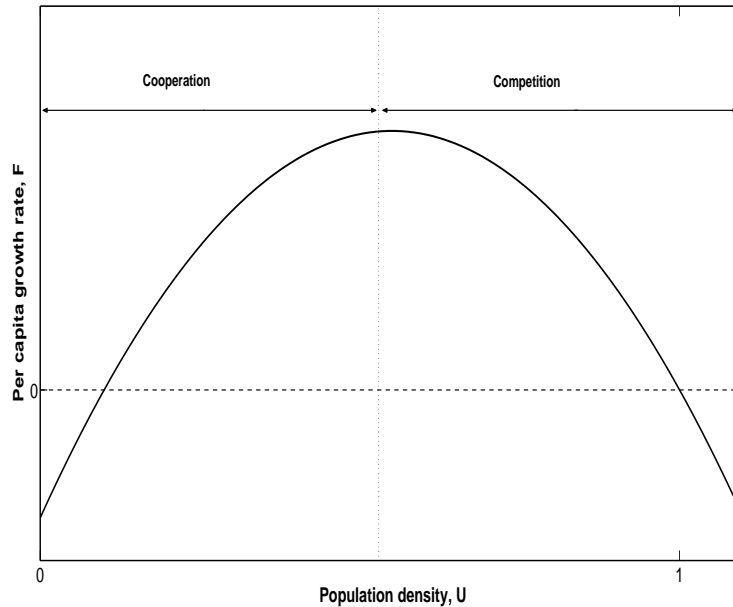

FIGURE 3.1: A sketch of the per capita growth rate $F(U)$ in the case of the strong Allee effect.

Hutchinson's equation (*Hutchinson 1948*):

$$\frac{dU}{dt} = \gamma U(t)(U(t) - \beta)(K - U(t - \tau)), \tag{3.5}$$

where τ is the time delay.

Throughout this section we have scaled both the carrying capacity K and the characteristic growth rate γ to unity, which implies the corresponding scaling for the variables U and t. Equation (3.5), as well as other delay differential equations (see eqs. (3.6) and (3.10–3.13) below) were solved by finite differences, in particular by the explicit Euler scheme. The time step was chosen to be sufficiently small, ensuring the accuracy and reliability of results, $\Delta t = 0.01$. Furthermore, we have checked the reliability of our solutions with Matlab's in-built solver for discrete delay differential equations (dde23). Unlike ordinary differential equations, in which defining initial conditions was sufficient, delay differential equations require us to define the population's "history", i.e. $U(t)$ for $-\tau < t < 0$. In all simulations, the history was chosen to be a constant function $U = U_0 = 0.5$ (except for $\beta = 0.5$ where we choose $U_0 = 0.6$ to ensure population survival). The Allee threshold density β is regarded as a controlling parameter and its value is varied between -1 and 0.5, which obviously includes both cases of the Allee effect, i.e. weak for $-1 < \beta \leq 0$ and strong for $0 < \beta < 0.5$. We choose the time delay τ as the second controlling parameter and observe the system's response to its variation. Following extensive computer simulations, we then summarise our findings as a map in the parameter plane (τ, β), Fig. 3.2.

Figure 3.2 shows the succession of different dynamical responses for a population subject to delayed competition, as described by Eq. (3.5). Some typical system's dynamics is shown in Fig. 3.3. For a given Allee threshold and a small time delay, the system quickly approaches the equilibrium state $U = 1$ with $U(t)$ being a monotonously increasing function (not shown). An increase in τ causes the solution to lose monotonicity (when τ exceeds the critical value shown by the dashed curve in Fig. 3.2) through the appearance of damped oscillations (Fig. 3.3, left). By further increasing τ, the system passes through the Hopf bifurcation (shown by the solid curve in Fig. 3.2) leading to the occurrence of limit cycles (Fig. 3.3, right). As the Allee threshold β increases, the population appears to be more stable as larger values of the time delay are needed to destabilise it. Also, as we have observed in our simulations, the population always persists and no extinction occurs even for a large time delay. Note that both the solid and dotted
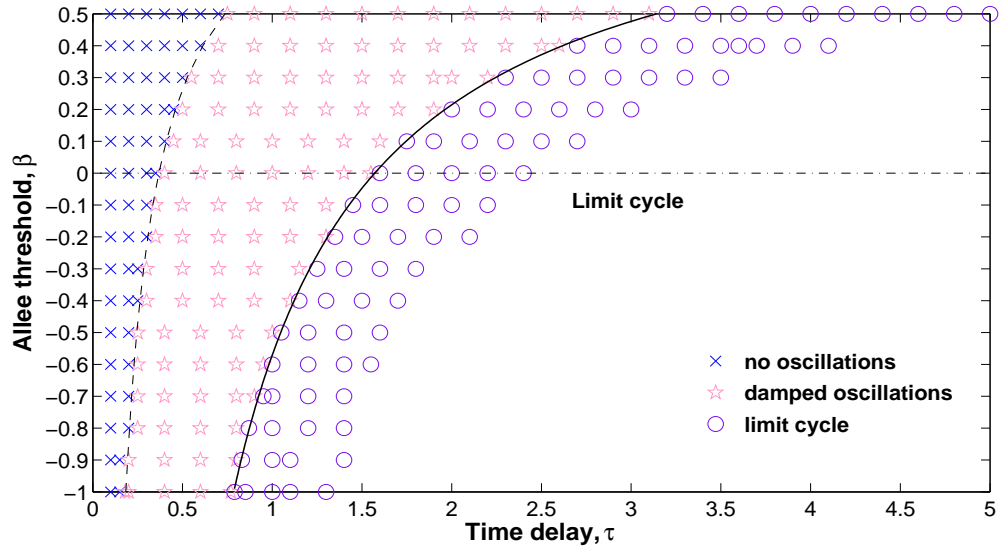
FIGURE 3.2: Summary of results for model (3.5). The solid line corresponds to the analytically calculated Hopf bifurcation curve (see Appendix B), the dotted line corresponds to the analytically calculated loss of monotonicity curve (see Appendix C), while the dash-dotted line acts as a visual aid to separate the weak and strong Allee effect.

curves in Fig. 3.2 are calculated analytically (see Appendices B and C) and are in excellent agreement with our numerical results.
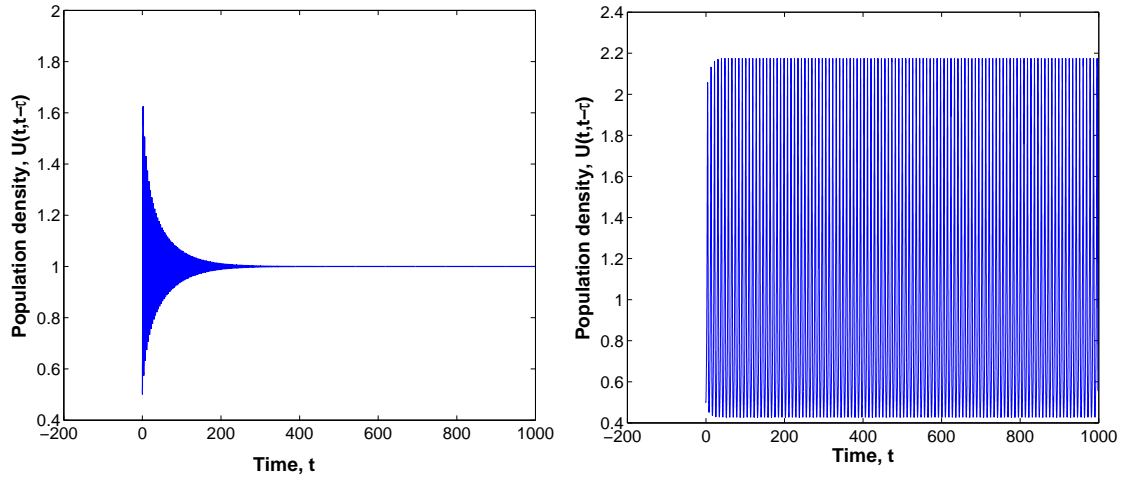
FIGURE 3.3: Temporal population dynamics for model (3.5). Parameters are $\beta = 0.7$, $\tau = 0.9$ (left) and $\beta = 0.1$, $\tau = 2$ (right).

As a next step we consider the effect of time delay on cooperation. Delayed cooperation in a population (when time delay is included into positive density

dependence) can be modelled as

$$\frac{dU}{dt} = \gamma U(t)(U(t-\tau) - \beta)(K - U(t)). \tag{3.6}$$

Contrary to model (3.5), increasing the time delay had no destabilising effect on solution behaviour, apart from minute changes in the slope (Figure 3.4). This was intuitively expected, as positive density dependent mechanisms do not regulate population density. For a sufficiently large time delay solutions monotonously approach the equilibrium $U = 1$, but at a slower rate.
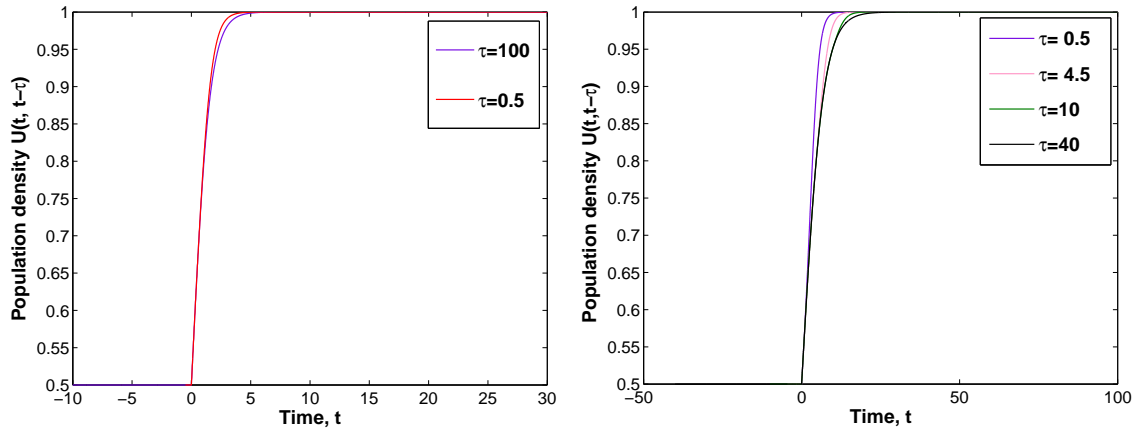
FIGURE 3.4: Solutions of model (3.6). Simulations presented are for the weak (left) and strong (right) Allee effect with $\beta = -0.8$ and $\beta = 0.2$, respectively. The corresponding time delays are given in the figure legend.

3.2.1 An alternative model

An apparent disadvantage of the baseline model (3.3) with the growth rate described by a cubic polynomial is that it accounts for the effects of competition and cooperation in a mixed, multiplicative way. Correspondingly, *Petrovskii et al. (2008)* have proposed an alternative, additive form of the per capita growth function $F(U)$:

$$F(U) = f(U) - m - A(U), \tag{3.7}$$

where $f(U)$ accounts for population multiplication due to reproduction, m is natural (density independent) mortality and $A(U)$ represents density dependent mortality (e.g. due to cannibalism), which is of significance in high density populations.

Unlike the previously introduced multiplicative form of the Allee effect, this additive form avoids the interference of different biological processes. The population dynamics can then be modelled by:

$$\frac{dU}{dt} = U(-m + f(U) - A(U)), \tag{3.8}$$

in which the particular parametrisation of functions depends on the system modelled.

Obviously, for different choices of functions f and A, model (3.8) can have various properties. Here we consider the growth term as $f(U) = aU$ and the density dependent mortality as $A(U) = \gamma U^2$ where a and γ are parameters. We then assume that the natural mortality rate m is proportional to the threshold density β, $m = \gamma\beta$. Since β has the meaning of the survival threshold, this is not completely unrealistic. Finally, in order to make model (3.8) directly comparable with (3.3) and to avoid additional parameters, we assume that $a = \gamma(1 + \beta)$. Equation (3.8) then takes the following form:

$$\frac{dU}{dt} = \gamma U(-\beta + (1 + \beta)U - U^2) \tag{3.9}$$

(in appropriately chosen dimensionless units). As before, γ is the characteristic growth rate, and β is the Allee threshold. Without time delay, model (3.9) is therefore identical to (3.3). However, different terms now possess different meaning and hence the time delay can be included differently. As the term $(1 + \beta)U$ apparently provides a positive feedback on the population growth, we associate it with cooperation. The term U^2 provides a negative feedback and hence should be associated with competition.

Since time delays in population models often account for maturation or gestation periods, we firstly include the time delay into the growth term:

$$\frac{dU}{dt} = \gamma U(t)(-\beta + (1 + \beta)U(t - \tau) - U^2(t)). \tag{3.10}$$

Following stability analysis (see Appendices B and C), one readily concludes that this inclusion of time delay should not affect population dynamics, as the equilibrium retains its stability. However, numerical simulations reveal interesting population dynamics resulting in the self-organized formation of intermediate quasi-stationary states; see Fig. 3.5. Namely, after a period of fast growth, the population density approaches an intermediate quasi-equilibrium at the close vicinity of
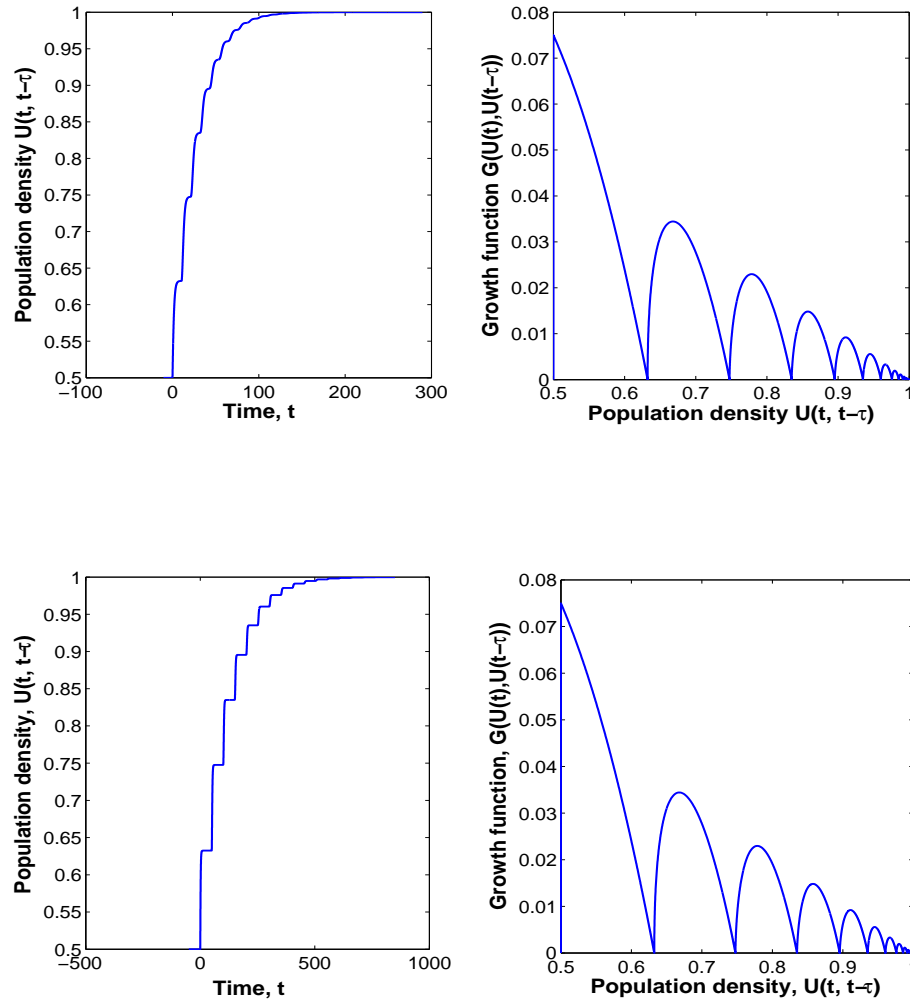
FIGURE 3.5: Solution behaviour as predicted by model (3.10); top for $\tau = 10.5$ and bottom for $\tau = 50$, the Allee threshold is $\beta = 0.2$. The figures on the left show the population density vs. time whilst the figures on the right show phase plane structure (growth function G vs population density). By increasing the time delay τ the step-like structures become more prominent (note the different range used for the t-axis in the top and bottom rows).

which it can remain for a considerable time. Subsequently, the population density leaves the vicinity and once again shows a fast growth before reaching another quasi-equilibrium. This pattern repeats itself until the system reaches its stable equilibrium $U = 1$ in the large-time limit, thus resulting in a step-like structure (Fig. 3.5, left column). As the time delay τ increases, the system remains at these "resting states" for longer and the transition between them becomes faster, making the step structure more prominent. Also, by increasing the time delay, more time is needed for the population to reach its equilibrium. Note that the values of τ

used in Fig. 3.5 are considerably larger than in the models considered above. We mention here that somewhat similar dynamics were observed in *So et al. (2001)* but for a more complex model involving a structured population on two patches. However, unlike our results their solutions lose monotonicity for a critical dispersal rate.

Using the additive model (3.9), populations subject to delayed competition can be modelled as

$$\frac{dU}{dt} = \gamma U(t)(-\beta + (1 + \beta)U(t) - U(t - \tau)U(t)). \qquad (3.11)$$

Figure 3.6 shows the parameter plane (τ, β) of the model (3.11) where different symbols correspond to different regimes of the system dynamics, as was obtained in computer simulations. The Hopf bifurcation curve (solid line) is a decreasing function and matches well with analytical results. For a given Allee threshold, an increase in time delay gradually leads to the loss of monotonicity and to the appearance of damped oscillations. A further increase in τ causes the system to lose stability and exhibit limit cycle behaviour. An obvious exception occurs at $\beta = -1$ as the system remains stable for any τ (see Appendix B). A key feature of this model is that a sufficiently large time delay may drive the population to extinction, only if subject to the strong Allee effect, whilst populations affected by the weak Allee effect persist.

Since Eq. (3.11) is a heuristic model, it is not immediately clear what the effect of delay on competition exactly is. Therefore, we consider an alternative model where additional mortality may be controlled by a purely delayed mechanism, so that population dynamics is modelled as:

$$\frac{dU}{dt} = \gamma U(t)(-\beta + (1 + \beta)U(t) - U^2(t - \tau)). \qquad (3.12)$$

The parameter plane of model (3.12) is structurally similar to that of model (3.11) whilst the bifurcation curve is monotonically decreasing, with a substantially steeper slope (Fig. 3.7). Again, populations can be driven to extinction only when a strong Allee effect is present.

Lastly, we consider the inclusion of both delayed competition and maturation (which is equivalent to delays in both cooperation and competition in the baseline model (3.3)):

$$\frac{dU}{dt} = \gamma U(t)(-\beta + (1 + \beta)U(t - \tau) - U^2(t - \tau)) \qquad (3.13)$$

FIGURE 3.6: Map of different scenarios as explained by the figure legend for model (3.11). The solid line corresponds to the analytically calculated Hopf bifurcation curve, the dotted line shows the analytically calculated loss of monotonicity curve, while the dash-dotted line acts as a visual aid to separate the weak and strong Allee effect.

FIGURE 3.7: Parameter map of different scenarios as explained by the figure legend for model (3.12). The solid line corresponds to the analytically calculated Hopf bifurcation curve, the dotted line shows the analytically calculated loss of monotonicity curve, while the dash-dotted line acts as a visual aid to separate the weak and strong Allee effect.

For this model, the map in the parameter space (τ, β) (see Fig. 3.8) appears to have a structure similar to that obtained in the corresponding multiplicative model (3.5) (see Fig. 3.2) where the delay was included only into the cooperation term. This seems to suggest that delay in competition may have a more prominent effect than delayed cooperation. One important difference though is that now, in case of the strong Allee effect ($\beta > 0$) and for sufficiently large time delays (see the top-right corner of the parameter plane), the population can be driven to extinction.

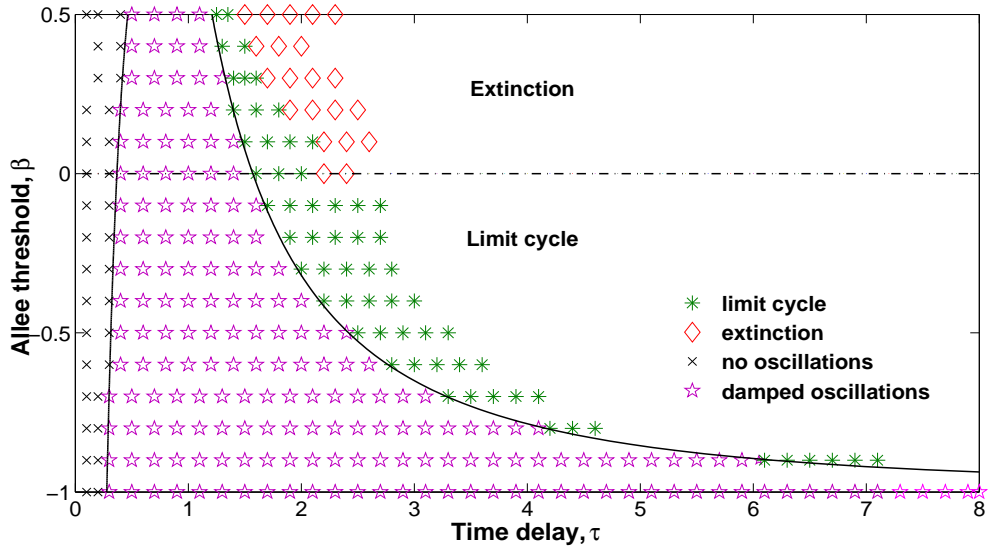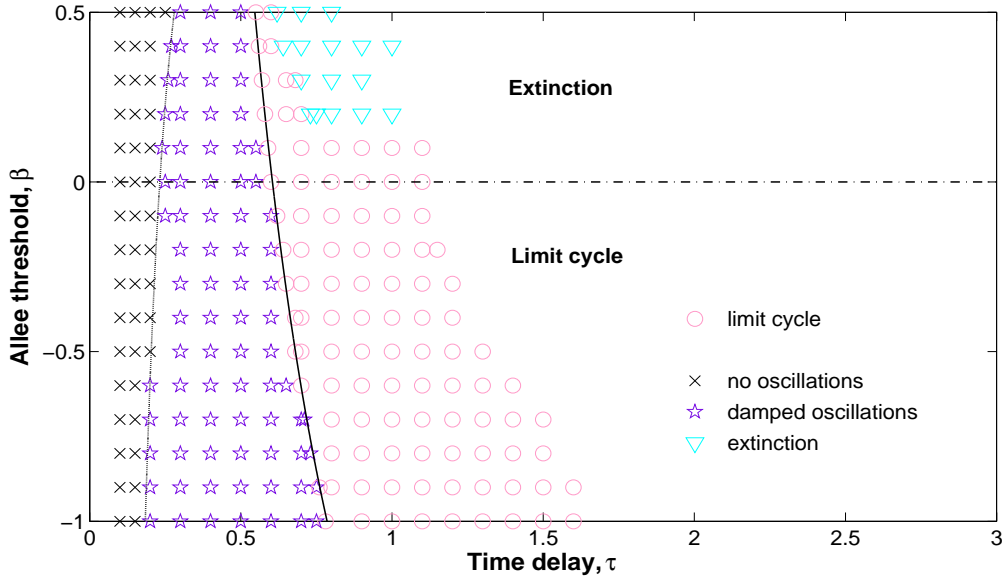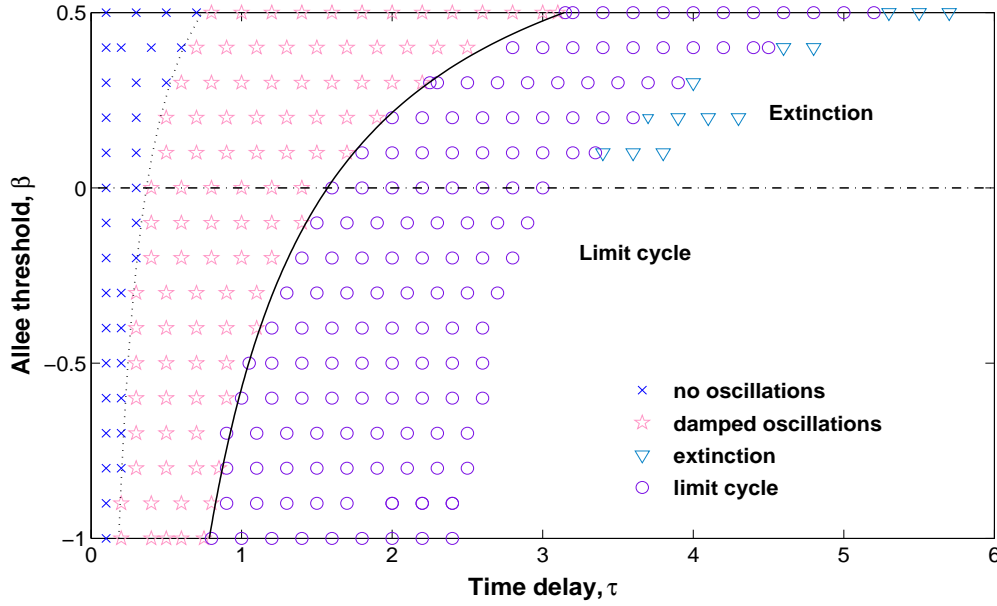

FIGURE 3.8: Map of different scenarios as explained by the figure legend for model (3.13).The solid line corresponds to the analytically calculated Hopf bifurcation curve, the dotted line shows the analytically calculated loss of monotonicity curve, while the dash-dotted line acts as a visual aid to separate the weak and strong Allee effect.

3.3   Discussion and Concluding remarks

The aim of this study is to address the interplay between time delays and the Allee effect. Using the single-species context, we study (both analytically and numerically) two different models of population dynamics where the effects of competition and cooperation are taken into account in either a multiplicative or additive way. The conditions for local stability are obtained analytically as a function of the Allee effect strength and are in full agreement with numerical results. We have found that the inclusion of time delay alone does not necessarily confer instability,

and the choice of the delayed underlying ecological process is an important determinant of overall population dynamics. However, a delay in negative feedback mechanisms such as intraspecific competition always results in instability and thus leads to population cycles or even to population extinction; see Figs. 3.2, 3.6, 3.7 and 3.8. We show that a delay in competition has a more dominant effect on population dynamics, compared to delays in positive feedback mechanisms arguably accounting for cooperative strategies which exert no consequences on the population's global stability. Even so, nontrivial transitional dynamics through self-organized formation of intermediate quasi-stationary states can be observed in models of this kind (Fig. 3.5). Our results are summarised in Table 3.1.

TABLE 3.1: Summary of the results. The succession of dynamical regimes from left to right corresponds to an increase in the value of time delay τ. Note that, since all models exhibit monotonous behaviour for sufficiently small τ this is not included into the table for the sake of brevity.

Model, type	Process delayed	Damped oscillations	Limit cycle	Quasistationary states ('steps')	Extinction
Eq. (3.5), multiplicative	competition	Yes	Yes	No	No
Eq. (3.6), multiplicative	cooperation	No	No	No	No
Eq. (3.10), additive	cooperation	No	No	Yes	No
Eq. (3.11), additive	competition	Yes	Yes	No	Yes
Eq. (3.12), additive	competition	Yes	Yes	No	Yes
Eq. (3.13), additive	competition, cooperation	Yes	Yes	No	Yes

Note that, in the corresponding real-world population dynamics, the intermediate states predicted by model (3.10) may not always be seen as they would likely be blurred by the effects of stochasticity and the transient nature of the environment. These intermediate states may therefore become "hidden" in the sense that they may be difficult to observe yet they affect the population dynamics (e.g. by considerably increasing the time required to converge to the 'true' steady state). That evokes the concept of "hidden states" that has been an issue of growing importance in ecology (*Clark and Bjørnstad 2004, Buckland et al. 2007*). It is thought that the existence of self-organised, hidden or intermediate states can, in some cases, provide an explanation to the complexity of ecosystems' dynamics (*Clark and Bjørnstad 2004*). The existence of such states can sometimes be linked to the population's heterogeneity, both in terms of its age and/or physiology and in its spatial structure (e.g. *So et al. 2001*). In our study, however, we have shown that

intermediate states can emerge in an unstructured single-species population as a result of the interplay between the time delayed cooperation and the Allee effect, a novel mechanism that has not been observed before. We also mention that the original concept of hidden states is used in a purely statistical context (*Buckland et al. 2007*); here we show that it can arise in a deterministic model as well.

Continuous population models are sometimes considered as limiting cases of their discrete counterparts. In time discrete population models, the Allee effect is thought to have a stabilising effect on system dynamics (in both delay and non-delay systems). In the works by *Scheuring (1999)* and *Fowler and Ruxton (2002)* logistic and Allee type difference models were presented and compared. Consequently, the per capita growth rates in Allee models were normalised to enable comparison of equivalent equilibrium stability. The inclusion of positive density dependence was shown to stabilise population dynamics, in particular with increasing Allee strength. *Çelik et al. (2008)* and *Merdan and Gümüş (2012)* confirm such findings in equivalent time delay models. In these studies, comparison was made between delayed competition models and delayed Allee effects. Analytical and numerical results suggest that even though delayed, positive density dependence remains a stabilising mechanism. In other words, a delay in cooperation does not alter the system's stability, proving it not to be a controlling feedback as is also readily observed in the continuous case; see Fig. 3.4.

Biological interpretation of the 'delayed cooperation' concept is difficult to grasp, though we suggest that cooperative behaviour itself may lead to a delay in reproduction, thereby increasing the population's time to converge to it's steady state (Figs. 3.4 and 3.5). Although cooperation in nature takes many forms, one specific form are cooperative breeding populations in which 'helpers' (individuals other than parents) provide care for offspring. In addition to such alloparental care, cooperative breeding populations exhibit two further characteristics: delayed dispersal and reproductive suppression (delayed reproduction). Reproductive suppression suggests that some social or physiological factor limits the individual's ability to reproduce. Possible sources and influences can greatly vary between species, ranked individuals and sexes. Cooperative breeding is a social phenomenon that has been observed in avian species (*Koenig and Dickinson 2004*) as well as across a rather diverse mammalian taxa (*Kramer 2010*): predominantly in wild canids, rodents, meerkats and some primates. Meerkats, *Suricata suricatta*, are highly gregarious species, obligate cooperative breeders, and live in groups of up to 50

individuals (*Clutton-Brock et al. 2008*). One dominant pair monolopolises repro-
duction, accounting for almost 80% of reproductive attempts (*Griffin et al. 2003*),
whilst helpers of both sexes assist in rearing young. The most striking form of help-
ing is such cooperative pup care which involves guarding pups in the natal burrow
and pup feeding. Like many other cooperative breeders subordinate females com-
monly attempt to breed but with substantially lower reproductive success than
dominant females. Behavioural tactics such as regular aggression, eviction and
infanticide are employed to achieve reproductive suppression (*Clutton-Brock et
al. 1998*, *Young et al. 2006*). Behavioural reproductive suppression is also seen in
grey wolf packs (*Asa and Valdespino 1998*). Young subordinates remain in their
natal pack, thus mating and reproduction are typically delayed. A common feature
of cooperative breeders is that the young the individuals helped to raise become the
individual's 'helpers', following their succession to breeding status in group (*Wiley
and Rabenold 1984*). Alloparental care is particularly prominent in South Amer-
ican marmosets and tamarins (*Solomon and French 1997*); see Fig. 3.9. Apart
from aggression as an effective mechanism limiting breeding by eviction (*Snowdon
and Pickhard 1999*), in the common marmoset, *Callithrix jacchus jacchus*, phys-
iological suppression is present, i.e. puberty is delayed in offspring that do not
disperse (*Abbott et al. 1981*).

FIGURE 3.9: Examples of species exhibiting delayed cooperation and competi-
tion: cottontop tamarins (left) and flour beetle (right). Taken from `http://`
`www.monkeyday.org/2013_09_01_archive.html` and `http://en.wikipedia.`
`org/wiki/Flour_beetle`.

Cyclic dynamics in populations have stimulated a great deal of research and de-
bate in ecology (*Elton 1924*, *Hutchinson 1948*, *Krebs 1996*, *Krebs and Myers 1974*).
Contrary to the ever enlarging data sets on population cycles, population ecolo-
gists continue to debate population regulation, in particular the role of density
dependence. Possibly the key issue in such disagreement is relating statistically

determined patterns to ecological mechanisms responsible for population fluctuations (*Williams and Liebhold 1995, Berryman and Turchin 1997*). Therefore, population regulation remains a fairly contentious field, open to further investigation of the "true" governing mechanisms. A common approach used to reveal dominant underlying ecological processes is time series analysis, and there seems to be consent amongst many authors as to density dependence being one of the main causal factors of population fluctuations (*Bjørnstad et al. 1998, Turchin et al. 1999, Berryman and Turchin 2001*). It is well known that populations are influenced by factors that are a function of the current population density (direct density dependence) and by factors that are functions of past population densities (delayed density dependence)[1]. The latter tends to destabilise population dynamics, making them more prone to cycle. There are numerous underlying causes of such second order dynamics, however the most commonly considered factors are: resource competition and cannibalism, predator-prey interactions (in particular the effect of specialist predators), parasitoids, pathogens, maternal effects, etc. Indeed, possible causes of delayed density dependence are linked to combinations of such factors, making the task of isolating one single mechanism quite difficult (*Krebs 1996*).

A classic example of fluctuating populations are the grey-sided vole populations, *Clethrionomys rufocanus*, in Kilpisjarvi, Finland (*Hansen et al. 1998*). Attempting to reveal causes of such dynamics, *Hansen et al. (1998)* obtained results that show delayed density dependence is crucial for generating $3 - 5$ year cycles within these populations. By testing two hypotheses of community dynamics, one caused by interaction with specialist predators, and the other relating to species specific trophic interaction (overgrazing of *Vaccinium*) and having excluded interspecific competition, *Hansen et al. (1998)* show that population cycles are rather caused by intrinsic factors such as overgrazing of *Vaccinium* or preferential predation by least weasels on grey-sided voles. A contrasting study on field-voles (*Microtus agrestis*) shows that predation by weasels, is neither a sufficient nor necessary condition to initiate and drive population cycles in Kielder forest populations (*Graham and Lambin 2002*), suggesting more inherent mechanisms such as intraspecific competition a more possible source of fluctuations. Under the assumption cyclic behaviour of both grey-sided and field vole populations is due to resource competition, we can suggest such population dynamics be described by delayed competition models such as Eq. (3.5). Depending on the specifics of intraspecific competition,

---

[1]Direct density dependence is often referred to as first order dynamics, whilst delayed density dependence is known as second (or higher) order dynamics, see *Turchin (1999)*

both Eqs. (3.11) and (3.12) would be appropriate to model observed population oscillations.

Predation was also shown to be an influential force controlling population cycles in the Asian tiger mosquito, *Aedes albopictus*, (*Walsh et al. 2012*) and the southern pine beetle, *Dendroctonus frontalis*, (*Turchin et al. 1999*). A common modeling approach would consist of formulating an appropriate predator-prey model (*Cushing 1976, Beretta and Kuang 1998*). Nonetheless, an alternative may be found in a single species system whereby predation effects would be implicitly incorporated as additional prey mortality. Such delayed density dependent mortality was shown to oscillate for sufficiently large time delay, so Eqs. (3.11) and (3.12) would be relevant. Also, we recall here that age-dependent predator-prey interactions may cause the emergence of Allee effects, cf. *De Roos and Persson 2002, De Roos et al. 2003*. However, one must be very careful in making a priori generalisations based on the intuition from simple models such as ours. Furthermore, the projection of single species dynamics to two or more species systems can also be misleading. In particular, *Hastings (1983, 1984)* showed that in an age-dependent predator prey system, delays in prey recruitment are critical for the system's stability; thus, delays in higher trophic levels seem less important than indicated from single species models. Even so, delays in prey recruitment were not the sole determinant of stability, but rather the combination with the functional response. Apart from biotic factors, abiotic factors such as season length, alone, have been shown to induce delayed density dependence therefore causing population fluctuations (*Smith et al. 2006*).

Since the focus of this study is on single species models, our efforts are directed at intrinsic factors influencing population dynamics. Ample evidence is available on fluctuating insect populations, and suggests that cannibalism is frequently observed therein. Unlike population cycles with a period of several to many generations (small mammals, temperate forest insect pests), another type of dynamics involves fluctuations with a period approximately equal to the animal's generation or developmental time occurring usually within insect populations (seasonally synchronised life cycles). These cycles are known as generation cycles, and have been mainly studied using flour beetles (*Tribolium*) and phycitine moths (*Pyralidae*). Intensive study of flour beetles has confirmed that cannibalism is able to trigger generation cycles. Namely, in *Tribolium* populations, egg and pupal cannibalism by adults occurs, with pupal cannibalism occurring in lower rates (*Chapman 1928, Park 1932, Desharnais 1997*). Generation cycles in *Tribolium* populations occur

only in juvenile, not adult-life stages, that is to say that when larvae/adults are abundant they manifest egg cannibalism, so inhibiting larval-adult recruitment. Furthermore, an increase in adult abundance leads to lower fecundity due to over-crowding effects. Both these consequences in turn result in a delayed decrease in the frequency of cannibalism, causing population fluctuations. Similar dynamics are observed in the Indian meal moth, *Plodia interpunctella*, in which competitive and cannibalistic effects exerted by large larvae on small larvae and/or eggs, are the main causes of delayed density dependence (*Bjørnstad et al. 1998, Briggs et al. 2000*). Intraspecific cannibalism seems to drive cyclic dynamics of the Indonesian lady beetle, *Coccinellidae*, which display clear generational cycles (*Nakamura et al. 2004*).

Clearly, to model cannibalistic behaviour in insect populations in a comprehensive way, one should formulate a stage-structured model accounting for all developmental stages and include time delay in the appropriate mechanism (*Cushing 1994*). Yet delayed density dependent mortality in a simpler model such as Eqs. (3.11) and (3.12) allow for inclusion of cannibalistic effects in principle, albeit indirectly, and can be used to qualitatively describe the dynamics of one (some) of those stages, i.e. larval population dynamics. Although, we do not have equations for other life stages, Eqs. (3.11), (3.12) and (3.5) alone are capable of producing population cycles. Moreover, an increase in time delay in the above models leads to population oscillations, a key feature of most insect populations.

Delays may occur as a consequence of developmental time and/or interaction between individuals of different stages (as mentioned above). As most forest insects, many species of *Lepidoptera* exhibit cyclic population dynamics. One possible mechanism is through maternal effects, namely, the nutritional environment of the parental generation significantly influences the growth and reproductive potential of the next generation through environmentally-based maternal effects. Numerous studies on the gypsy moth, *Lymantria dispar*, have confirmed the existence of such effects, that is the nutritional experience of the parental generation affects the length of the pre-feeding period, development time and pupal weight in the subsequent generation (*Rossiter 1991*). These traits are thought to be critically important in insect population dynamics because of their influence on natality and mortality. Moreover, these effects take place with a time lag, and are able to destabilise the population, leading to the occurrence of cyclic behaviour (*Ginzburg and Taneyhill 1994*). *Ginzburg and Taneyhill (1994)* developed a time discrete maternal effect system coupled with delayed logistic growth and fitted the results

to data of six species of forest moths (including gypsy moths). The maternal model predicts cycle periods very close to observed values; however, an important factor that has been shown to influence gypsy moth populations has been overlooked – namely, the Allee effect (*Liebhold and Bascompte 2003*, *Tobin et al. 2009*, *Vercken et al. 2011*). Thus, an interesting future extension to this work would be to test multi-annual gypsy moth dynamics with a time continuous maternal model including a delayed Allee effect such as given by Eqs. (3.5), (3.11), (3.12) and (3.13).

We emphasise that the interplay between time delay and the Allee effect can be subtle and rather counterintuitive. In our study, we revisit the notable destabilising effect of time delays, as for a fixed Allee threshold an increase in time delay leads to oscillatory behaviour, in most models. However, depending on the particular description of the delayed process, the shape of the bifurcation curves can change significantly; see Figs. 3.2, 3.6 and 3.7. In all three corresponding models the same underlying ecological process (i.e. competition) is subject to delay, yet the results are considerably different. In addition, the possibility of the population driven to extinction occurs only in the additive formulation of the Allee effect (Figs. 3.6, 3.7 and 3.8) but not in the multiplicative one (Fig. 3.2). Also, the pattern of population growth can be remarkably different depending on whether the time delayed cooperation is described by multiplicative or additive formulations of the model, cf. Figs. 3.4 and 3.5. These results indicate strong dependence on the choice of functional form (parametrisation), thereby evoking the controversial issue of model sensitivity (*Adamson and Morozov 2012*, *Fussmann and Blasius 2005*).

The majority of population fluctuations are described by the generally accepted specialist predator (or parasitoid) hypothesis, with just a few exceptional cases involving other kinds of trophic interactions (*Turchin 2003*). This of course does not guarantee nor imply that intrinsic controlling mechanisms are completely absent in populations. However, to date such inherent hypotheses have not fully provided theoretically sound and empirically supported population models (due to tenuous connections to data). We emphasise that our intention was not to develop a comprehensive framework or provide a unique solution to population cycles, but rather to demonstrate and gain informative insight into the consequences of delayed feedback mechanisms and their interaction with density dependence through the Allee effect. Time delays are integral parts of ecological systems, and as such may aid in explaining underlying mechanisms of complex population dynamics such as population fluctuations. A common standpoint is that in stable (non-oscillating)

populations these time lags are insufficiently large to cause fluctuations, therefore are disregarded. We hereby tentatively propose that even non-fluctuating populations may be subject to delayed processes that do not alter population stability, such as positive density dependent mechanisms, i.e. cooperation.

Chapter 4

Power laws, time delays and population dynamics

4.1   Introduction

Contributing to the controversy surrounding population variability is its inability
to be straightforwardly quantified (*Pimm and Redfearn 1988*). The understanding
of amplitude and frequency patterns of population fluctuations, why some pop-
ulations fluctuate cyclically, and others exhibit a lesser degree of periodicity is
closely related to the contentious issue of population regulation, touched upon in
the previous chapter. The long-standing debate over whether populations are reg-
ulated through internal, biotic mechanisms such as competition, or whether they
are mostly dominated by environmental forcing is very much ongoing, taking on
many other guises (*Sugihara 1995*). Though it is certain that both intrinsic and
extrinsic factors strongly influence population dynamics with the prevalence of one
or the other being case specific (*Steele 1985*), particular difficulty lies in outlining
the contribution of each (*Kaitala and Ranta 1996*). Ecological time series offer
some insight into the underlying ecological processes driving population dynamics
(*Turchin et al. 1999*), though are all too often of insufficient length to suggest a
more general explanation.

A common feature of long-term ecological time series ($>$ 30 years) is the in-
creasing temporal variability of population abundance (*Akçakaya et al. 2003*).
The fact that population abundance does not converge but rather fluctuates has
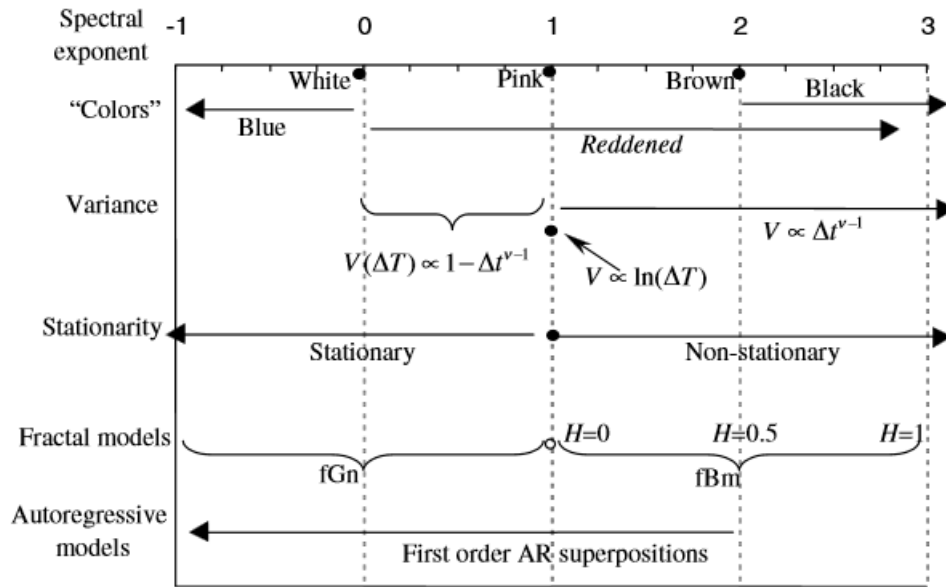
FIGURE 4.1: Classification of different types of "coloured" noise in terms of spectral exponent. The figure shows basic properties of coloured noise such as the variance, and gives an overview of models that take into account and generate such processes. Common characteristics of time series such as spectral exponent, ν, and Hurst exponent, H, indicate the "colour" of noise. Taken from *Halley and Inchausti 2004.*

prompted the proposal of various mechanisms and models to account for this phenomenon including environmental variability (*Lawton 1988*), age-structure (*McArdle 1989*), stochastic delayed dependence (*Kaitala and Ranta 1996*), spatial subdivision (*White et al. 1996*) and $1/f$ noise (*Halley 1996*). In general, statistical properties (e.g. colour) of ecological time series are determined by Fourier analysis, which results in the relationship between a range of frequencies and their relative importance to the given data set (power spectrum). The prevalence of long-term, low frequency trends in time series data results in the "reddening" of the power spectrum[1], estimated by the spectral exponent (see Fig. 4.1). Typically, ecological time series display behaviour intermediate between the two mathematically favoured, contrasting processes: white noise and random walk (see *Vasseur and McCann 2007*), despite the fact that modelling efforts show a strong tendency to overlook the subject of correlation structure altogether (*Halley 1996*). If, on the other hand, attempts to include correlation structure are made, they are usually limited to autoregressive processes characterised by exponentially decaying memory which lead to mathematically tractable models and imply a relatively short-lived dependence on past events. Emerging and growing evidence suggests

---

[1] The terminology "reddening of power spectrum" is an analogy made with the optical spectrum, as a surplus of low frequency, long wavelength light makes it appear redder.

that observed properties of ecological time series can be adequately represented by coloured noise, in particular the family of $1/f^\nu$ noise ($0 < \nu < 2$). All $1/f^\nu$, or power law noises as they are sometimes referred to, are defined by their power spectrum which is inversely proportional to the frequency:

$$S(\omega) \propto \frac{1}{\omega^\nu} \sim \frac{1}{f^\nu}\,, \tag{4.1}$$

where $\omega = 2\pi f$ is the angular frequency. Power-law noise shares important features with ecological time series such as fractality, variance growth and long-term memory. In addition, the autocorrelation function ψ has a power law dependence on the time delay:

$$\psi(\tau) \propto \frac{1}{\tau^{1-\nu}} \quad for \quad \nu < 1\,. \tag{4.2}$$

Defining autocorrelation functions for non-stationary members of the $1/f^\nu$ family proves more difficult due to the logarithmic dependence not only on the time lag, τ, but also on the (current) time of observation, Δt (*Kasdin 1995*). Specifically, the memory of pink noise ($\nu = 1$) has been studied in detail, and shows the longest memory with approximately equal correlation of recent and very distant events to present ones (*Keshner 1982*).

Recent theoretical studies stress the importance of these "reddened" spectra for population dynamics and estimation of expected extinction likelihood (*Halley and Kunin 1999, Cuddington and Yodzis 1999, Lawton 1988*). Growing population variability along with reddened spectra was found in data of 123 species out of 544 natural populations over a 30 year time span (*Inchausti and Halley 2002*). Similar independent studies carried out by *Ariño and Pimm (1995)* and *Vasseur and Yodzis (2004)* also corroborate such findings. In particular, it has been hypothesised that marine environments and populations tend to be redder than terrestrial ones (*Steele 1985*). Spatial variability of bird species' abundance has been shown to exhibit reddened spectra (*Storch et al. 2002*), alongside reddened spectra of both temporal and spatial dynamics of grasshopper populations in the western US (*Lockwood and Lockwood 1997*).

Although a comprehensive understanding of the underlying ecological mechanisms responsible for the distinctive population dynamics exhibiting $1/f^\nu$ noise traits is yet to be found, the most common explanation is attributed to extrinsic, fluctuating environmental conditions (*Lawton 1988, Vasseur and McCann 2007, Ruokalainen et al. 2009*). In some cases, environmental stochasticity merely superimposes noise on the time series thereby corrupting it, though in others this

forcing may significantly alter qualitative features of population dynamics, even completely masking deterministic elements which consequently may lead to an increased risk of extinction estimation (*Lundberg et al. 2000*). Therefore, the dominance of low frequency events in fluctuations of the abiotic environment is merely mirrored in ecological time series. Alternatively, experimental studies of the spatiotemporal dynamics of isolated, laboratory insect populations indicate the pervasiveness of low frequencies in time series (*Miramontes and Rohani 1998*), suggesting more intrinsic mechanisms influencing population dynamics. Furthermore, reddened time series of population dynamics have been shown to be independent of the colour of environmental noise (*Petchey 2000*). These studies seem to suggest that reddened population dynamics may not necessarily need to be explained through extrinsic influences, but rather efforts should be directed towards some possible within population mechanisms.

Motivated by the prevalence of time delays in ecology and the clear influence of $1/f^\nu$ noise-like dynamics, we aim to combine these two concepts into a rather simple population model. We consider a deterministic single species model with logistic growth and incorporate a distributed time delay, resulting in an integro-differential equation. We then analyse and compare the system's response to different delay kernels i.e. rates of decay: the null model of exponentially decaying kernel versus the power law memory kernel prompted by $1/f$ noise dynamics. Despite the abundant literature on time delay population models, to the best of our knowledge the interplay between logistic growth and a power law memory kernel still remains unaddressed. In the following section, we introduce some basic properties of $1/f$ noise, relevant to ecology, and then in Section 4.3 we revisit proof that a $1/f$ noise spectrum implies a power law governed autocorrelation function. Subsequently, in Section 4.4 we introduce our modelling framework and present simulation results. A brief summary of results is given in Section 4.5.

4.2   The importance of $1/f$ noise

Processes shaping population dynamics have been shown to act on different time scales in a correlated manner (*Balkind et al. 2013*) and as a consequence of this multi-scaled randomness "reddening" of time series' power spectra appears. Contrary to the expectation that both rare and frequent events are of equal importance, reddened power spectra indicate the longer-lasting influence of low frequency ones,

bringing assumptions of the hitherto default white noise hypothesis into question. Indeed, the majority of populations show long-term trends in abundance, albeit for different reasons and in different ways (*Pimm and Redfearn 1988*). Unfortunately, the available population data is often sparse as it is rarely long enough to sustain sensible spectral analyses, however some conjectures can still be made and there is good reason to believe $1/f$ noise can offer a reasonable description.

Spectral analysis is a commonly used tool in studying population dynamics (*Schaffer 1984, Storch et al. 2002, Tamburello et al. 2013*) and allows for the decomposition of ecological time series into frequency components. The resulting power spectra indicate the contribution of frequencies to the variance of the time series and suggest the form of correlation[2]. Before progressing further, I introduce the terminology that will be used hereafter: $1/f$ noise will refer to $1/f^\nu$ noise with the spectral exponent $0 < \nu < 2$, near pink noise has spectral exponent $0.5 \leq \nu \leq 1.5$, pink noise refers to the case in which $\nu = 1$, and white noise corresponds to $\nu = 0$. The inverse proportionality of spectral density on frequency and autocorrelation on time delay is a signature trait of $1/f$ noise, alongside a long memory. On the contrary, the accepted null model of ecological variability has no memory and is constituted of an equal partition of frequencies – white noise ($\nu = 0$):

$$S(f) \sim \frac{1}{f^\nu} = 1 \quad \text{for} \quad \nu = 0\,, \tag{4.3}$$

resulting in a flat spectral density (see Fig. 4.2). This even distribution of different 'disturbances' over different timescales would be a reasonable modelling assumption, as it seemingly contains no bias. However, spectral density is only one of many ways of describing a power spectrum and bias-free depictions of variability are a matter of perspective (*Halley and Inchausti 2004*). Looking into the relative significance given to timescales is also of interest, and it reveals the biased nature of white noise. Whilst white noise contains all frequencies it favours shorter timescales, and on the other side of the spectrum Brown noise assigns more importance to longer timescales. What sets apart the family of $1/f$ noise is exactly that it contains memory of all past events equally on all timescales (*Keshner 1982*). Translated to population dynamics, population densities are not only a function of their recent past, but also are influenced by long-term history events in an invariant manner, which is typical of many ecological time series (*Storch et al. 2002*).

---

[2]An additional measure of a stochastic process is its power spectrum or spectral density, describing how the 'signal' of a time series is distributed over different frequencies. This helps to identify any periodicities and define correlation structures (*Blackman and Tukey 1958*).
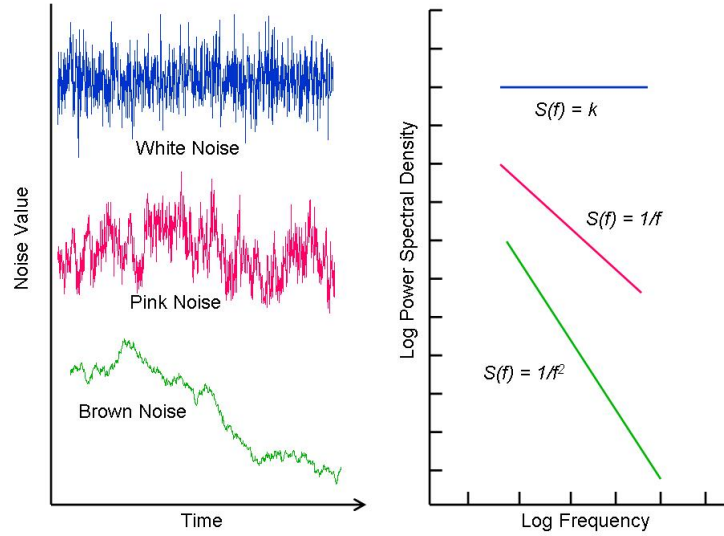
FIGURE 4.2: An illustration of power spectra of white, brown and pink noise. Figure taken from `http://www.scholarpedia.org/article/File:Scholarpedia_fig1.jpg`.

Indeed, *Ariño and Pimm (1995)* explicitly calculated Hurst exponents [3] for time series of 58 different species and concluded that the mean exponent lies "halfway between Brownian and white noise", indicating the ubiquity of $1/f$ noise in natural populations.

The longer the time series, the more variation is observed, and this "more time means more variation" (*Lawton 1988*) concept is another feature that makes $1/f$ noise attractive for modelling purposes. Growing variance is another key feature of $1/f$ noise, and for an observation time Δt the dependence is as follows (*Halley and Inchausti 2004*):

$$\sigma^2(\Delta t) \quad \propto \quad 1 - \Delta t^{\nu-1}, \quad \forall \nu < 1 \tag{4.4}$$

$$\sigma^2(\Delta t) \quad \propto \quad ln(\Delta t), \quad \nu = 1 \tag{4.5}$$

$$\sigma^2(\Delta t) \quad \propto \quad \Delta t^{\nu-1}, \quad \forall \nu > 1, \tag{4.6}$$

with the apparent singularity for $\nu < 1$ not being relevant as we are dealing with long time series (Δt is large). New empirical evidence of $1/f$ noise in natural populations is constantly emerging as the topic gradually receives more attention. Power law relationships in ecology seem to be more common than first anticipated.

---

[3]Hurst exponents act as a measure of long-term time series, and relate to the autocorrelation of time series. The Hurst exponent for Brown noise is $H = 0.5$, and $0 < H < 0.5$ indicates positive correlation between observations and $0.5 < H < 1$ indicates a negative correlation (Fig. 4.1).

In the following section we revisit the proof that a power law governed spectral density implies a power law autocorrelation function.

4.3   Power law spectral density and autocorrelation

The results presented in this section have been known for long and are by no means novel (*Keshner 1982, Watanabe 2005, Szendro et al. 2001*), however the motivation to include them was based on the potential to better understand our proposed mathematical framework (Section 4.4) and justify our model formulation. In the following we demonstrate that the spectral density corresponding to $1/f$ noise results in a power law autocorrelation function with respect to time delay. Following the discovery of $1/f$ noise in 1925 (*Johnson 1925*), the widespread occurrence of processes exhibiting such behaviour called for a generally recognised physical explanation of the phenomenon. Though mathematical descriptions such as Fractional Brownian Motion offer some insight, a well-established theory is still lacking. One of the proposed methods is described in *Watanabe (2005)* which we follow. Under the assumption that the average decay of a fluctuating quantity, X, follows an exponential relaxation, the autocorrelation function is given as:

$$\psi_\tau(t) = \overline{X}^2 \mathrm{e}^{-t/\tau} \, , \tag{4.7}$$

where τ is the relaxation (decay) time. The spectral density, $S_\tau(f)$, can then be found as a Fourier transform of $\psi_\tau(t)$ (Wiener-Khinchine theory):

$$S_\tau(f) = \overline{X}^2 \frac{4\tau}{1 + (2\pi f\tau)^2} = \overline{X}^2 \frac{4\tau}{1 + (\omega\tau)^2} \, . \tag{4.8}$$

The ansatz is that the $1/f$ spectrum can be generated by the summing of simple 'Lorentzian' like spectra described by Eqs. (4.7) and (4.8), over a wide range of relaxation times in the interval between τ_1 and τ_2, given the weighting function $g(\tau)$:

$$g(\tau) = a\tau^{-\alpha} \, . \tag{4.9}$$

In order to obtain a $1/f$ spectrum by summation of Lorentzian spectra the distribution of relaxation times (τ's) should be as in Eq. (4.9) (*Hooge and Bobbert 1997*).

We then normalise the distribution weight:

$$\int_{\tau_1}^{\tau_2} a\tau^{-\alpha}d\tau = \frac{a}{1-\alpha}\left(\tau_2^{1-\alpha} - \tau_1^{1-\alpha}\right) = 1 \; , \tag{4.10}$$

and to determine the value of constant a, we distinguish between two cases:

$$\alpha = 1: \quad a = \frac{1}{ln(\tau_2/\tau_1)} \tag{4.11}$$

$$\alpha \neq 1: \quad a = \frac{1-\alpha}{\tau_2^{1-\alpha} - \tau_1^{1-\alpha}} \; . \tag{4.12}$$

The linear superposition of Lorentzian spectra results in a $1/f$ spectrum with the autocorrelation function and spectral density taking the following form:

$$\psi(t) = \overline{X}^2 \int_{\tau_1}^{\tau_2} g(\tau)\mathrm{e}^{-t/\tau}d\tau \tag{4.13}$$

$$S(f) = \overline{X}^2 \int_{\tau_1}^{\tau_2} g(\tau)\frac{4\tau}{1+(2\pi f\tau)^2}d\tau \; . \tag{4.14}$$

Then, the power spectral density can be rewritten as:

$$S(\omega) = \overline{X}^2 \int_{\tau_1}^{\tau_2} \frac{a}{\tau^\alpha}\frac{4\tau}{1+(\omega\tau)^2}d\tau = \frac{4a\overline{X}^2}{\omega^{2-\alpha}}\int_{\omega\tau_1}^{\omega\tau_2}\frac{(\omega\tau)^{1-\alpha}}{1+(\omega\tau)^2}d\omega\tau \; . \tag{4.15}$$

By letting $\tau_1 \to 0$ and $\tau_2 \to \infty$, the integral becomes:

$$\int_0^\infty \frac{(\omega\tau)^{1-\alpha}}{1+(\omega\tau)^2}d\omega\tau \; . \tag{4.16}$$

By solving the above integral, the spectral density takes the form:

$$S(\omega) = \frac{4a\overline{X}^2}{\omega^{2-\alpha}}\frac{\pi}{2}\csc\frac{\alpha\pi}{2} = 2\pi\frac{a\overline{X}^2}{\omega^{2-\alpha}}\csc\frac{\alpha\pi}{2} \; , \tag{4.17}$$

or a more simplified version:

$$S(\omega) = A\omega^{-2+\alpha} \; , \quad \text{for} \quad 0 < \alpha < 2 \quad \text{and} \quad \alpha \neq 1, \tag{4.18}$$

which indicates the spectral density being inversely proportional to the angular frequency ω. The constant A is specified as:

$$A = \frac{(1-\alpha)\overline{X}^2}{\tau_2^{1-\alpha} - \tau_1^{1-\alpha}}2\pi\csc\frac{\alpha\pi}{2} \; . \tag{4.19}$$

To obtain the autocorrelation function, we differentiate Eq. (4.13):

$$\frac{d\psi(t)}{dt} = \frac{d}{dt}\left\{ a\overline{X}^2 \int_{\tau_1}^{\tau_2} \tau^{-\alpha}\mathrm{e}^{-t/\tau}d\tau \right\} = -a\overline{X}^2 \int_{\tau_1}^{\tau_2} \tau^{-\alpha-1}\mathrm{e}^{-t/\tau}d\tau \ . \qquad (4.20)$$

Following a straightforward change of variables, $T = 1/\tau$, Eq. (4.20) can be written as:

$$\frac{d\psi(t)}{dt} = a\overline{X}^2 \int_{1/\tau_1}^{1/\tau_2} T^{\alpha-1}\mathrm{e}^{-tT}dT. \qquad (4.21)$$

By integrating, we obtain the final expression for the autocorrelation function $\psi(t)$, now containing two relaxation times (delays), τ_1 and τ_2:

$$\psi(t) = C - \overline{X}^2\Gamma(\alpha)\frac{t^{1-\alpha}}{\tau_2^{1-\alpha} - \tau_1^{1-\alpha}} \quad \text{for} \quad 0 < \alpha < 1\,, \qquad (4.22)$$

where Γ is the gamma function and C is the integration constant which can be found by defining appropriate initial conditions. A power law dependence on time delay is also found for the case $1 < \alpha < 2$ (see *Watanabe (2005)* for a full discussion). It is readily seen that instead of an exponential dependence, the autocorrelation function now is inversely related to the decay time, τ, following a power law. This analysis holds for all members of the $1/f$ noise family, with the exception of pink noise. For the case of pink noise, corresponding to $\alpha = 1$, the autocorrelation function follows a logarithmic law (*Keshner 1982, 1979, Hooge and Bobbert 1997*):

$$\psi(t) = \overline{X}^2\,\frac{\ln\left(\frac{\tau_2}{t}\right)}{\ln\left(\frac{\tau_2}{\tau_1}\right)} \quad \text{for} \quad \tau_1 < t < \tau_2\,. \qquad (4.23)$$

4.4   Model and results

From the spatiotemporal variability of orchids (*Gillman and Dodd 1998*) to shell-changing behaviour of hermit crabs (*Kitabayashi et al. 2002*) power laws seem to be more common than first thought. Correspondingly, we formulate a single species population model with distributed time delay, such that the delay follows a power law decay. The motivation behind such an assumption lies in the ubiquity of $1/f$ noise-like behaviour in natural populations and their power law autocorrelation functions. We first test our null model of exponentially decaying memory both analytically and numerically, and subsequently formulate an alternative model consisting of a power law memory kernel. Under the spatial homogeneity

assumption, we consider a population governed by logistic growth subject to a distributed time delay:

$$\frac{dU}{dt} = rU(t) \left[1 - \frac{1}{K} \int_{-\infty}^{t} G(t-s)U(s)ds \right],$$ (4.24)

where K is the carrying capacity and G is the memory kernel indicating the amount of emphasis that should be given to the size of the population at earlier times in order to determine the present effect on population dynamics (*Murray 2002*). In general, the memory kernel is normalised:

$$\int_{0}^{\infty} G(s)ds = 1,$$ (4.25)

so that discrete delay is a limiting case when $G(s)$ is the Dirac function, $\delta(t-\tau)$:

$$\int_{-\infty}^{\infty} \delta(t-\tau-s)U(s)ds = U(t-\tau).$$ (4.26)

Different forms of memory kernels are employed depending on the topic of research, with exponential kernels prevailing in the literature, due to their mathematical tractability. As a starting point we choose a fairly simple step kernel to test the model predictions and then gradually increase complexity:

$$G(t-s) = a \quad \text{for} \quad 0 < t-s < \frac{1}{a} \quad \text{otherwise} \quad G(t-s) = 0,$$ (4.27)

where $a > 0$ acts as the time delay parameter. The units of a should be inversely proportional to time, therefore a higher value of a should correspond to a smaller time delay, whilst lower values of a should instigate oscillatory behaviour, with the upper equilibrium losing stability. The model was solved by finite-differences using the explicit Euler scheme as a numerical approximation (see Appendix A), and the integral itself was solved by implementing the trapezium rule. Furthermore, as an immediate consequence of the normalisation condition, Eq. (4.25), we take the integration limits to be $t - 1/a$ and t. We have chosen a sufficiently small time step to avoid numerical errors which ensures the accuracy of our results (see Fig. 4.3). For the population's history a constant function ($U_0 = 0.5$) has been chosen, as other, more complicated forms did not show qualitative or quantitative effects on solution behaviour or stability. Examples of typical solution behaviour are given in Fig. 4.4. For a relatively large value of a, the solution shows a monotonous approach to the system's carrying capacity, and by gradually decreasing a the solution loses monotonicity, resulting in damped oscillations. For a sufficiently
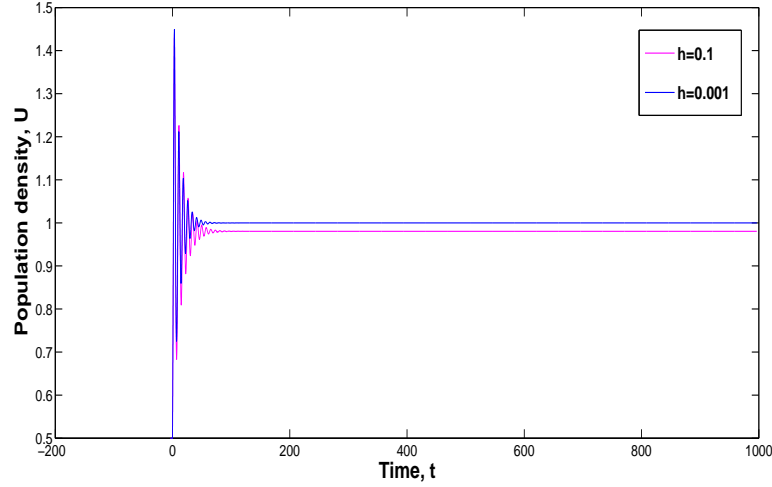
FIGURE 4.3: Impact of changing the time step on solution accuracy for the constant memory kernel. Value of bifurcation parameter in simulations is $a = 0.3$. The intrinsic rate of growth and the carrying capacity are as follows: $r = 1$ and $K = 1$.

small a the solution loses stability through the Hopf bifurcation, and limit cycles appear ($a = 0.2$). A further decrease in a results in an increase in amplitude of the limit cycle with the solution staying in the vicinity of the extinction equilibrium for longer.

As a next step we choose the delay kernel to be of exponential form, exhibiting a rapid decay and short memory. Such a thin-tailed distribution kernel allows for analytical analysis of the corresponding model. Accordingly, the system is modelled by:

$$\frac{dU}{dt} = rU(t)\left[1 - \frac{1}{K}\int_{-\infty}^{t} ae^{-a(t-s)}U(s)ds\right]. \tag{4.28}$$

The analytical method for studying such systems is known as the linear chain trick, and consists of the transformation of a delay differential equation into a system of ODEs, by simply redefining the integral:

$$\frac{dU}{dt} = rU\left(1 - \frac{Q}{K}\right) \tag{4.29}$$

$$\frac{dQ}{dt} = a(U - Q), \tag{4.30}$$

where $Q = \int_{-\infty}^{t} U(s)G(t-s)ds$. Following standard linear stability analysis we conclude that the positive equilibrium (K, K) is always stable for positive a (Fig. 4.6). This prediction fits well with our simulation results, as for smaller a we
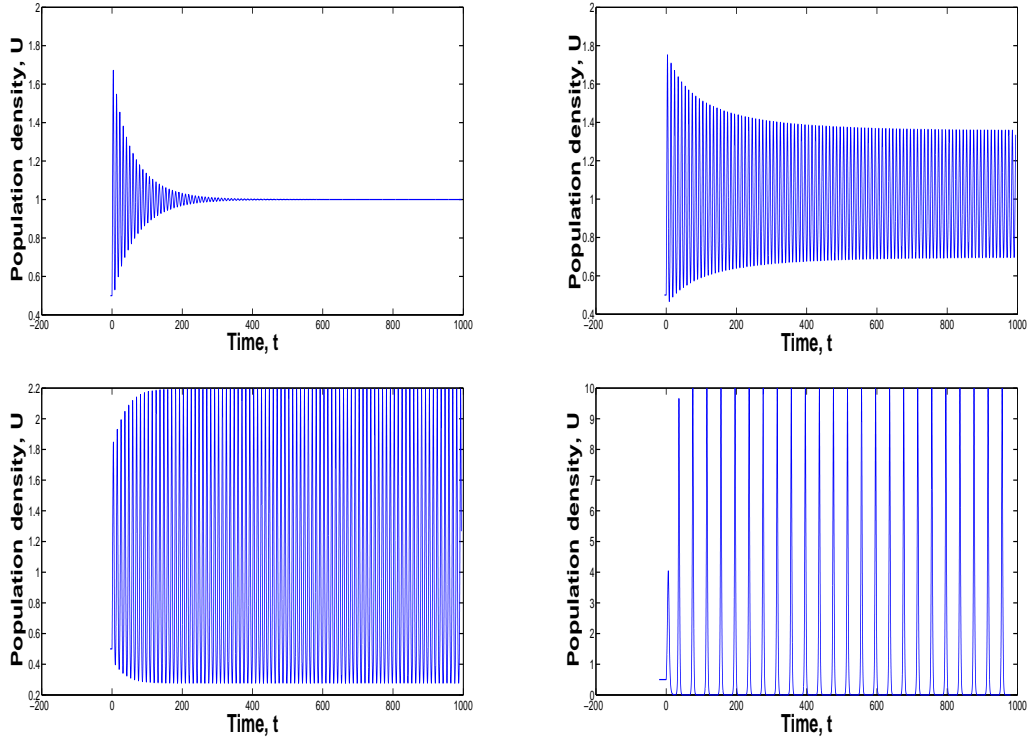
FIGURE 4.4: By decreasing the bifurcation parameter, a, we can clearly distinguish between different scenarios (from left to right, top to bottom): damped oscillations, limit cycle at bifurcation point and limit cycles beyond bifurcation point (bottom row). Respectively, the values of bifurcation parameter a are 0.22, 0.2, 0.18 and 0.05. The intrinsic rate of growth and the carrying capacity are as follows: $r = 1$ and $K = 1$.

observe damped oscillations, and for an increase in the bifurcation parameter they disappear (i.e. solution is monotonous). With increasing complexity of the delay kernel the sensitivity to numerical approximation also increases (see Fig. 4.5), as does the computational effort due to the larger integration domains required.

Based on the significant ecological literature and evidence indicating the ubiquity of $1/f$ noise dynamics (see Sections 4.1 and 4.2), we now investigate a population model in which the significance of past populations decays according to a power law:

$$G(t - s) = \frac{1}{a^p + (t - s)^p} \quad \text{for} \quad p \geq 0 \ . \tag{4.31}$$

We then normalise the memory kernel, which results in:

$$\frac{dU}{dt} = rU \left(1 - \frac{C}{K} \int_{-\infty}^{t} \frac{U(s)}{a^p + (t - s)^p} ds \right), \tag{4.32}$$

where $C = pa^{(p-1)}/\pi \csc(\pi/p)$. We choose a as the controlling parameter, and observe the system's response to its variation, where higher values of a correspond
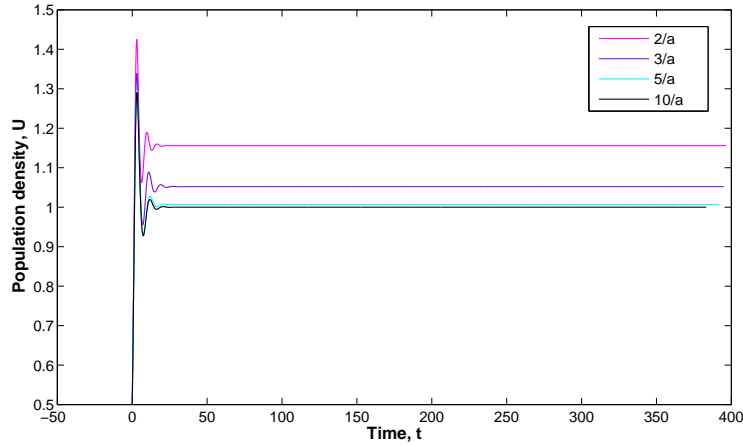
FIGURE 4.5: Impact of different integration limits on solution accuracy for the exponential kernel. The bifurcation parameter is $a = 0.6$. The intrinsic rate of growth and the carrying capacity are as follows: $r = 1$ and $K = 1$.
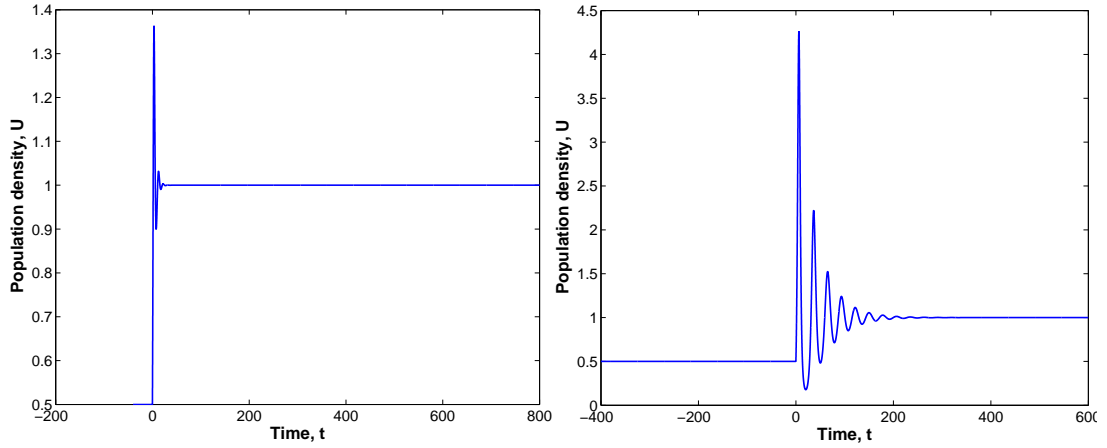

FIGURE 4.6: Snapshots of temporal behaviour of solution for different values of bifurcation parameter a for model (4.28). From left to right the bifurcation parameter a decreases tenfold, i.e. from 0.5 to 0.05. The intrinsic rate of growth and the carrying capacity are as follows: $r = 1$ and $K = 1$. The lower limit of integration is $t - 20/a$

to a larger "delay" and therefore should destabilise the system. Results presented include only numerical simulations, which were done for a range of values of the degree of kernel. The integration limits were chosen accordingly to ensure necessary accuracy of results and in particular for smaller values of p larger integration domains were needed (e.g. for $p = 2$ the integration domain is $\sim 150a$). For all tested values of $p \geq 2$, an increase in the bifurcation parameter a leads to the occurrence of limit cycle behaviour. Interestingly, lower powers $(p = 2)$ are more robust to the effect of time delay, as significantly higher values of a are needed to destabilise the system, however for $p < 2$ we could not find any bifurcation values.

TABLE 4.1: Summary of bifurcation values for different degrees of the memory kernel. Note that bifurcation values have been checked up to $a = 300$. Bifurcation values checked for $r = 1$ and $K = 1$.

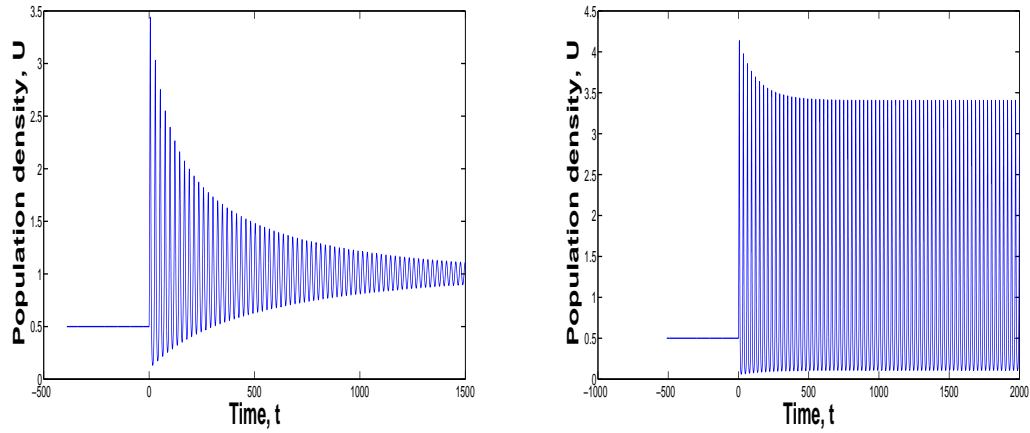| Degree of memory kernel, p	Bifurcation value, a
1.5	no bifurcation value
2	81
3	15
4	9
5	7
6	7
7	6
8	6
9	6
10	6
15	6
20	5
30	5
50	5

FIGURE 4.7: Temporal behaviour of solution for power law memory kernel. The simulation parameters are $p = 3$, $a = 13$ (left) and $a = 17$(right). Other parameters are taken to be $r = 1$ and $K = 1$.

Table 4.1 shows the dependence of the bifurcation value on the kernel degree.

Our main interest was on temporal dynamics, but we have also looked into the spatial dynamics by incorporating diffusive effects into the simplest model with a constant memory kernel, resulting in an integrodifferential equation:

$$\frac{\partial U}{\partial t} = D\frac{\partial^2 U}{\partial x^2} + rU\left[1 - \frac{1}{K}\int_{t-1/a}^{t} aU(s)ds\right], \qquad (4.33)$$

where D is the diffusion coefficient. As before, we used finite-differences to solve
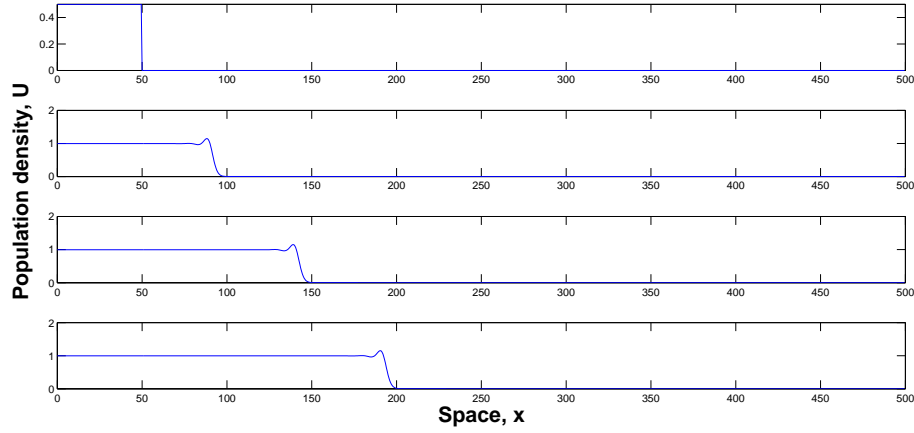
FIGURE 4.8: Spatial propagation of travelling front given at equidistant moments in time for model (4.33): $t = 1$, $t = 334$, $t = 667$ and $t = 999$. The parameters are as follows: $a = 0.7$, $r = 1$, $K = 1$ and $L = 100$.

the equation, and the trapezium rule to approximate the integral. We choose a as the controlling parameter, and choose sufficiently small mesh steps ($\Delta t = 0.01$, $\Delta x = 0.5$) to ensure the accuracy of the solution. The spatial domain was chosen to be sufficiently large to avoid the impact of boundaries, and at the boundaries Neumann "no flux" conditions were implemented. The initial condition is chosen as:

$$U(x,0) = U_0 \quad \text{if} \quad |x| \leq \frac{L}{2}, \quad \text{otherwise} \quad U(x,0) = 0, \qquad (4.34)$$

where $U_0 > 0$ is the initial population density and L determines the size of the initially occupied patch ($L = 1000$). As before, we choose the population's history to be a constant function equal to the population's initial density, $U_0 = 0.5$. For a sufficiently large value of a, Fig. 4.8 shows the spatial propagation of the population front at equidistant moments in time. As the solution is symmetric with respect to the origin, Figs. 4.8-4.10 show only the right-hand side of the domain. The population fronts are travelling waves which exhibit nonmonotonous decaying oscillations at the leading edge. Fig. 4.8 shows a small hump at the edge of the front which with decreasing a becomes more prominent and for a sufficiently small value of a regular oscillations appear, forming a wavetrain (Fig. 4.9). The value of the controlling parameter, a, when the system passes through the Hopf bifurcation and begins to cycle corresponds to the nonspatial system ($a = 0.2$). Regular oscillations are also observed in the temporal dynamics, recorded at half the numerical spatial domain, of this system for the corresponding parameter set (Fig. 4.10).
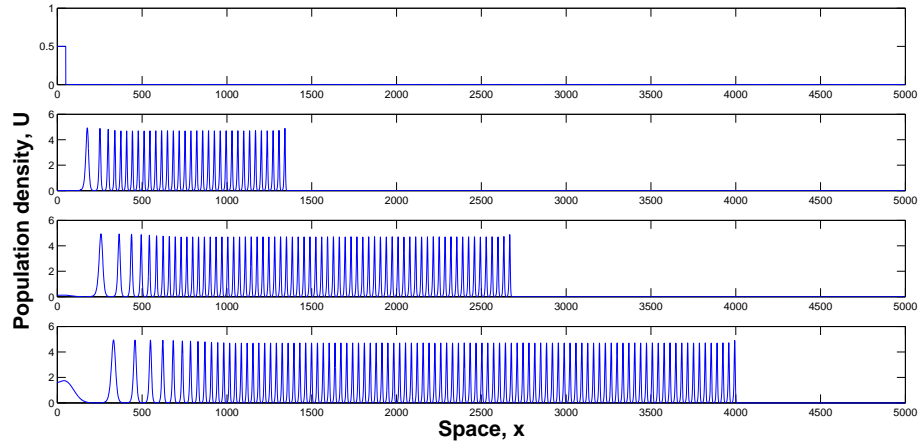
FIGURE 4.9: Spatial propagation of travelling front given at equidistant moments in time for model (4.33): $t = 10$, $t = 673$, $t = 1336$ and $t = 1999$. The parameters are as follows: $a = 0.1$, $r = 1$, $K = 1$ and $L = 100$.
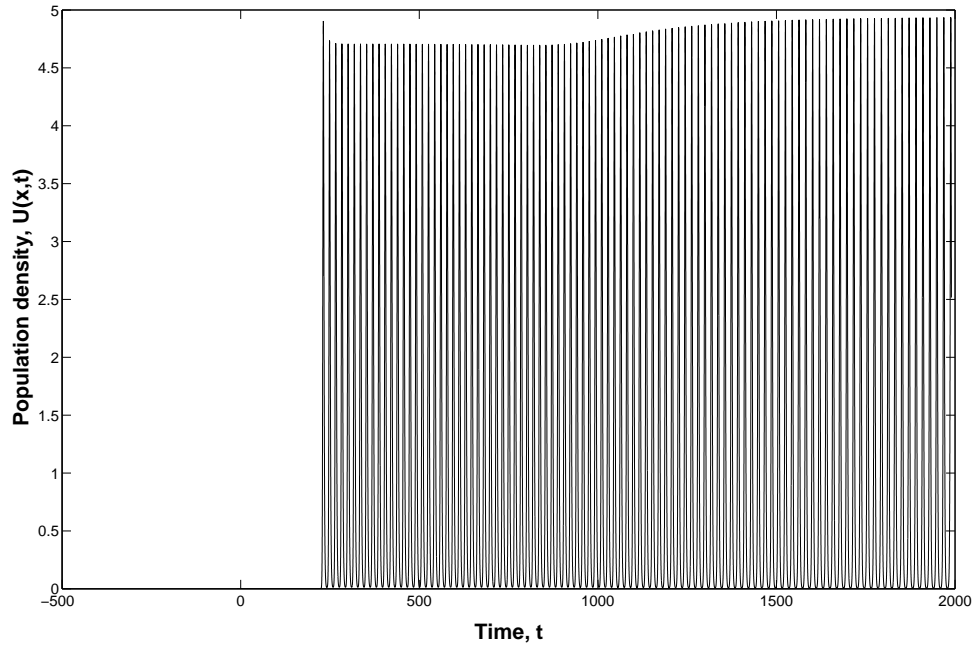

FIGURE 4.10: Temporal propagation of travelling front for model (4.33) with $a = 0.1$, $r = 1$, $K = 1$ and $L = 100$.

4.5 Discussion and Concluding remarks

Our intention in this chapter was to combine two concepts that have been gaining growing attention from the theoretical ecology community: time delay and $1/f$ noise-like dynamics. Building upon the questions addressed in the previous chapter, our interest here lies not only in determining the conditions of destabilising time delay effects, but also on ecologically relevant forms of such. Both mathematically and ecologically a distributed time delay gives a more realistic description of population dynamics. However, models dominating the literature are mostly chosen due to their tractability, rather than on the observed natural populations. Using a single-species context we study, mostly numerically, three different types of memory kernels and their effect on the system's stability. The main focus is on population fluctuations (temporal dynamics), but we have extended our study to incorporate some spatial effects as well. We investigate the interplay between logistic growth and distributed time delay, and particularly motivated by the plenitude of evidence supporting $1/f$ noise-like dynamics we combine a key feature, the power law autocorrelation, with the concept of distributed delay. By comparing the resulting population dynamics with differing rates of decay, we conclude that depending on the rate of decay of memory kernels time delays are not necessarily destabilising, as thin tailed kernels such as an exponential one do not generate population cycles.

Chapter 5

Delay driven chaos in single species population models

5.1   Introduction

Factors and mechanisms determining the spatial population distribution of ecological species are a major focus of interest in ecology (*Fortin and Dale 2005*, *Ritchie 2010*). Often the distribution shows remarkable spatial variability, which is usually referred to as patchiness (*Levin 1994*, *Rietkerk et al. 2004*), where areas or "patches" of high population density are separated from areas where the given species is either present at a very low density or is absent altogether. A classical example of such a patchy spatial distribution is given by plankton (*Levin and Segel 1976*, *Martin 2003*), although terrestrial species, in particular insects, often exhibit considerable spatial variability as well (*Liebhold et al. 2013*).

One obvious explanation of this phenomenon is swarming behaviour (*Okubo 1986*). On a larger spatial scale, an intuitive explanation of the spatial heterogeneity in species distribution relates it to the variability of the environment, e.g. being driven by the heterogeneous distribution of resources (*Liebhold et al. 1994*, *Grünbaum 2012*). However, in many cases this does not seem to be the case as the observed population distributions appear to be largely uncorrelated with the environment (*Powell et al. 1975*, *Sharov et al. 1997*). The heterogeneous spatial population distribution can also arise as a result of biotic interactions. In particular, there is a large body of literature showing, both theoretically and empirically, that a spatial pattern can be a result of prey-predator or host-parasite interactions

(*Hassell et al. 1991, Hastings et al. 1997, Davis et al. 1998, Petrovskii and Mal-chow 1999, Jankovic and Petrovskii 2013*), or multi-specific competition (*Petrovskii et al. 2001, Adamson and Morozov 2012, Mimura and Tohma 2014*). Note that, in the case of biotic-driven pattern formation, the patterns can be regarded as self-organised, i.e. they are not related to any external forcing; in particular, they can arise in a uniform environment.

Formation of a self-organised pattern is often related to instability of the spatially uniform distribution; a classical example of such instability is given by the Turing instability (*Segel and Jackson 1972, Klausmeier 1999*). However, a necessary condition of the Turing instability is the differing diffusivity of interacting species; in order to make the instability practically observable (i.e. to occur in a reasonably broad range of population dynamics' parameters), the diffusion coefficients have to be different by at least an order of magnitude. This large difference in the mobility of a prey and its predator does not often happen, and hence the ecological importance of the Turing scenario of pattern formation is rather limited (but see *Sherratt 2013*).

An alternative mechanism is sometimes referred to as biological turbulence[1] or a "wave of chaos" (*Petrovskii and Malchow 2001*) and it appears to be possible when the dynamics of the interacting species are oscillatory. In the theoretical context, this is usually related to the existence of a stable limit cycle, e.g. see *Turchin (2003)*. The properties of the population's spatial distribution emerging due to this mechanism were shown to be in agreement with field observations (*Medvinsky et al. 2002, Petrovskii et al. 2003, Malchow et al. 2008*). However, the capacity of biological turbulence to explain patchiness of ecological populations is somewhat limited too, as the existence of the limit-cycle population oscillations requires interaction of the given species (prey) with its specialist predator (cf. *Rosenzweig 1971, May 1972*). Specialist predators are relatively rare in nature and that may explain why the genuine predator-prey cycles are not often seen[2]. As far as the predator is a generalist, in a realistic multi-species community predator-prey cycles are unlikely to occur, as the changes in the density of prey becomes uncoupled from that of the predator because of the complicated switching behaviour of the latter (*Comins and Hassell 1976, Holt 1983, Van Leeuwen et*

---

[1]The term "biological turbulence" was suggested to Sergei Petrovskii by Lutz Schimansky-Geier in a private discussion in 1999.

[2]The famous hare-lynx cycle (*Elton and Nicholson 1942, May 1975*) is sometimes regarded as the only available example, although there are different opinions on that (cf. *Sherratt and Smith 2008*) and the discussion is by no means over.

al. 2013, Morozov and Petrovskii 2013). Heterogeneous population distribution is therefore a far more general phenomenon than the theoretical mechanisms that have by far been brought forward as its explanation.

As was demonstrated in previous chapters, another feature of population dynamics as ubiquitous as species heterogeneity, is time delay. Delayed density dependence is thought to be one of the main factors causing population fluctuations (*Berryman and Turchin 1997*). The most commonly considered causal mechanisms are resource competition (*Hansen et al. 1998*), cannibalism (*Briggs et al. 2000*), and maternal effects (*Ginzburg and Taneyhill 1994*) where the nutritional environment of the parental generation can influence the growth and reproductive potential of the next generation. Delays may also occur as a consequence of developmental time and/or interaction between individuals of different stages (*Royama 1981*). In mathematical terms, the destabilisation of a positive steady state, both in non-spatial and spatial systems, usually occurs through the Hopf bifurcation (*Green and Stech 1981, Fowler 1982, Busenberg and Huang 1996, Li et al. 2008, Su et al. 2009*) that leads to the limit-cycle oscillatory behaviour (but see Chapter 3 for a counter-example of the effects of time delay and a further discussion of this issue). In this chapter, we examine the inherent relation between these two phenomena, i.e. time delays and pattern formation. We are especially interested in the possibility of the onset of spatiotemporal chaos and, respectively, the formation of irregular spatial patterns. We mention here that, whilst the dynamics of time-delayed non-spatial systems are understood relatively well, time-delayed spatial systems pose a much bigger challenge. Although there is a large body of literature concerned with time-delayed spatially explicit population dynamics (e.g. see the references above), the vast majority of it is concerned with either a travelling front or a periodic pattern (*Ashwin et al. 2002, Yoshida 1982, Su et al. 2009*). Meanwhile, in population systems where limit cycles appear for other reasons (i.e. not related to time delay), travelling waves and periodic patterns are known to be only a part of the rich spectrum of spatiotemporal dynamics (*Petrovskii and Malchow 2000*) that, in particular, may exhibit chaotic oscillations (*Sherratt et al. 1995, Sherratt 2001, Petrovskii et al. 2001*). Correspondingly, the possibility of spatiotemporal pattern formation and chaos in a single species population with time delay is our main interest here. We first consider pattern formation triggered by travelling population fronts in a heuristic delayed diffusion-reaction equation where the delay is included into the per capita growth, and reveal the onset of spatiotemporal chaos in the wake of the front. We then consider a somewhat more realistic model

where the delay is appropriately spatially averaged (*Ashwin et al. 2002, Gourley and Bartuccelli 1995, Gourley and Chaplain 2002, Britton 1990*), which results in an integro-differential model, and show that it exhibits some qualitatively similar properties such as, in particular, the onset of chaos.

5.2 Modelling framework and some analytical results

The generic model describing temporal dynamics of a single species population was introduced earlier (Chapter 3) and consists of an ordinary differential equation. For many populations the observed biological reality imposes a saturation level, known as the carrying capacity, which forms a numerical upper bound on growth. Correspondingly, the simplest form of such, the classic Verhulst-Pearl logistic equation is frequently used to model self-limiting populations:

$$\frac{dU}{dt} = rU\left(1 - \frac{U}{K}\right),\tag{5.1}$$

where r is the intrinsic rate of growth and K is the carrying capacity. Logistic growth implies rapid initial growth at low population densities and a nearly exponential decay to the population's carrying capacity due to the negative feedback through intraspecific competition. Admittedly a simple model, such behaviour is in qualitative agreement with observed dynamics of many populations, especially under laboratory, resource-limited, conditions. In nature, though, events do not often occur instantaneously as predicted by the above model. For this reason, *Hutchinson (1948)* suggested a more appropriate and biologically sound model including a time delay accounting for hereditary terms contained in the regulatory mechanisms controlling growth, such as resource regeneration, maturation and gestation times. From *Hutchinson's (1948)* seminal paper and thereafter, time delay models have gained significance and become a much studied topic in mathematical ecology. The model proposed is a delay differential equation:

$$\frac{dU}{dt} = rU\left(1 - \frac{U_\tau}{K}\right),\tag{5.2}$$

where $\tau > 0$ is the time delay, and $U_\tau = U(t-\tau)$. Even though the choice of delayed mechanism still remains questionable, the above model was used extensively to model natural populations with reasonable success, see *May (1975)*.

Therefore, aiming to describe both spatial and temporal population dynamics, the model results in a delay reaction-diffusion equation:

$$\frac{\partial U}{\partial t} = D\frac{\partial^2 U}{\partial x^2} + rU\left(1 - \frac{U_\tau}{K}\right), \tag{5.3}$$

where D is the diffusion coefficient. In what follows, we present both analytical and numerical results to investigate the effect of time delay in Eq. (5.3). We consider Eq. (5.3) in the context of biological invasion (*Shigesada and Kawasaki 1997*), so that the 'initial' population distribution $U(x,t)$ for $-\tau < t < 0$ is assumed to be a function of compact support.

A general standpoint is that the addition of diffusive term will not change the system's dynamical structure, cf. *Huang 1998*. However, below we will show that this is not necessarily true and that a spatial model can exhibit dynamical regimes that are not possible in its nonspatial counterpart. Whilst the nonspatial Hutchinson's model is only capable of exhibiting periodic oscillations, its spatial counterpart can display chaos. Some of our results will then be extended, using numerical simulations, to include the corresponding 2D case:

$$\frac{\partial U}{\partial t} = D\left(\frac{\partial^2 U}{\partial x^2} + \frac{\partial^2 U}{\partial y^2}\right) + rU\left(1 - \frac{U_\tau}{K}\right), \tag{5.4}$$

where we also demonstrate the onset of chaotic oscillations.

5.2.1 Linear Stability Analysis

It is worth noting that single ordinary differential equations, unlike delay differential equations (DDEs), cannot exhibit oscillatory, limit cycle behaviour (see Fig. 5.1). While qualitative features of DDEs for population growth dynamics near bifurcation points, including analytical solutions, may be found (*Fowler 1982*), the investigation of quantitative properties is done mostly numerically (*Banks 1977*). In this section, we first revisit some results of the linear stability analysis to obtain the stability condition on τ. We then further our study by obtaining the loss of monotonicity condition for the travelling front solution of Eq. (5.3), cf. *Ashwin et al. (2002)*.

We begin by recalling the spatially homogeneous Hutchinson's equation which will serve as the baseline model. Stability is examined only for the positive steady state
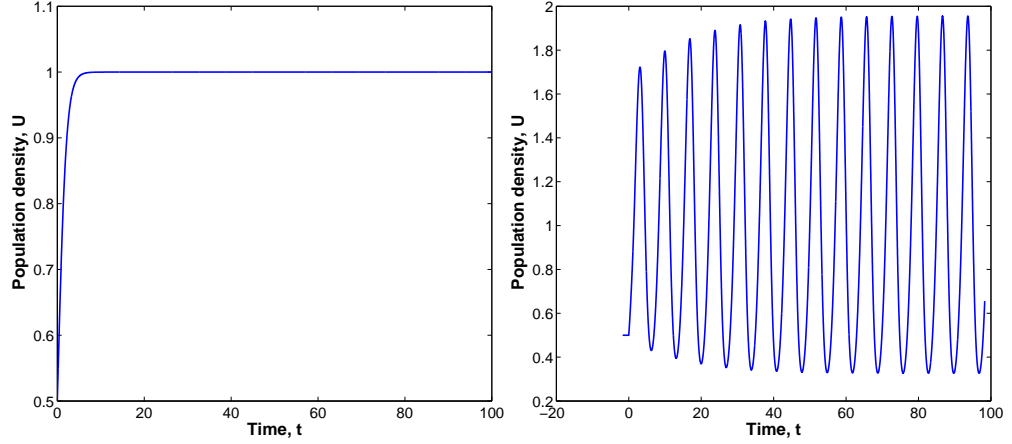
FIGURE 5.1: Snapshots of solution behaviour for the instantaneous logistic equation (left) and Hutchinson's equation (right), with delay parameter $\tau=1.7$. Other parameters are $r = 1$ and $K = 1$.

$U_* = K$, as the extinction steady state, $U_* = 0$, is always unstable. We nondimensionalise the equation, thereby decreasing the number of parameters (*Murray 2002*):

$$\frac{d\widetilde{U}(\tilde{t})}{d\tilde{t}} = \widetilde{U}(\tilde{t}) \left(1 - \widetilde{U}(\tilde{t} - \tilde{\tau}) \right), \qquad (5.5)$$

where $\widetilde{U} = \frac{U}{K}$, $\tilde{t} = rt$ and $\tilde{\tau} = r\tau$. Suppose $\tilde{u}$ is a small perturbation from the steady state $\widetilde{U_*} = 1$, such that:

$$\tilde{u} = \widetilde{U} - \widetilde{U_*}. \qquad (5.6)$$

By linearising, and omitting higher order terms, we obtain the following equation:

$$\frac{d\tilde{u}(\tilde{t})}{d\tilde{t}} \approx -\tilde{u}(\tilde{t} - \tilde{\tau}), \qquad (5.7)$$

for which solutions must be of exponential form $\tilde{u}(\tilde{t}) = ce^{\lambda \tilde{t}}$, where c is a constant and λ are the eigenvalues that, when substituted into Eq. (5.7), leads to the transcendental characteristic equation:

$$\lambda = -e^{-\lambda \tilde{\tau}}, \qquad (5.8)$$

so that λ is a function of the (dimensionless) delay $\tilde{\tau}$.

The equilibrium point $\widetilde{U_*} = 1$ is asymptotically stable if all eigenvalues have negative real parts. For this reason we set $\lambda = \mu + \imath \omega$, substitute into Eq. (5.7),

and separate the real and imaginary parts:

$$\mu = -e^{-\mu\widetilde{\tau}}\cos\omega\widetilde{\tau}, \qquad (5.9)$$

$$\omega = e^{-\mu\widetilde{\tau}}\sin\omega\widetilde{\tau}. \qquad (5.10)$$

Considering two cases, when the eigenvalues are real and complex, we determine the stability condition on $\widetilde{\tau}$. The case of real eigenvalues is trivial and perturbations are damped, thus the steady state is always stable. In the latter case, if eigenvalues are complex, the stability condition reads $\mu < 0$ therefore implying $\omega\widetilde{\tau} < \pi/2$. The Hopf bifurcation point is found for $\mu(\widetilde{\tau}) = 0$, thus $\omega\widetilde{\tau} = \pi/2$. From Eq. (5.9) the only viable solution is $\omega = 1$, hence $\widetilde{\tau} = \pi/2$. Scaling back to dimensional quantities, the equilibrium $U_* = K$ is stable if $0 < r\tau < \pi/2$, and unstable otherwise ($r\tau > \pi/2$). Stability conditions obtained for Hutchinson's equation are easily extended to the diffusive logistic equation and verified by simulations, which will be done in the following sections.

5.2.2 Loss of monotonicity

Before the positive steady state loses its stability, another change in the solution's properties takes place, namely, the loss of monotonicity. Let us rewrite the Eq. (5.8) for the eigenvalues in the following form:

$$F(\lambda;\tilde{\tau}) = \lambda + e^{-\lambda\tilde{\tau}} = 0. \qquad (5.11)$$

Obviously, function F has a unique minimum and it is readily seen that, when $\tilde{\tau}$ is sufficiently small, this minimum lies in the third quarter of the (λ, F) plane, so that Eq. (5.11) has two real negative roots. The positive steady state is stable and the solution approaches it monotonously, e.g. as can be seen from the left panel of Fig. 5.1. When $\tilde{\tau}$ increases, the minimum is pushed upwards; correspondingly, the two roots move towards each other so that finally, for some $\tilde{\tau} = \tilde{\tau}_*$, they merge and 'disappear', which actually means that they become complex. For $\tilde{\tau} = \tilde{\tau}_h > \tilde{\tau}_*$, the Hopf bifurcation takes place, but for the values of $\tilde{\tau}$ just slightly larger than $\tilde{\tau}_*$ the real part of the eigenvalues is still negative. It means that the positive steady state is still stable but the solution approaches it in an oscillatory manner.

More quantitatively, in order to obtain the value of $\tilde{\tau}_*$, one needs to consider Eq. (5.11) together with the tangency condition:

$$\frac{\partial F}{\partial \lambda} = 1 - \tau e^{-\lambda \tilde{\tau}} = 0. \tag{5.12}$$

Having solved the system (5.11–5.12), one readily obtains that $\tilde{\tau}_* = 1/e$ (*Kakutani and Marcus 1958, Yoshida 1982*). In original dimensional parameters, it means that solutions of Hutchinson's equation start oscillating for $r\tau > 1/e$.

We now consider how the loss of monotonicity condition can be applied to Eq. (5.3). A compact initial population distribution is known to converge to two travelling fronts propagating in the opposite directions with the same speed c, i.e. $U(x,t) \to \widetilde{U}(x - ct) \cup \widetilde{U}(x + ct)$. Consider, for instance, the front propagating to the right, $U(x,t) = \widetilde{U}(\xi)$ where $\xi = x - ct$, which is the solution of the following equation (in dimensionless variables):

$$\frac{d^2\widetilde{U}(\xi)}{d\xi^2} + c\frac{d\widetilde{U}(\xi)}{d\xi} + \widetilde{U}(\xi)(1 - \widetilde{U}(\xi + c\tau)) = 0, \tag{5.13}$$

corresponding to the conditions at infinity as $\widetilde{U}(\xi) \to 0$ for $\xi \to \infty$ and $\widetilde{U}(\xi) \to 1$ for $\xi \to -\infty$.

If we linearise around the steady state $\widetilde{U}_* = 1$, by setting $\widetilde{U} = 1 + \widetilde{v}$, where $\widetilde{v}$ is a small perturbation, it gives a second order differential equation:

$$\widetilde{v}_{\xi\xi} + c\widetilde{v}_\xi - \widetilde{v}(\xi + c\tau) = 0. \tag{5.14}$$

As before, we try a solution of exponential form $\widetilde{v} = e^{\lambda\xi}$ and obtain the characteristic equation:

$$F(\lambda; \tau) = \lambda^2 + c\lambda - e^{\lambda c\tau}. \tag{5.15}$$

When the delay is zero, the eigenvalue equation has two real roots of opposite sign. By increasing the time delay the positive root branches into two roots, which get closer to each other and eventually coalesce, then turn complex. Loss of monotonicity is associated with the loss of real positive eigenvalues and this coalescence which occurs at a critical value, τ_{cr}; see Fig. 5.2. We denote the double root itself, λ_*, and it must satisfy both:

$$F(\lambda_*; \tau_{cr}) = 0; \qquad \frac{\partial F}{\partial \lambda}(\lambda_*; \tau_{cr}) = 0. \tag{5.16}$$
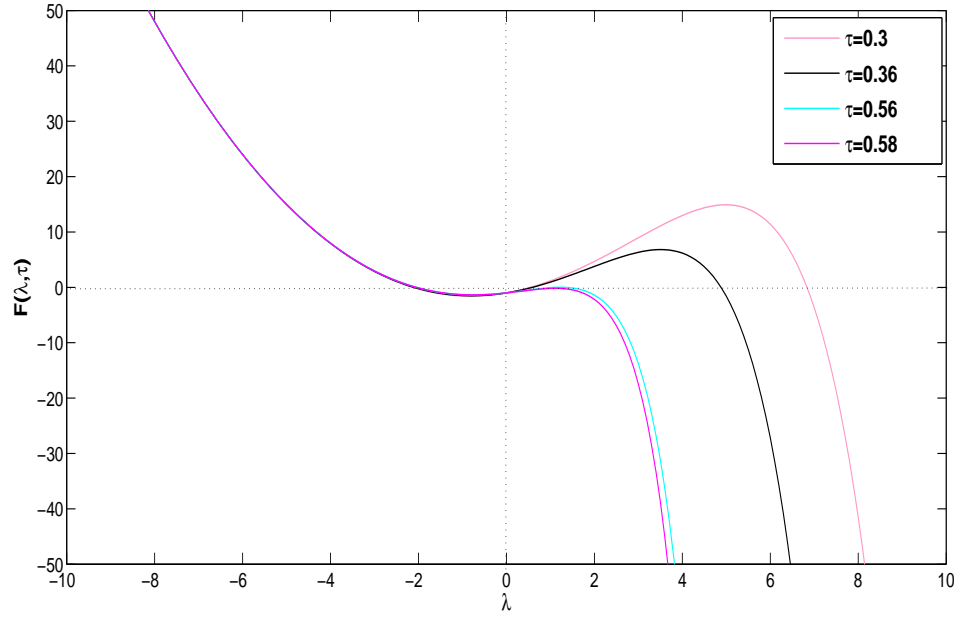
FIGURE 5.2: Plot of $F(\lambda; \tau)$ for different values of τ. The critical value, when loss of monotonicity occurs, is calculated as $\tau_{cr} \approx 0.5608$ for the minimum wave speed $c = 2$.

Following some standard calculations, one can find the loss of monotonicity condition as the following implicit expression (*Ashwin et al. 2002*):

$$\frac{2}{c\tau} + \sqrt{\frac{4}{c^2\tau^2} + c^2} = c\tau \exp\left(1 + \sqrt{1 + \frac{c^4\tau^2}{4}} - \frac{c^2\tau}{2}\right). \qquad (5.17)$$

For any given value of the front speed c, Eq. (5.17) determines the critical value of τ. We now notice that the travelling wave equation (5.13) linearised in the vicinity of the extinction state $\widetilde{U}_* = 0$, i.e. at the leading edge of the front, coincides with the linearised Fisher equation, and hence the same argument can be used resulting in the condition $c \geq 2$. Indeed, compact initial conditions are known to converge to a travelling front propagating with the minimum speed $c = 2$ (e.g. *Ashwin et al. 2002*). In this case, eq. (5.17) takes a somewhat simpler form:

$$\frac{1}{\tau} + \sqrt{\frac{1}{\tau^2} + 4} = 2\tau e^{1 + \sqrt{1 + 4\tau^2} - 2\tau}. \qquad (5.18)$$

Equation (5.18) is solved numerically resulting in $\tau_{cr} \approx 0.5608$.

5.3 Simulations

Apart from the results discussed above, it is difficult to establish other solution properties analytically, so we have to resort to simulations. We begin with the 1D diffusive logistic equation, Eq. 5.3. We write it in dimensionless variables:

$$\frac{\partial U}{\partial t} = \frac{\partial^2 U}{\partial x^2} + U\left(1 - U_\tau\right), \tag{5.19}$$

and solve it numerically by finite-differences for different values of the time delay τ, hence considering τ as the controlling parameter. The mesh steps, Δt and Δx, were taken to be sufficiently small ($\Delta t = 0.1$ and $\Delta = 0.5$), ensuring accuracy and reliability of our results. The spatial domain is chosen to be sufficiently large in order to minimize the impact of boundaries. At the domain boundaries, the Neumann type "no flux" conditions are used.

The initial condition is used in the following form:

$$U(x,0) = U_0 \quad \text{if} \quad |x| \leq \frac{L}{2}, \quad \text{otherwise} \quad U(x,0) = 0, \tag{5.20}$$

where $U_0 > 0$ is the initial population density and L determines the size of the initially occupied patch. Since Eq. (5.19) involves a time delay, we supplement the initial condition with the population's "history", i.e. the data on $U(x,t)$ for $-\tau < t < 0$. For this purpose we choose a constant function equal to the initial population density:

$$U(x,t_0) = U_0 \quad \forall \quad t \in (-\tau, 0). \tag{5.21}$$

For a sufficiently small time delay ($\tau_{cr} < \tau < \pi/2$), Fig. 5.3 shows snapshots of the spatial propagation of population fronts at equidistant moments in time. (Note that, since the mathematical problem is symmetric with respect to the origin, in Figs. 5.3–5.4 and 5.6–5.8 only the right-hand half of the domain is shown.) The fronts are travelling wave solutions exhibiting nonmonotonous, decaying oscillations at the leading edge. These damped oscillations grow in amplitude with increasing τ and can become prominent but decay promptly behind the front. An increase in τ alters the solution's behaviour significantly, as the system surpasses the Hopf bifurcation and apparent spatially irregular oscillations emerge in the wake (Fig. 5.4). Connecting the two dynamically differing scenarios, chaos in the wake and damped oscillations at its leading edge, a quasi-homogeneous plateau appears. This plateau is nontrivial as it corresponds to the system's unstable equilibrium

point, $U_* = K$, acting as a dynamical stabiliser. Qualitatively similar dynamics were observed in systems of coupled instantaneous reaction-diffusion equations, such as prey-predator models (*Sherratt et al. 1995, Petrovskii and Malchow 2000, Malchow and Petrovskii 2002*). Similarly, the length of the plateau increases with simulation time, see Fig. 5.4. The dynamical stabilisation is a spatiotemporal feature that cannot be linked to dynamics in the corresponding nonspatial system. As far as we are aware, this type of dynamics is usually attributed to multi-species models, and is a novel concept in the context of single species population models. We would also like to emphasise here that the patterns emerging are purely self-organised and do not depend on any "environmental" heterogeneity, as the parameters are space-independent. Furthermore, the spatiotemporal patterns are self-sustained as following the onset of apparent chaos, no qualitative changes in the system's dynamics occur. Namely, for longer simulation time, as the fronts propagate, the aperiodic behaviour slowly occupies the whole numerical domain; see the bottom of Fig. 5.6. We have also investigated the temporal dynamics of the system, see Fig. 5.5. The population density profile was recorded at half of the spatial numerical domain and clearly suggests irregular oscillations. This result contradicts the temporally periodic oscillations observed by *Ashwin et al. (2002)* for the equivalent system.
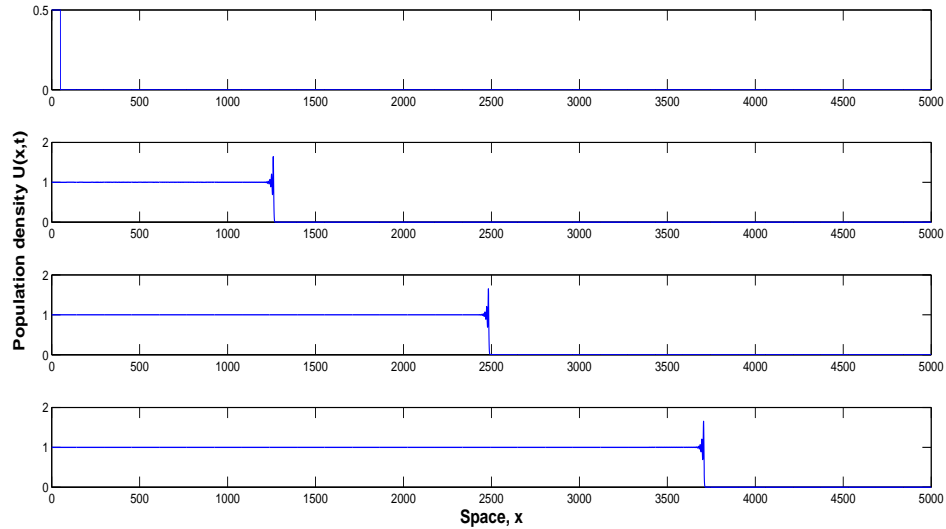

FIGURE 5.3: Snapshots of spatial propagation of population front at equidistant moments in time: $t = 1$, $t = 667$, $t = 1333$ and $t = 1999$. With the time delay parameter set to $\tau = 1.5$, we observe damped oscillations at the leading edge, and the monotonous approach to the stable equilibrium in the wake of the population front. Other parameters are $r = 1$, $K = 1$, $U_0 = 0.5$ and $L = 100$.
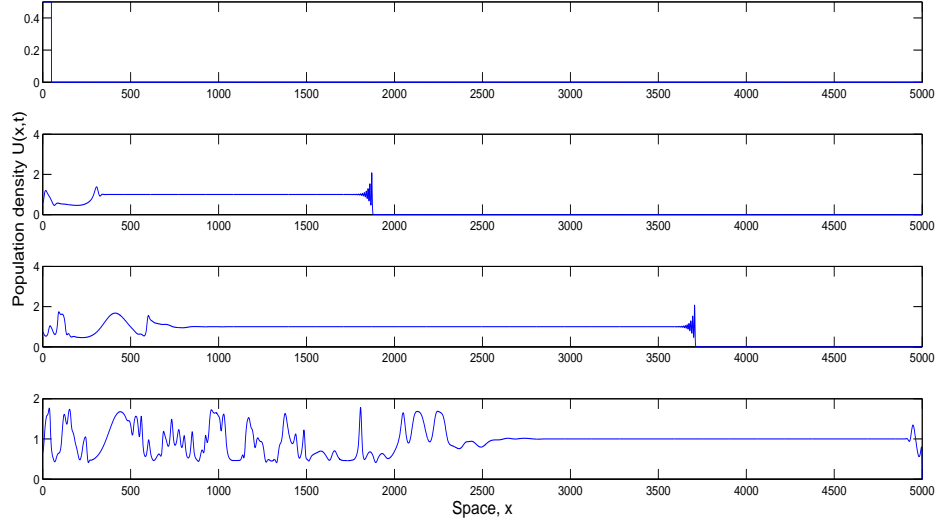
FIGURE 5.4: Snapshots of spatial propagation of population front at equidistant moments in time: $t = 1$, $t = 1001$, $t = 2000$ and $t = 2999$. The time delay parameter is set to $\tau = 1.7$, ensuring instability of stable steady state. Damped oscillations are observed at the leading edge, with apparent chaotic behaviour developing in the wake of the front. Connecting the two dynamical scenarios is the "steady state" plateau.
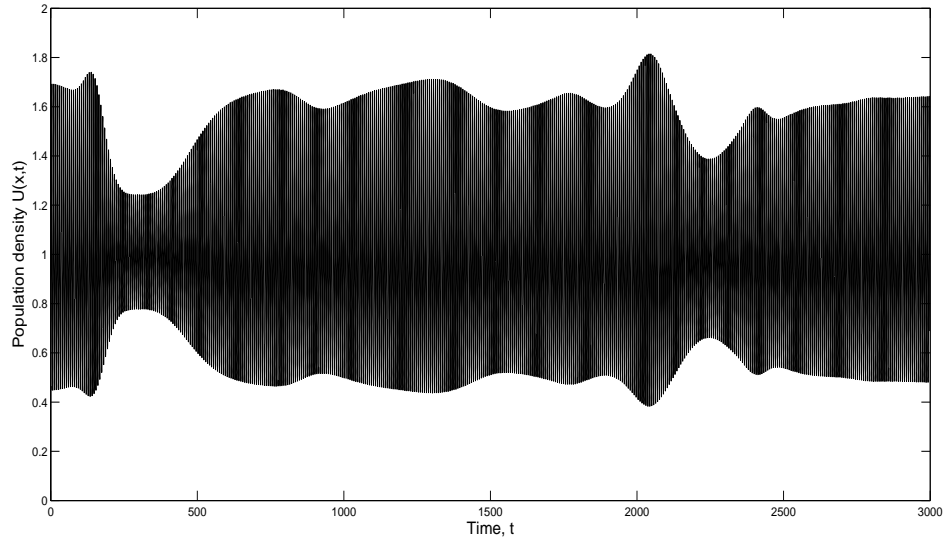

FIGURE 5.5: Snapshots of temporal propagation of population front. Prominent irregular oscillatory behaviour is observed. Time delay parameter is set to 1.7. Other parameters are $r = 1$, $K = 1$, $U_0 = 0.5$ and $L = 200$. The recording was taken at half the spatial numerical domain after chaotic oscillations have occupied the whole domain.
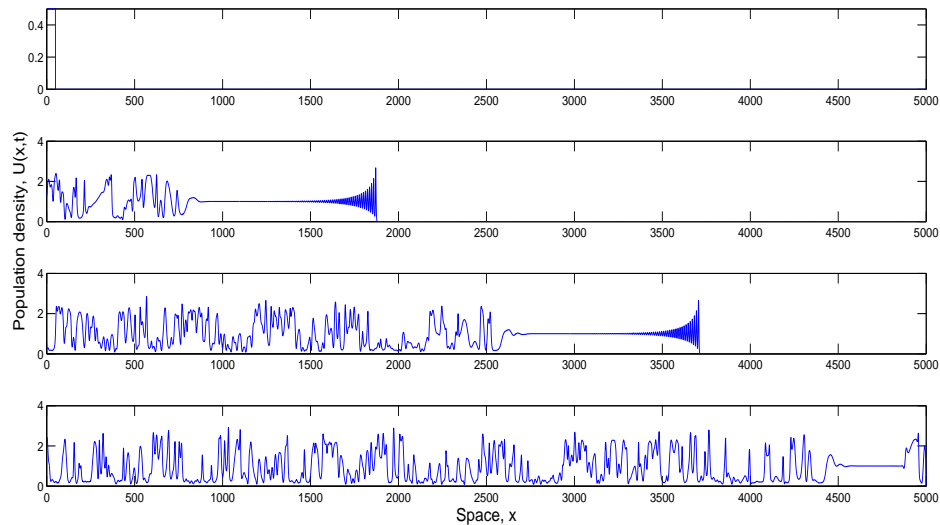
FIGURE 5.6: Snapshots of spatial propagation of population front at equidistant moments in time: $t = 2$, $t = 1001$, $t = 2000$ and $t = 2999$. Time delay parameter is set to 1.94 and other parameters are $r = 1$, $K = 1$, $U_0 = 0.5$ and $L = 200$. Apparent chaotic behaviour develops in the wake of the front, preceded by the "dynamical stabilisation" of the unstable equilibrium.

By even further increasing the controlling parameter, τ, one would expect more prominent oscillatory behaviour, as was observed (Figs. 5.6 and 5.7). Interestingly, for a sufficiently large τ, instead of the quasi-homogeneous distribution, a wave-train of periodic oscillations is formed behind the propagating population front. Our simulations indicate that these periodic oscillations appear abruptly without any gradual transition: a slight difference in τ results in a completely different pattern, cf. Figs. 5.6 and 5.7. This seems to suggest that the sudden change in dynamics should not be attributed to the Hopf bifurcation. We mention that a further increase in τ (not shown here for the sake of brevity) does not lead to any qualitative changes; in fact, even the amplitude of the periodic oscillations shows almost no change.

To verify the irregular spatiotemporal patterns are in fact chaotic, we tested the sensitivity of solutions to initial conditions. Fig. 5.8 shows spatial propagation of two population fronts with slightly different initial conditions. Indeed, as simulation time is increased, small perturbations grow and induce large scale differences between the fronts, which in turn leads to the conclusion that the behaviour is in fact chaotic.

Chaotic behaviour is also apparent in the phase plane (Fig. 5.9) where the axes
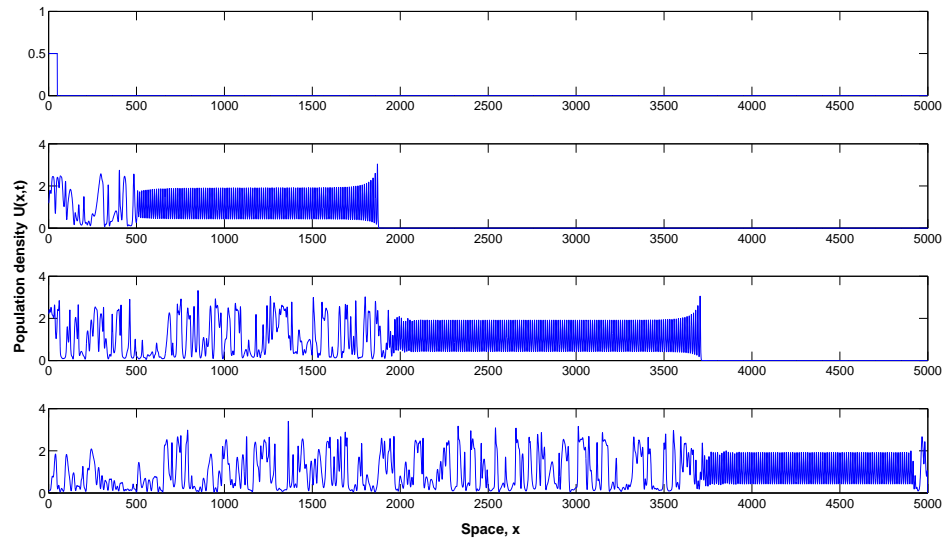
FIGURE 5.7: Snapshots of spatial propagation of population front at equidistant moments in time: $t = 2$, $t = 1001$, $t = 2000$ and $t = 2999$. Time delay parameter is set to 1.95 and other parameters are kept as above. Prominent chaotic behaviour develops in the wake of the front and is preceded by a wavetrain.

FIGURE 5.8: Spatial propagation of population fronts with different initial conditions. The time delay parameter is chosen to be 1.7 in simulations, whilst the unperturbed (original) initial condition is taken to be $U_0 = 0.5$ and the perturbed condition is set as $U_0 = 0.502$.

show population densities at the same position in space but at different time moments, hence being separated by a certain time lag. The trajector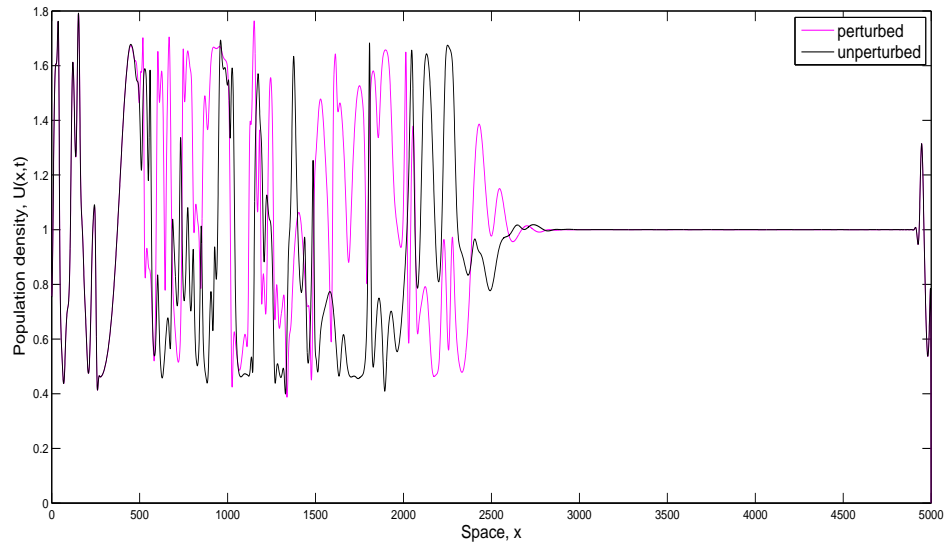ies are intricate and indicate quite complex behaviour of solutions. Numerical simulations suggest a cascading sequence of bifurcating solutions which become chaotic. Note that, by decreasing the time lag, the trajectory in the phase plane eventually shrinks to the bisector line. Correspondingly, the oscillations in the population density become highly correlated; however, behaviour still remains chaotic.
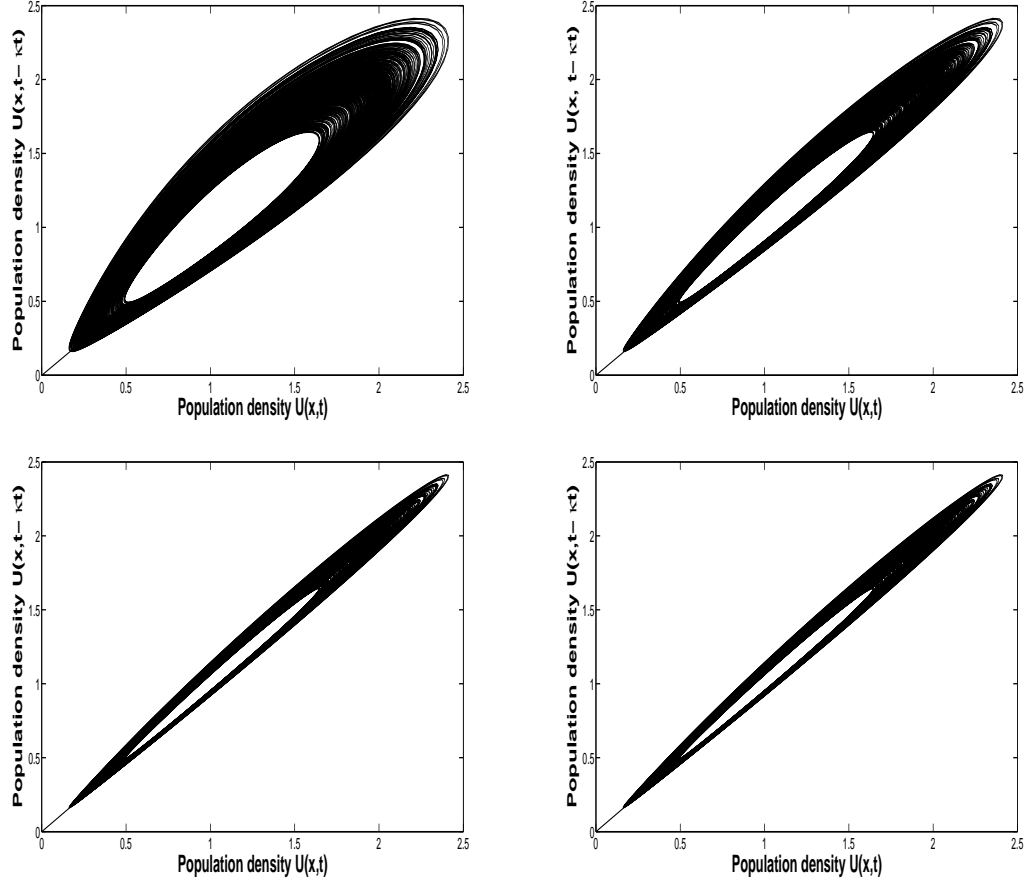
FIGURE 5.9: Phase plane of Eq. (5.19) where axes show population densities at the same location in space but at different moments, i.e. separated by a time lag. By decreasing the time lag between solutions a higher correlation is observed (from top to bottom, left to right). The corresponding values of κ are 1/4, 1/10, 1/16 and 1/35 with $\tau = 1.8$.

We have also investigated such spatiotemporal pattern formation in the 2D case, (Fig. 5.10). Since the system is symmetric with regards to reflection ($x \to -x$ and $y \to -y$), simulation results are shown only in the first quadrant. As can be seen, the system mirrors the dynamics of the corresponding 1D model. Namely, for a significantly large τ, the travelling population front exhibits decaying oscillations at the front. Damped oscillations are followed by a plateau emerging due to the

dynamical stabilisation of the unstable equilibrium. For larger simulation time irregular spatiotemporal patterns emerge in the wake of the front. These chaotic oscillations develop gradually and eventually spread throughout the numerical domain. Patchiness in the wake is an inherent property of the delayed system and is induced by a sufficiently large time delay. As before, the patterns are triggered by the population fronts themselves, i.e. are self-organised and self-sustained.
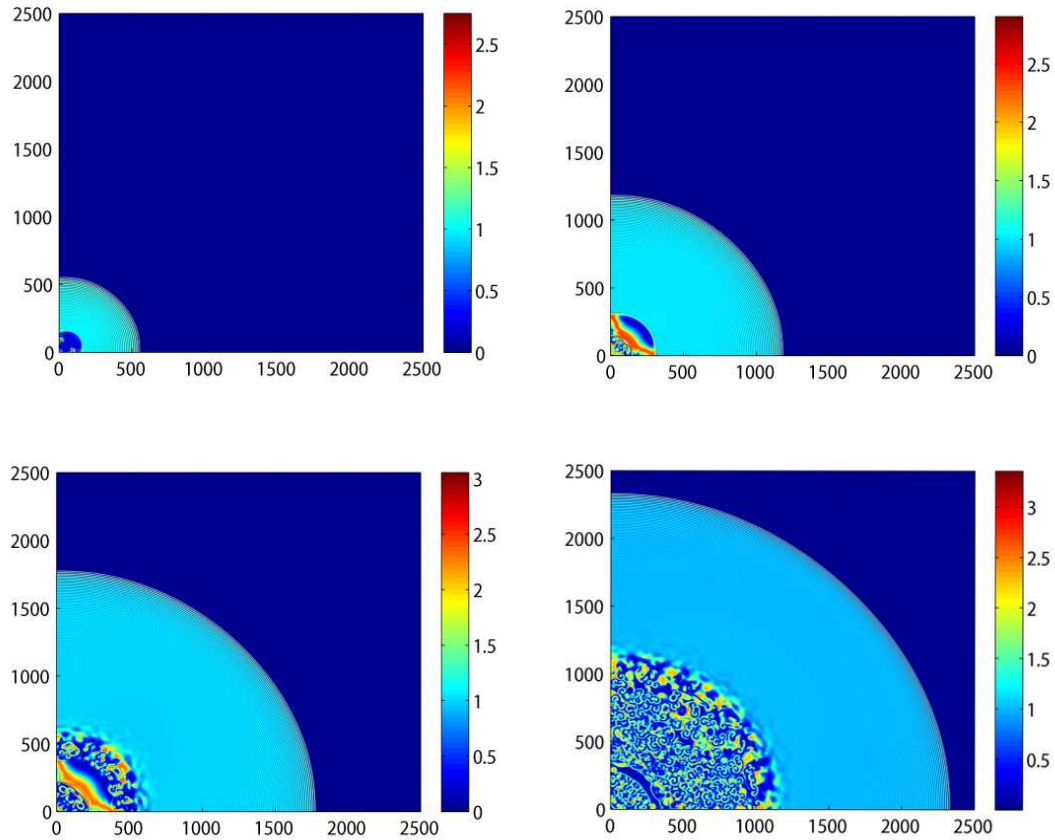
FIGURE 5.10: Snapshots of spatial propagation of population front in two dimensions. Snapshots are given for simulation times: $t = 280$, $t = 600$, $t = 940$ and $t = 1280$. The time delay is $\tau = 1.9$ and other parameters are $\Delta t = 0.1$, $\Delta x = \Delta y = 1$, $K = 1$, $r = 1$, $U_0 = 0.5$.

It has recently been recognised (*Britton 1990, Gourley and Chaplain 2002*) that the inclusion of diffusion into delay equations such as Eq. (5.19) is not biologically relevant. In particular, the underlying assumption of diffusion is that individuals freely and randomly move around, without any preferred direction. Though, there is a higher probability of individuals choosing nearby positions compared to further away ones, and to account for this phenomenon we introduce a spatial convolution

(*Gourley and Chaplain 2002, Ashwin et al. 2002, Gourley and Bartuccelli 1995*):

$$f(x,t) = \frac{1}{\sqrt{4\pi t}} e^{-\frac{x^2}{4t}} \delta(t - \tau), \qquad (5.22)$$

which when substituted into eq. 5.19 results in:

$$\frac{\partial U}{\partial t} = D\frac{\partial^2 U}{\partial x^2} + rU\left(1 - \frac{1}{K}\int_{-\infty}^{\infty} \frac{1}{\sqrt{4\pi\tau}} e^{\frac{-(x-y)^2}{4\tau}} U(y, t - \tau)dy\right) \qquad (5.23)$$

for the 1D case. The chosen kernel is normally distributed with a dependence on time delay. Our model now allows for the spatial drift of individuals and is considered ecologically more viable. The additional integral was approximated by the trapezium rule, and numerical results are presented in Figs. 5.11–5.16. The qualitative dynamics have not been altered by this addition, and still include the emergence of spatiotemporal chaos for significantly large τ, see Figs. 5.12 and 5.13. As before, at the leading edge of the front we observe damped oscillations, which are followed for a "small" value of time delay, τ, by periodic oscillations in the wake, see Fig. 5.11. An increase in τ replaces these periodic oscillations with quite irregular behaviour, both spatially and temporally, and for longer simulation time this apparent spatiotemporal chaos slowly occupies the whole numerical domain (Fig. 5.13). We have tested the sensitivity to initial conditions for slight perturbations and concluded that the irregular oscillations in the wake are in fact chaos, as a small difference in initial conditions gradually grows and induces a large difference between observed population fronts. Temporal dynamics of the system have also been investigated and confirm irregular oscillatory behaviour (see Fig. 5.14). Furthermore, we have compared the spatial dynamics for a larger time delay, $\tau = 2.0$, with its corresponding phase plane (population densities recorded at same spatial location, separated by a time lag equal to the delay), which confirms our hypothesis of spatiotemporal chaotic dynamics (Fig. 5.16). For a higher value of τ, the wavetrain preceding spatiotemporal chaos in the wake, emerges (Fig. 5.17). Again, all spatiotemporal patterns are completely self-organised and self-sustained, and arise as a consequence of the interplay between delay, spatial averaging and local interactions.
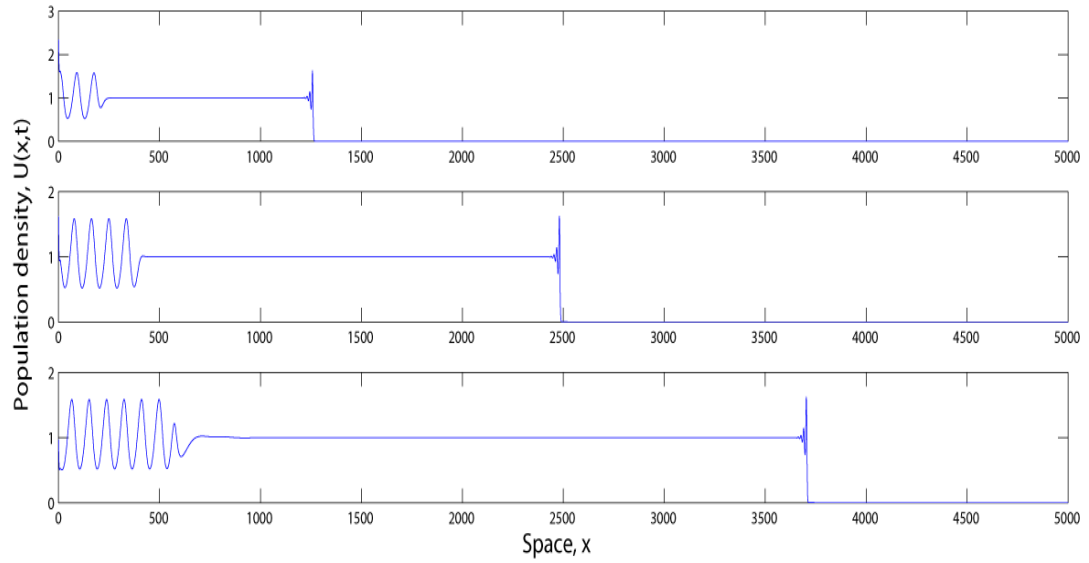
FIGURE 5.11: Snapshots of spatial propagation of population front with spatial averaging taken at equidistant moments in time: $t = 667$, $t = 1333$ and $t = 1999$. The time delay parameter is chosen to be 1.7, and other parameters are $r = 1$, $K = 1$, $L = 100$.
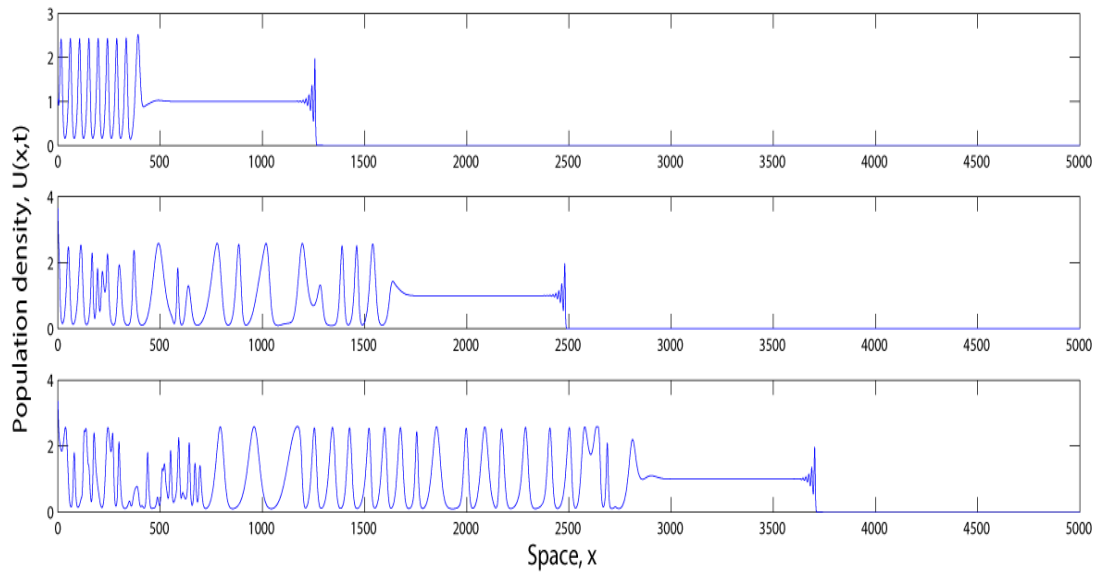
FIGURE 5.12: Snapshots of spatial propagation of population front with spatial averaging taken at equidistant moments in time: $t = 2665$, $t = 3331$ and $t = 3997$. The time delay parameter is chosen to be 1.95, and other parameters are $r = 1$, $K = 1$, $L = 100$.
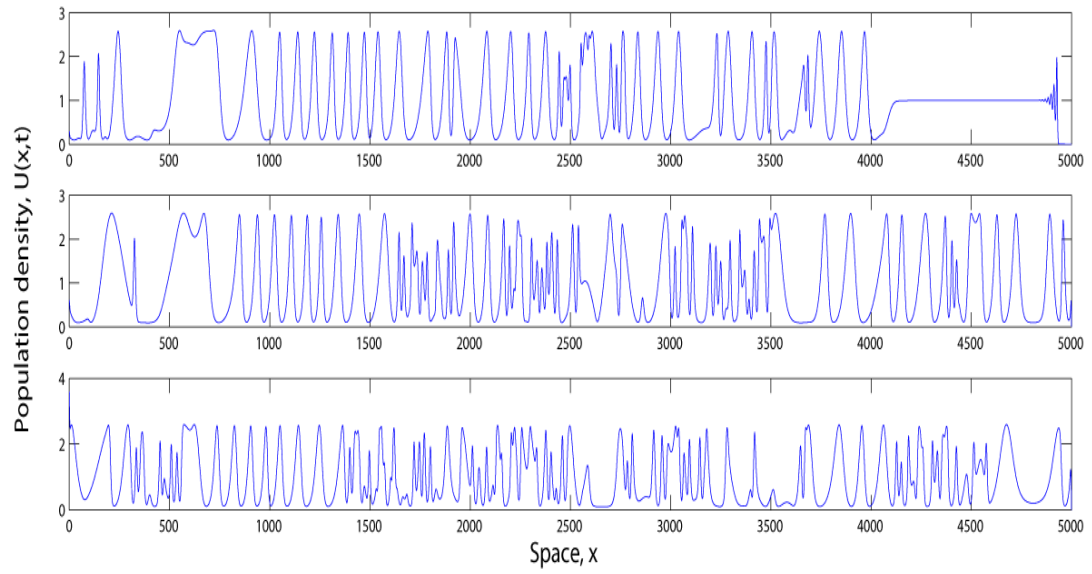
FIGURE 5.13: Snapshots of spatial propagation of population front with spatial averaging for longer simulation time. The time delay parameter is chosen to be 1.95.
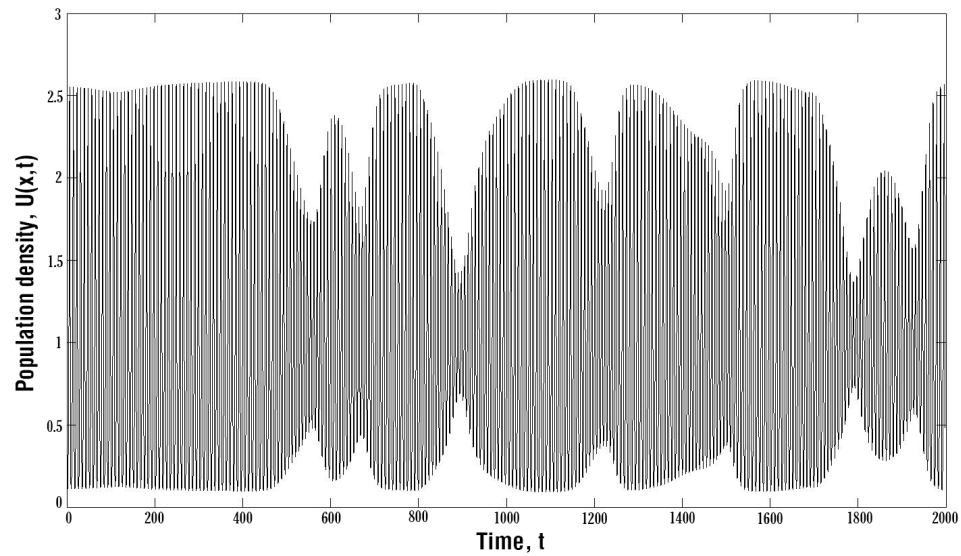
FIGURE 5.14: Temporal dynamics of population front with spatial averaging. The time delay parameter is chosen to be 1.95.
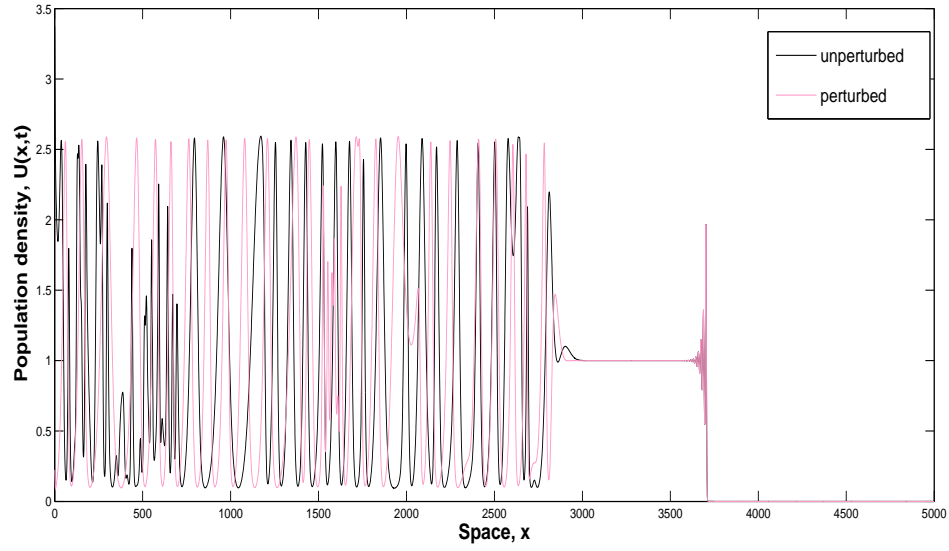
FIGURE 5.15: Sensitivity to the initial conditions: spatial propagation of population fronts with different initial conditions. The unperturbed initial condition is taken as $U_0 = 0.5$ and the perturbed one is $U_0 = 0.505$.
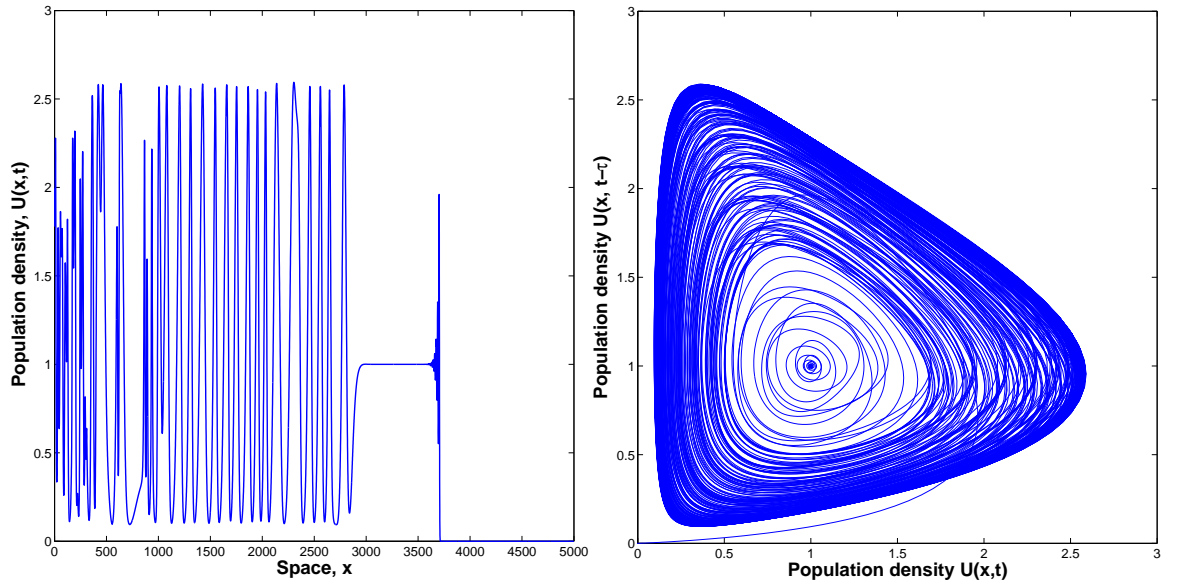
FIGURE 5.16: Spatial propagation of population front for $\tau = 2.0$ (left) and corresponding phase plane (right) whereby the population densities are recorded at the same spatial position but at different time moments.
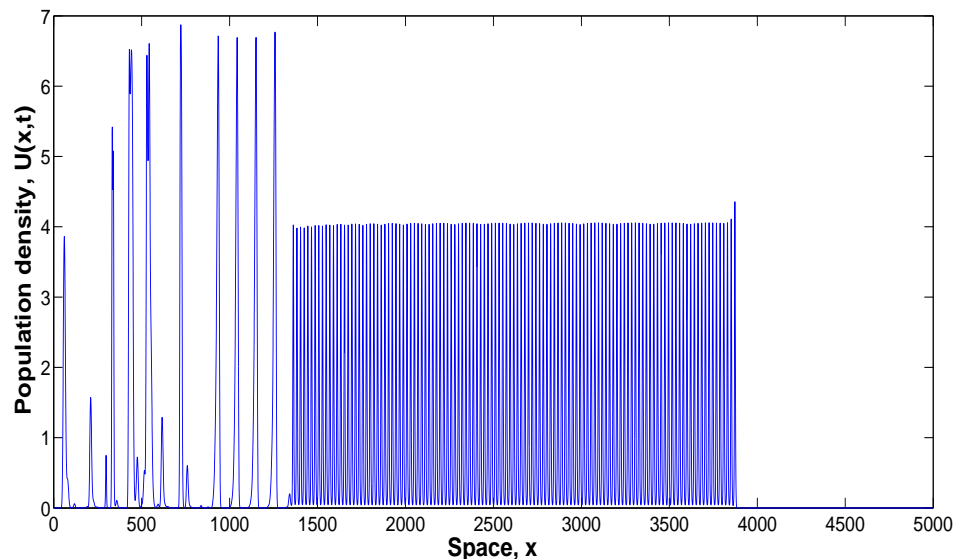
FIGURE 5.17: Spatial propagation of population front for $\tau = 3$. The wavetrain preceding spatiotemporal chaos in the wake emerges.

5.4 Discussion and Concluding remarks

The aim of this study is to investigate the interplay between time delay and logistic growth. For this purpose, we use the delayed diffusive logistic model. We show that travelling population fronts are capable of generating rich dynamics, resulting in an array of different spatiotemporal patterns. Using standard linearisation techniques, we revisit known analytical results and obtain the local stability condition of the upper steady state $U_* = K$, and loss of monotonicity condition for solutions. Our results are verified through numerical simulations, and extended to the 2D case as well. The destabilising effect of time delays is not new, however the resulting spatiotemporal patterns can be nontrivial. As the time delay, τ, increases from zero, the population front loses monotonicity through the appearance of a single hump which evolves into damped oscillations. These oscillations increase in amplitude with increasing τ, though decay promptly as the upper equilibrium $U_* = K$ is still stable. For a sufficiently large τ, irregular oscillations in the wake of the front appear. These spatiotemporal patterns are sometimes referred to as "biological turbulence" (*Malchow et al. 2008*) and are self-organised, thus are an inherent property of the time delayed system. The observed dynamics are self-sustained, as following the onset of chaos, no further qualitative changes appear. Connecting the nonmonotonous damped oscillations at the leading edge and spatiotemporal patterns in the wake for a particular parameter set, is

the emerging quasi-homogeneous distribution of species. Peculiarly, this plateau coincides with the otherwise unstable equilibrium, and is abruptly displaced by periodic oscillations for a slight change in parameters. Qualitatively similar dynamics were observed in various instantaneous coupled reaction-diffusion systems, as a consequence of trophic interactions (*Malchow and Petrovskii 2002*). Here, these complex dynamics arise due to the delayed density dependent controlling mechanism.

Whether in nature we can really observe such spatiotemporal dynamics is quite a long standing, disputable and largely open question (*Turchin and Taylor 1992*, *Hassell et al. 1976*). Despite the abundant theoretical literature, studies on self-organised pattern formation in real ecological communities are limited. There are numerous mechanisms underlying the spatial distribution of species, however the most common ones include environmental heterogeneity (*Kareiva et al. 1990*, *Klausmeier 1999*), trophic interactions (*Bjørnstad et al. 2002*), intrinsic mechanisms (such as delayed density dependence), and various other biotic and abiotic factors (*Ranta et al. 1995*). Indeed, such spatial patterns are most likely a consequence of the synergetic effect of various mechanisms, rather than a single one (*Rietkerk and van de Koppel 2007*). *Turchin and Taylor (1992)* examined 36 time series of insect and vertebrate populations concluding that the complete spectrum of dynamical behaviour as observed in mathematical models can be found in natural populations, ranging from monotonous and nonmonotonous stability to chaos. In the quest of revealing irregular spatial distributions the most intuitive starting point would be amongst cyclic populations, as they tend to be regulated by highly nonlinear interactions (*Bjørnstad et al. 2002*). Populations of octopus, *Joubini Robson*, despite being territorial animals (meaning they are more likely to be evenly distributed) show clumped, patchy distributions. Amongst many factors influencing this irregular spatial pattern formation, the presence of empty molluscan shells is thought to be the most prominent factor affecting distribution (*Mather 1982*). Habitat features are also suggested to heavily influence the distribution of bottlenose dolphins (*Davis et al. 2002*, *Baumgartner 1997*), however newer studies relate observed patterns to foraging (*Hastie et al. 2004*). Self-organised patterns are noted in beds of blue mussel populations, *Mytilus edulis*, on intertidal flats with significant variability in mussel density observed on larger scales of meters, but with no apparent within-cluster difference. It is suggested that the interaction between individual mussels is the only underlying mechanism of such pattern formation (*van de Koppel et al. 2008*, *Gascoigne et al. 2005*).

Self-organised spatial and temporal chaotic patterns emerge in the wake of the front for a sufficiently large time delay in both our models. In the diffusive logistic model this apparent chaos is preceded by a quasi-homogeneous species distribution, due to the "dynamical stabilisation" of the unstable equilibrium. A slight change in parameters replaces this "homogeneous" distribution with periodic oscillations. The inclusion of spatial averaging as a more realistic biological concept does not alter the observed succession of spatiotemporal dynamics. Although the concept of spatiotemporal patterns in the wake of fronts is not new in an ecological context (*Petrovskii and Malchow 2000, Malchow and Petrovskii 2002, Sherratt 1994, Sherratt et al. 1995*), it has usually been observed in multi-species models. However, we have demonstrated here that such patterns can arise in a single species population model.

Chapter 6

Conclusions

Both public and academic recognition of biological invasions and problems associated with invasive species have grown substantially in recent years, mostly due to the detrimental effects of non-native species. Now posing a serious threat to biodiversity and resulting in vast economic losses, the call for a more integrated and interdisciplinary approach is needed to predict and control biological invasions. Indeed, mathematical modelling has proven to be a powerful research tool in theoretical ecology, as the biological factors underpinning the dynamics of invasive species are often difficult to observe, quantify and manipulate in natural settings. Though the approaches to model building can be very different, the great variety of models have considerably furthered our understanding of processes underlying biological invasions. However, despite the ever-enlarging empirical and experimental data, the interface between theory and observation still remains weak.

Understanding the spatiotemporal dynamics of populations is one of the main pursuits in modelling biological invasions, and in this thesis our main motivation was to examine both spatial and temporal pattern formation in ecological systems. The results of this dissertation have been twofold: from gaining insight into the underlying regulatory mechanisms and modelling the spatial spread of gypsy moth in the US, to identifying the effects of time delays on both spatial and temporal dynamics in single species populations.

In Part I (Chapter 2) we documented a case study of gypsy moth, *Lymantria dispar*, invasion in the US. A distinct feature of gypsy moth spread is its heterogeneous, patchy spatial distribution. With the possible impact of environmental forcing excluded, this phenomenon is usually attributed to the inadvertent transport of egg masses to new locations, in which they develop into new gypsy moth

colonies. However, this theory disagrees with the existence of the strong Allee effect, known to affect gypsy moth populations, which turns the successful establishment of new colonies into a rare event, driving small populations extinct. Therefore, we propose an alternative hypothesis to demonstrate that the pattern of gypsy moth spread can be explained by the interplay between two natural factors: wind dispersal and a viral infection (or predation). Depending on the density of gypsy moth populations, the dynamics are strongly affected by either predation or a naturally occurring viral infection (NPV); Section 2.5. Correspondingly, using a reaction-diffusion framework, we formulate a predator-prey and susceptible-infected model and find that within a certain parameter range, both models exhibit spatial patterns qualitatively similar to what is observed in natural gypsy moth populations. Following an extensive literature search, we aim to identify a biologically relevant parameter range, and using the diffusive SI model we were able to estimate the spread rate of gypsy moth populations which is comparable to historical data. Our intention was not to develop a comprehensive model of gypsy moth population dynamics, but rather to illustrate that the spatial patchiness can be alternatively explained. Forthcoming work should include a combination of dispersal modes, both wind and human-assisted dispersal, alongside other specifics such as weather conditions affecting virus dynamics, though parametrisation of such models may prove troublesome. Our interpretation of the SI model entails implicit consideration of virus particles, however another interesting extension would be to explicitly model all three stages: healthy susceptible larvae, infected larvae and virus particles, and the interactions between them. One of the underlying assumptions of the SI model is that transmission of disease occurs instantaneously, which in many cases, including gypsy moth, is not true. Ultimately, we would also like to investigate the effect of this time delay on gypsy moth population dynamics as a part of future research.

Understanding the amplitude and frequency of population fluctuations and factors underlying such dynamics are of equal interest and importance to the study of biological invasions as are the corresponding spatial patterns. Populations of many species tend to fluctuate nearly periodically over time and both theoretical and empirical studies agree that delayed density dependence instigates cyclic behaviour. The underlying ecological processes through which this occurs are often difficult to determine and are species-dependent, thus a more general explanation is still lacking. Nonetheless, time delays are integral parts of ecology and as such should be included into modelling efforts. Part II of this dissertation provides a

study of the effects of different forms of time delays and time delayed models on single species population dynamics.

In particular, Chapter 3 shows that contrary to the generally accepted idea of time delays being potent sources of instability, this is not always the case. By using two different mathematical formulations of the Allee effect, we analyse the role of time delays in the dominant ecological feedback mechanisms – cooperation and competition. Interestingly, depending on the chosen delayed mechanism even large time delays may not necessarily destabilise the population's dynamics. A more dominant effect on population dynamics was observed in controlling, negative feedback mechanisms in which sufficiently large time delays always led to limit cycle behaviour. We also show that in the case of delayed cooperation, time delays are not destabilising, but may lead to the self-organised formation of quasi-stationary states. Even though time delays in positive feedback mechanisms do not instigate population cycles, they increase the time needed for the population to converge to its equilibrium (Figs. 3.4 and 3.5) which is observed in natural cooperative breeding populations. Consequently, we suggest that even 'stable' populations are subject to delayed processes which should be accounted for in modelling efforts. However, in making a priori generalisations based on the intuition from simple models such as ours, one must be very careful. The projection of single species dynamics to two or more species systems can be misleading. In this case, a more detailed investigation of the interaction between time delay and different functional responses may be needed, and will also be part of future work, especially in making the connection with gypsy moth population dynamics.

Furthering the concept of time delayed dynamics, in Chapter 4 we study a single species population model with logistic growth and distributed delay resulting in an integrodifferential model. With ecological time series of many populations showing "reddened" power spectra and indicating the prevalence of $1/f^{\nu}$ noise dynamics, we examine the effect of different memory kernels on population dynamics, in particular the effect of a power-law kernel. We compare the resulting temporal dynamics of a constant, exponentially decaying and power-law memory kernel, concluding that descriptions with longer memory (fat-tailed kernels with a slower decay rate) can be destabilised by sufficiently large time delays. Additionally, spatiotemporal dynamics of the model with constant memory kernel also suggest periodicity for a sufficiently small time delay. A more comprehensive investigation of spatiotemporal dynamics is required for all other models to determine whether the dynamics remain periodic or if there is a possibility of the onset of spatiotemporal chaos. Due

to the increased computational effort needed for this further research, we would need to optimise our numerical approximation of models e.g. through the use of Fourier transforms. An outstanding question then would be the applicability of such models to real ecological populations and their corresponding dynamics.

It is well known that the propagation of travelling population fronts in multi-species models is capable of generating rich dynamics and an array of different spatiotemporal patterns. However, can the interplay between time delay and diffusion do the same in a single species model? In Chapter 5 we revisit the diffusive logistic type delayed equation and investigate the possibility of spatiotemporal pattern formation and chaos. For a relatively small time delay, the model exhibits dampening oscillations at the leading edge and a monotonous convergence to the stable equilibrium, however an increase in time delay alters the solution's behaviour significantly. As the system surpasses the Hopf bifurcation, the onset of spatiotemporal chaos is evident in the wake of the front, which is connected to the damped oscillations at the leading edge through either dynamical stabilisation of the unstable equilibrium or an abruptly appearing wavetrain. Including a spatially homogeneous time delay into a model with diffusion has been proven not to be self-consistent, and for that reason we introduce the concept of spatial averaging. As a consequence of including spatial averaging there was no qualitative effect on population dynamics. For a sufficiently large time delay, the onset of spatiotemporal chaos in the wake of the front is observed along with either a plateau or regular oscillations preceding it. Other studies on spatially explicit time delayed models have mainly been concerned with either travelling fronts or periodic patterns, and thus the onset of spatiotemporal chaos in the wake, to the best of our knowledge is a novel feature in both our models, but also in the context of single species population models. Finally, establishing the link between the obtained theoretical results and observed ecological populations is also a potential future research topic. The debate on regular vs. irregular spatiotemporal pattern formation in nature is very much ongoing and the theoretical results in this study are a stepping stone to a better understanding of potential underlying mechanisms.

Appendix A

A comment on numerical methods: finite differences

For a function u which has single-valued, finite and continuous derivatives with respect to the time coordinate t, we can use a Taylor expansion to approximate the following:

$$u(t + \Delta t) = u(t) + \Delta t u'(t) + \frac{1}{2}(\Delta t)^2 u''(t) + \frac{1}{6}(\Delta t)^3 u'''(t) + ... \quad \text{(A.1)}$$

$$u(t - \Delta t) = u(t) - \Delta t u'(t) + \frac{1}{2}(\Delta t)^2 u''(t) - \frac{1}{6}(\Delta t)^3 u'''(t) + ..., \quad \text{(A.2)}$$

where Δt is an increment of the variable t. By simply re-arranging the above expansions and neglecting higher order terms, we are able to obtain an approximation for the second derivative of u:

$$u''(t) \simeq \frac{1}{(\Delta t)^2} \left(u(t + \Delta t) - 2u(t) + u(t - \Delta t) \right). \quad \text{(A.3)}$$

Similarly, subtraction of eqs. A.1 and A.2 leads to the expression for the first derivative:

$$u'(t) \simeq \frac{1}{2\Delta t} \left(u(t + \Delta t) - u(t - \Delta t) \right), \quad \text{(A.4)}$$

that has an error order of $(\Delta t)^2$, and is known as the *central difference* approximation. Throughout this thesis, the preferred method was the *forward difference* approximation given by:

$$u'(t) \simeq \frac{1}{\Delta t} \left(u(t + \Delta t) - u(t) \right). \quad \text{(A.5)}$$

126

However, another approximation method involves the use of backward differences:

$$u'(t) \simeq \frac{1}{\Delta t} \left(u(t) - u(t - \Delta t) \right) . \tag{A.6}$$

For both forward and backward differences the leading errors are both $O(\Delta t)$.

Let u be a function of two independent variables x and t, satisfying the parabolic diffusion equation:

$$u_t = D u_{xx} \quad for \quad t > 0, \quad 0 < x < L \tag{A.7}$$

$$u(0, t) = u(L, t) = 0 \quad \forall t \in [0, T_f] \tag{A.8}$$

$$u(x, 0) = u_0(x) \quad \forall x \in [0, L], \tag{A.9}$$

where D is the diffusion coefficient. We discretise both the spatial and temporal domain by constructing a spatial grid with $N_x + 1$ equally spaced mesh points with $\Delta x = \frac{L}{N_x}$ and one in the time-direction with $N_t + 1$ equally distributed mesh points $\Delta t = \frac{T_f}{N_t}$ with $x = i\Delta x$ and $t = j\Delta t$, where i and j are integers. Then, by applying forward differences, we obtain:

$$u_t \approx \frac{u(x, t + \Delta t) - u(x, t)}{\Delta t} \tag{A.10}$$

$$u_{xx} \approx \frac{u(x + \Delta x, t) - 2u(x, t) + u(x - \Delta x, t)}{(\Delta x)^2}, \tag{A.11}$$

and by substituting into the diffusion equation:

$$\frac{\partial u(x, t)}{\partial t} - D \frac{\partial^2 u(x, t)}{\partial x^2} \approx \frac{u(x_i, t_{j+1}) - u(x_i, t_j)}{\Delta t} - D \frac{u(x_{i-1}, t_j) - 2u(x_i, t_j) + u(x_{i+1}, y_j)}{(\Delta x)^2} = 0. \tag{A.12}$$

The positive integers i and j take values $i = 1, 2, ... N_x$ and $j = 0, 1, ... N_t$. To simplify the notation $u(x_i, t_j)$ will be written as $u_{i,j}$. Therefore, the above expression may be rewritten in a more suitable form:

$$u_{i,j+1} = u_{i,j} + \sigma(u_{i-1,j} - 2u_{i,j} + u_{i+1,j}), \tag{A.13}$$

where $\sigma = D \frac{\Delta t}{(\Delta x)^2}$ is known as the Courant number and determines the stability of the scheme (stable if $0 \leq \sigma \leq \frac{1}{2}$). Furthermore, the proposed method can be extended to two spatial dimensions:

$$\frac{\partial u}{\partial t} = D \left(\frac{\partial^2 u}{\partial x^2} + \frac{\partial^2 u}{\partial y^2} \right), \tag{A.14}$$

by constructing grids such as:

$$x = i\Delta x, \quad y = j\Delta y \quad and \quad t = n\Delta t\,, \tag{A.15}$$

where i,j and n are positive integers, such that $i = 1, 2..N_x$, $j = 1, 2, ..N_y$ and $n = 0, 1, ..., N_t$, with:

$$u(x_i, y_j, t_n) = u_{i,j,n}\,. \tag{A.16}$$

Similarly, we obtain the forward difference approximation:

$$u_{i,j,n+1} - u_{i,j,n} = \frac{\Delta t}{(\Delta x)^2}(u_{i-1,j,n} - 2u_{i,j,n} + u_{i+1,j,n}) + \frac{\Delta t}{(\Delta y)^2}(u_{i,j-1,n} - 2u_{i,j,n} + u_{i,j+1,n}) \tag{A.17}$$

whereby the stability condition now reads:

$$\sigma = D\Delta t \left\{ \frac{1}{(\Delta x)^2} + \frac{1}{(\Delta y)^2} \right\} \leq \frac{1}{2} \tag{A.18}$$

The above stability condition poses a serious drawback on explicit finite difference schemes, and a convenient alternative would be an implicit method such as the Crank-Nicholson scheme. By replacing the approximation of the second derivative $\partial^2 u/\partial x^2$ with the mean of its finite differences on subsequent time rows ($j + 1$ and j) eq. A.7 is now approximated by:

$$\frac{u_{i,j+1} - u_{i,j}}{\Delta t} = \frac{D}{2} \left\{ \frac{u_{i+1,j+1} - 2u_{i,j+1} + u_{i-1,j+1}}{(\Delta x)^2} + \frac{u_{i+1,j} - 2u_{i,j} + u_{i-1,j}}{(\Delta x)^2} \right\}. \tag{A.19}$$

Therefore, it is possible to write out:

$$-\sigma u_{i-1,j+1} + (1 + 2\sigma)u_{i,j+1} - \sigma u_{i+1,j+1} = \sigma u_{i-1,j} + (1 - 2\sigma)u_{i,j} + \sigma u_{i+1,j} \tag{A.20}$$

where $\sigma = D\frac{\Delta t}{2(\Delta x)^2}$. The above expression cannot be solved explicitly as the left hand side contains three unknowns, but rather amounts to solving $N_x - 1$ equations simultaneously for each time row. The error order is $O((\Delta x)^2)$, and the scheme is unconditionally stable.

These results are found in any standard textbook on numerical solutions of PDEs (*Smith 1978, 1965*).

Appendix B

Linear Stability Analysis: delay differential equations

The general approach adopted in this and the following appendix is based on the standard linearisation technique coupled with basic knowledge of ODE theory used to obtain a bifurcation value of the time delay parameter, τ. Since the method in question can be easily extended and applied to all models introduced in Chapter 3, stability analysis will be shown for one model as an illustrative example, and results for other models listed. Stability of the upper positive equilibrium is considered as it is known that the intermediate equilibrium $U_* = \beta$ is always unstable.

Suppose x is a small perturbation from the steady state $U_* = K = 1$:

$$x = U - U_* \tag{B.1}$$

To determine equilibrium stability we investigate the behaviour of this small perturbation, whether it grows or decays, and for that purpose we linearise around the steady state, ignore higher order terms of model (3.5), which gives:

$$\frac{dx}{dt} = (\beta\gamma - \gamma)x_\tau. \tag{B.2}$$

Note that we treat the delayed variables, $U(t - \tau) = U_\tau$ and $x(t - \tau) = x_\tau$ as separate variables throughout linearising. We look for solutions of form $x = ce^{\lambda t}$, where c is a constant and λ are the eigenvalues of the system which determine its stability. By substituting this solution form in (B.2) we obtain the transcendental

Model	Stability Condition
$\gamma U(U_\tau - \beta)(K - U)$	$\lambda = \beta - 1$
$\gamma U(-\beta + (1 + \beta)U_\tau - U^2)$	$\tau_c = \dfrac{\arccos\left(\frac{2}{1+\beta}\right)}{\sqrt{\frac{1+\beta}{2}}}$
$\gamma U(-\beta + (1 + \beta)U - U_\tau U)$	$\tau_c = \dfrac{\arccos \beta}{\sin(\arccos \beta)}$
$\gamma U(-\beta + (1 + \beta)U - U_\tau^2)$	$\tau_c = \dfrac{\arccos\left(\frac{\beta+1}{2}\right)}{\sqrt{4 - (\beta+1)^2}}$
$\gamma U(-\beta + (1 + \beta)U_\tau - U_\tau^2)$	$\tau_c = -\dfrac{\pi}{2(\beta-1)}$

TABLE B.1: Note that $U(t) = U$, $U(t - \tau) = U_\tau$ and parameter $\gamma = 1$.

characteristic equation:

$$\lambda = (\beta\gamma - \gamma)e^{-\lambda\tau}, \tag{B.3}$$

for which analytical solutions are difficult to find. Nevertheless, from a stability viewpoint it is important to find whether there are any solutions with $Re\lambda > 0$ which implies instability (since the perturbation grows exponentially with time). By setting $\lambda = i\omega$, we assume $Re\lambda = 0$, and obtain an expression for the critical value at which the system passes through the Hopf bifurcation, below which stability prevails and above which instability occurs. Substituting into (B.3) and separating real and imaginary parts of the transcendental equation, we obtain the system:

$$-(\beta\gamma - \gamma)\cos(\omega\tau) = 0 \tag{B.4}$$

$$\omega = -(\beta\gamma - \gamma)\sin(\omega\tau) \tag{B.5}$$

Following some elementary calculations we are able to find the critical value of τ:

$$\tau_c = -\frac{\pi}{2(\beta\gamma - \gamma)} \tag{B.6}$$

In all subsequent analysis, the characteristic growth rate was taken as $\gamma = 1$. In the below table we summarise stability conditions for all other models used.

For the delayed cooperation model (3.6) stability analysis confirmed that the equilibrium remains stable as:

$$\lambda = \beta - 1 \tag{B.7}$$

thus the eigenvalue is always negative for all biologically viable values of β. Loss of stability does not occur for the model incorporating time delay in the maturation

term (3.10), as the stability condition in this case reads:

$$\lambda = \frac{\arccos\left(\frac{2}{1+\beta}\right)}{\sqrt{\frac{1+\beta}{2}}} \tag{B.8}$$

Since $-1 \leq \beta \leq 0.5$, $\arccos\left(\frac{2}{1+\beta}\right)$ is not defined, there are no bifurcation values, τ_c. As for the model incorporating time delay in direct competition (3.11) we were able to map all critical values, τ_c:

$$\tau_c = \frac{\arccos\beta}{\sin(\arccos\beta)} \tag{B.9}$$

with the exception of $\beta = -1$ as it is a singularity. Addition of another delayed term into direct competition results in model (3.12) for which the stability condition reads:

$$\tau_c = \frac{\arccos\left(\frac{\beta+1}{2}\right)}{\sqrt{4-(\beta+1)^2}} \tag{B.10}$$

Analytically defining bifurcation values, τ_c, for the model with two delayed terms (3.13) is the same as in model with delayed competition (3.5).

Appendix C

Loss of Monotonicity: delay differential equations

Following the linearisation method previously described, we obtain expressions (and subsequently values) for the time delay parameter, τ, when the system loses monotonicity, i.e. when the solution still approaches the stable equilibrium $U_* = K$, but in a nonmonotonous manner (referred to as damped oscillations). We introduce the conditions of monotonicity, solving for one model, and list results for all others, as in Appendix B.

We consider model (3.5) and its corresponding characteristic equation:

$$F(\lambda; \tau) = \lambda + e^{-\lambda\tau}(\gamma - \beta\gamma) = 0 \qquad (\text{C.1})$$

In general, whether the solution is monotone or not depends on the roots of this eigenvalue equation and loss of monotonicity is associated with the total loss of all relevant real eigenvalues. Obviously, when $\tau = 0$, the eigenvalue is negative for all biologically relevant values of β. The minimum of the characteristic polynomial, F, lies in the third quarter of the (λ, F) plane, and has two negative roots for sufficiently small time delay, τ. By increasing τ, the minimum is pushed upwards and for a particular $\tau = \tau_*$, the two roots merge and disappear – go complex (Fig. C.1).

At this critical value the two roots coalesce and the following condition holds:

$$\frac{\partial F}{\partial \lambda}(\lambda; \tau) = 0 \qquad (\text{C.2})$$
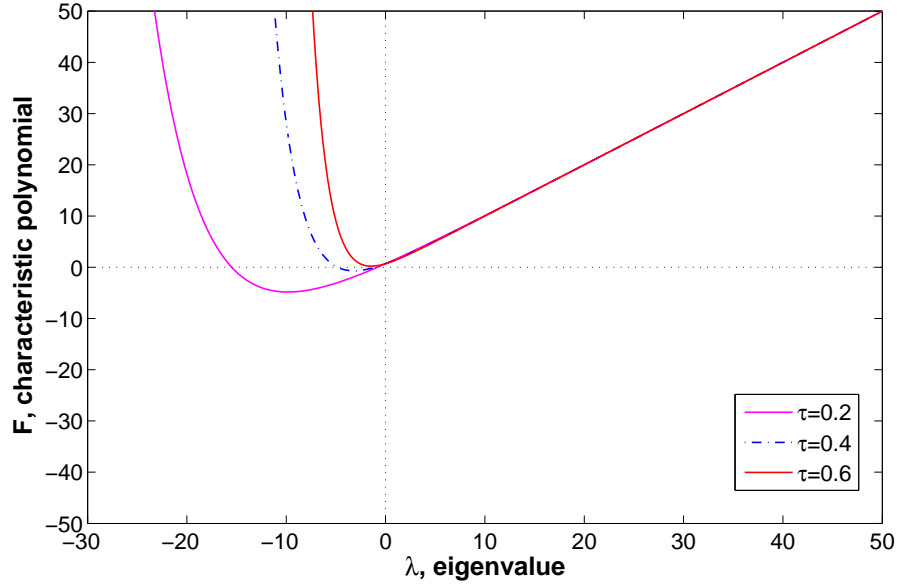
FIGURE C.1: Plot of $F(\lambda;\tau)$ for different values of τ. The simulation was done for $\beta = 0.3$, and the critical value at which the loss of monotonicity occurs is calculated as $\tau_* = 0.53$.

Model	Stability Condition
$\gamma U(U_\tau - \beta)(K - U)$	$\lambda = \beta - 1$
$\gamma U(-\beta + (1+\beta)U_\tau - U^2)$	$\frac{1}{\tau_*(\beta+1)} + e^{1+2\tau_*} = 0$
$\gamma U(-\beta + (1+\beta)U - U_\tau U)$	$\frac{1}{\tau_*} - e^{1-\beta\tau_*} = 0$
$\gamma U(-\beta + (1+\beta)U - U_\tau^2)$	$\frac{1}{2\tau_*} - e^{1-(1+\beta)\tau_*}$
$\gamma U(-\beta + (1+\beta)U_\tau - U_\tau^2)$	$\tau_* = \frac{1}{e(1-\beta)}$

TABLE C.1: Note that $U(t) = U$, $U(t - \tau) = U_\tau$ and parameter $\gamma = 1$.

On elimination of λ, using elementary calculus, one finds an explicit condition for τ:

$$\tau_* = \frac{1}{e(\gamma - \beta\gamma)} \qquad (C.3)$$

and so loss of monotonicity is predicted for $\tau \geq \tau_*$. Note this is the only case in which we may obtain an explicit expression, as with all other models implicit expressions are presented. In the below table we summarise all critical values, τ_* for which solutions lose monotonicity, for all subsequent models.

In Eq. (3.6) the solution remains monotonous as the eigenvalues are always negative for all applicable values of the Allee threshold ($\lambda = \beta - 1$).

Model (3.10), yielding the most interesting step-like results, clearly preserves monotonicity throughout all possible values of the time delay parameter, τ, as the monotonicity condition does not have any roots, and reads:

$$\frac{1}{\tau(\beta+1)} + e^{1+2\tau} = 0 \qquad (C.4)$$

For model (3.11) the implicit expression for the critical time delay is:

$$\frac{1}{\tau} - e^{1-\beta\tau} = 0 \qquad (C.5)$$

A differing monotonicity condition is obtained for a fully delayed density dependent mortality (model (3.12)):

$$\frac{1}{2\tau} - e^{1-(1+\beta)\tau} \qquad (C.6)$$

Our two delay model yielded the same condition as in model (3.5), as was expected and confirmed in numerical simulations.

Bibliography

[1] Abbott O H, McNeilly A S, Lunn S F, Hulme M J, Burden F J (1981) Inhibition of ovarian function in subordinate marmoset monkeys (*Callithrix jacchus jacchus*). Journal of Reproduction and Fertility 63(2):335-345.

[2] Adamson M W, Morozov A Y (2012) Revising the role of species mobility in maintaining biodiversity in communities with cyclic competition. Bull. Math. Biol. 74: 2004–2031.

[3] Adamson M W, Morozov A Y (2013) When can we trust our model predictions? Unearthing structural sensitivity in biological systems. Proceedings of the Royal Society A: Mathematical, Physical and Engineering Sciences 469 (2149).

[4] Akçakaya H R, Halley J M, Inchausti P (2003)Population level mechanisms for reddened spectra in ecological time series. Journal of Animal Ecology 72:698-702.

[5] Allsopp P G (1996) Japanese beetle, *Popillia japonica* Newman (*Coleoptera: Scarabaeidae*): rate of movement and potential distribution of an immigrant species. Coleopterists Bulletin 50:81-95.

[6] Amarasekara P (1998a) Interactions between local dynamics and dispersal: Insights from single species models. Theoretical Population Biology 53(1):44-59.

[7] Amarasekara P (1998b) Allee effects in metapopulation dynamics. The American Naturalist 152(2):298-302.

[8] Andow D, Kareiva P, Levin S, Okubo A (1990) Spread of invading organisms. Landscape ecology 4:177-188.

[9] Ariño A, Pimm S L (1995) On the nature of population extremes. Evol. Ecol. 9:429-443.

[10] Asa C S, Valdespino C (1998) Canid reproductive biology: an integration of proximate mechanisms and ultimate causes. American Zoologist 38(1):251-259.

[11] Ashwin P, Bartuccelli V, Bridges T J, Gourley S (2002) Travelling fronts for the KPP equation with spatio-temporal delay. Z.angew. Math. Phys. 53:102-122.

[12] Balkind M D, Jacobs K R, Güneralp B, Basurto X (2013) Resilience, social-ecological rules, and environmental variability in a two species artisanal fishery. Ecology and Society 18(4):50.

[13] Banks H T (1977) Delay systems in biological models: approximation techniques. In Nonlinear Systems and Applications (ed. Lakshmikantham V.), pp. 21-38. New York: Academic Press.

[14] Barlow N D, Caldwell N P, Kean J M, Barron M C (2000) Modelling the use of NPV for the biological control of Asian gypsy moth *Lymantria dispar* invading New Zealand. Agricultural and Forest Entomology 2(3):173-184.

[15] Baumgartner M F (1997) The distribution of Risso's dolphin (Grampus Griseus) with respect to the physiography of the northern Gulf of Mexico. Marine Mammal Science 13(4):614-638.

[16] Beddington J R, May R M (1975) Time delays are not necessarily destabilizing. Mathematical Biosciences 27:109-117.

[17] Belnap J, Phillips S L (2001) Soil biota in an ungrazed grassland: response to annual grass (Bromus tectorum) invasion. Ecological Applications 11:1261-1275.

[18] Beretta E, Kuang Y (1998) Global analyses in some delayed ratio-dependent predator-prey systems. Nonlinear Analysis: Theory, Methods and Applications 32(3): 381-408.

[19] Berryman A A, Stenseth N C, Isaev A S (1987) Natural regulation of herbivorous forest insect populations. Oecologia 71:174-184.

[20] Berryman A, Turchin P (1997) Detection of delayed density dependence: Comment. Ecology 78:318-320.

[21] Berryman A, Turchin P (2001) Identifying the density-dependent structure underlying ecological time series. Oikos 92:265-270.

[22] Bjørnstad O N, Begon M, Stenseth N C, Falk W, Sait S M, Thompson D J (1998) Population dynamics of the Indian meal moth: Demographic stochasticity and delayed regulatory mechanisms. Journal of animal ecology 67: 110-126.

[23] Bjørnstad O N, Peltonen M, Liebhold A M, Baltensweiler W (2002) Waves of larch budmoth outbreaks in the European Alps. Science 298:1020-1023.

[24] Blackburn T M, Pyšek P, Bacher S A , Carlton J T, Duncan R P, Jarošík V, Wilson J R U, Richardson D M (2011) A proposed unified framework for biological invasions. Trens in Ecology and Evolution 26(7):333-339.

[25] Blackman R B, Tukey J W (1958) The measurement of power spectra from the point of view of communications engineering-Part I. The Bell System Technical Journal 37:185-282.

[26] Briggs C J, Sait S M, Begon M, Thompson D J, Godfray H C J (2000) What causes generation cycles in populations of stored-product moths? J Anim Ecol 69(2):352–366.

[27] Britton N F (1990) Spatial structures and periodic travelling waves in an integro-differential reaction-diffusion population model. SIAM Journal on Applied Mathematics 50(6):1663-1688.

[28] Brown M W, Cameron E A (1982) Natural enemies of *Lymantria dispar* (*Lep: Lymantriidae*) eggs in Central Pennsylvania, U.S.A, and the review of the world literature on natural enemies of *L. dispar* eggs. Entomophaga 27(3):311-321.

[29] Brown R G B (1970) Fulmar distribution: a Canadian perspective. Ibis 111:44-51.

[30] Buckland S T, Newman K B, Fernandez C, Thomas L, Harwood J (2007) Embedding population dynamics models in inference. Stat. Sci. 22(1):44-58.

[31] Busenberg S, Huang W (1996) Stability and Hopf bifurcation for a population delay model with diffusion effects. Journal of Differential Equations 124:80-107.

[32] Buss L, McCullough D, Smitley D R (2001) *Entomophaga maimaiga*: a Natural enemy of gypsy moth. Michigan State University Extension Bulletin E-2604.

[33] Campbell R W (1969) Studies on gypsy moth population dynamics. Forest Insect Population Dynamics: 29-44. Proceedings of the Forest Insect Population Dynamics Workshop, 1967. United States Department of Agriculture Forest Service Research Paper NE 125:29-34.

[34] Campbell R W, Sloan R J (1977) Natural regulation of innocuous gypsy moth populations. Environmental Entomology 6(2):315-322.

[35] Camphuysen C J, Garthe S (1997) An evaluation of the distribution and scavenging habits of northern fulmars (*Fulmarus glacialis*) in the North Sea. ICES Journal of Marine Science 54:654-683.

[36] Cantrell R S, Cosner C (2003) Spatial ecology via reaction-diffusion equations. Wiley.

[37] Cao Y, Gard T C (1995) Ultimate bounds and global asymptotic stability for differential delay equations. Rocky Mountain Journal of Mathematics 25(1):119-131.

[38] Caughley G (1970) Eruption of ungulate populations with emphasis on Himalayan thar in New Zealand. Ecology 51:53-72.

[39] Çelik C, Merdan H, Duman O, Akin Ö (2008) Allee effects on population dynamics with delay. Chaos, Solitons and Fractals 37:65-74.

[40] Chapman R N (1928) The quantitative analysis of environmental factors. Ecology 9:111-122.

[41] Clark J, Bjørnstad O (2004) Population time series: process variability, observation errors, missing values, lags and hidden states. Ecology 85:3140âĂŞ-3150.

[42] Clutton-Brock T H, Brotherton P N M, Smith R, McIlrath G M, Kansky R, Gaynor D, O'Riain M J, Skinner J D (1998) Infanticide and expulsion of females in a cooperative mammal. Proceedings: Biological Sciences 65(1412):2291-2295.

[43] Clutton-Brock T H, Hodge S J, Flower T P (2008) Group size and the suppression of subordinate reproduction in Kalahari meerkats. Animal Behaviour 76(3):689-700.

[44] Comins H N, Hassell M P (1976). Predation in multi-prey communities. J Theor Biol 62: 93-114.

[45] Cooke K L, Grossman Z (1982) Discrete delay, distributed delay and stability switches. Journal of Mathematical Analysis and Applications 86:592-627.

[46] Coulson R N, Witter J A (1984) Forest entomology: ecology and management. Wiley, New York.

[47] Courchamp F, Berec L, Gascoigne J (2008) Allee effects in Ecology and Conservation. Oxford University Press.

[48] Courchamp F, Clutton-Brock T, Grenfell B (1999) Inverse density dependence and the Allee effect. TREE 14(10):405-410.

[49] Cuddington K M, Yodzis O (1999) Black noise and population persistence. Proc. R. Soc. Lond. Ser. B-Biol. Sci. 264:1841-1847.

[50] Cushing J M (1976) Predator-prey interactions with time delays. Journal of Mathematical Biology (3-4):369-380.

[51] Cushing J M (1994) Oscillations in age-structured population models with an Allee effect. Journal of Computational and Applied Mathematics 52:71-80.

[52] D'Amico V, Elkinton J S, Dwyer G, Burand J P, Buonaccorsi J P (1996) Virus transmission in gypsy moths is not a simple action mass process. Ecology 77(1):201-206.

[53] Davis M A (2009) Invasion biology. Oxford University Press, Oxford, UK.

[54] Davis M B, Calcote R R, Sugita S, Takahara H (1998) Patchy Invasion and the Origin of a Hemlock-Hardwoods Forest Mosaic. Ecology 79:2641-2659.

[55] Davis R W, Ortega-Ortis J G, Ribic C A, Evans W E, Biggs D C, Ressler P H, Cady R B, Leden R R, Mullin K D, Wursig B (2002) Cetacean habitat in the northern oceanic Gulf of Mexico. Deep Sea Research Part I: Oceanographic Research Papers 49(1):121-142.

[56] De Roos A M, Persson L (2002) Size-dependent life-history traits promote catastrophic collapses of top predators. Proceedings of the National Academy of Sciences 99(20):12907-12912.

[57] De Roos A M, Persson L, Thieme H R (2003) Emergent Allee effects in top predators feeding on structured prey populations. Proceedings of the Royal Society B 270:611-618.

[58] Dennis B (1989) Allee effects: Population growth, critical density and the chance of extinction. Natural Resource Modeling 3:481-538.

[59] Desharnais R A (1997) Population dynamics of *Tribolium.* Pages 303-328 in Structured Population Models in Marine, Terrestrial, and Freshwater Systems, S. Tuljapurkar and H. Caswell (editors), Chapman & Hall, New York.

[60] Dobzhansky T, Wright S (1943) Genetics of natural populations. X. Dispersion rates in *Drosophila Pseudoobscura.* Genetics 28(4):304-340.

[61] Dunbar S R (1983) Travelling wave solutions of diffusive Lotka-Volterra equations. J.Math.Biol. 17:11-32.

[62] Dunlap T R (1980) The gypsy moth: a study in science and public policy. Journal of Forest History 24(3):116-126.

[63] Dwyer G (1991) The role of density, stage and patchiness in the transmission of an insect virus. Ecology 72(2):559-574.

[64] Dwyer G (1992) On the spatial spread of insect pathogens: theory and experiment. Ecology 73(2):479-494.

[65] Dwyer G, Dushoff J, Elkinton J S, Levin S A (2000) Pathogen-driven outbreaks in forest defoliators revisited: building models from experimental data. The American Naturalist 156(2):105-120.

[66] Dwyer G, Elkinton J S (1993) Using simple models to predict virus epizootics in gypsy moth populations. Journal of Animal Ecology 62(1):1-11.

[67] Dwyer G, Elkinton J S, Buonaccorsi J P (1997) Host heterogeneity in susceptibility and disease dynamics: tests of a mathematical model. The American Naturalist 150(6):685-707.

[68] Elkinton J S, Burand J P, Murray K D, Woods S A (1990) Epizootiology of gypsy moth nuclear polyhedrosis virus. USDA Gypsy Moth Research Review.

[69] Elkinton J S, Dwyer G, Sharov A (1995) Modelling the epizootiology of gypsy moth nuclear polyhedrosis virus. Computers and Electronics in Agriculture 13:91-102.

[70] Elkinton J S, Healy W M, Buonaccorsi J P, Boettner G H, Hazzard A M, Smith H R, Liebhold A M (1996) Interactions among gypsy moths, white-footed mice, and acorns. Ecology 77(8):2332-2342.

[71] Elkinton J S, Liebhold A M (1990) Population dynamics of gypsy moth in North America. Annual Review of Entomology 35:571-596.

[72] Elton C and Nicholson M (1942) The ten-year cycle in numbers of the lynx in Canada. J. Anim. Ecol. 11:215-244.

[73] Elton C S (1924) Periodic fluctuations in the number of animals: their causes and effects. British Journal of Experimental Biology 2:119-163.

[74] Elton C S (1958) The ecology of invasions by animals and plants. Chapman & Hall, London.

[75] Fagan W F, Lewis M A, Neurbert M G, van der Driessche P (2002) Invasion theory and biological control. Ecol. Lett. 5:148-157.

[76] Fisher J (1952) The fulmar. New Naturalist Monograph 6. Collins, London.

[77] Fisher J (1966) The fulmar population of Britain and Ireland, 1959. Bird Study 13:5-76.

[78] Fisher R A (1937) The wave of advance of advantageous genes. Annals of Eugenics 7:255-369.

[79] Fortin M J, Dale M R T (2005) Spatial Analysis: A Guide for Ecologists. Cambridge: Cambridge University Press.

[80] Fowler A C (1982) An asymptotic analysis of the delayed logistic equation when the delay is large. IMA Journal of Applied Mathematics 28:41–49.

[81] Fowler M S, Ruxton G D (2002) Population dynamic consequences of Allee effects. Journal of Theoretical Biology 215:39-46.

[82] Freedman H I, Gopalsamy K (1986) Global stability in time delayed single species dynamics. Bulletin of Mathematical Biology 48(5):485-492.

[83] Fussmann GF, Blasius B (2005) Community response to enrichment is highly sensitive to model structure. Biology Letters 1:9-12.

[84] Gascoigne J C, Beadman H A, Saurel C, Kaiser M J (2005) Density dependence, spatial scale and patterning in sessile biota. Oecologia 145(3):371-381.

[85] Gerardi M H, Grimm J K (1979) The history, biology, damage and control of the gypsy moth, *Porthetria dispar* (*L.*). Fairleigh Dickinson University Press (Rutherford N.J.).

[86] Gillman M P, Dodd M E (1998) The variability of orchid population size. Bot. J. Linnean Soc. 126:65-74.

[87] Ginzburg L R, Taneyhill D E (1994) Population cycles of forest *Lepidoptera*: a maternal effect hypothesis. J Anim Ecol 63:79-92

[88] Gopalsamy K, Ladas G (1990) On the oscillation and asymptotic behaviour of $\dot{N}(t) = N(t)[a + bN(t-T) - cN^2(t-T)]$. Quarterly of Applied Mathematics 3:433-440.

[89] Gould J R, Elkinton J S, Wallner W E (1990) Density-dependent suppression of experimentally created gypsy moth, *Lymantria dispar* (*Lepitoptera: Lymantriidae*) populations by natural enemies. Journal of Animal Ecology 59(1):213-233.

[90] Goulson D, Hails R S, Williams T, Hirst M L, Vasconcelos D, Green B M, Carty T M, Cory J S (1995) Transmission dynamics of a virus in a stage-structured insect population. Ecology 76(2):392-401.

[91] Gourley S A , Bartuccelli M V (1995) Length scales in solutions of a scalar reaction-diffusion equation with delay. Physics Letters A 202:79-87.

[92] Gourley S A, Chaplain M A J (2002) Travelling fronts in a food-limited population model with time delay. Proceedings of the Royal Society of Edinburgh 132A:75-89.

[93] Graham I S, Lambin X (2002)The impact of weasel predation on cyclic field vole survival: The specialist predator hypothesis contradicted. Journal of Animal Ecology 71(6):946-956.

[94] Green D, Stech H W (1981) Diffusion and hereditary effects in a class of population models. In Differential equations and applications in ecology, epidemics and population problems (Ed Busenberg S and Cooke K L) pp. 19-28. Academic Press, New York.

[95] Greene D F, Calogeropoulos C (2001) Measuring and modelling seed dispersal for terrestrial plants. In Dispersal Ecology, pp. 3-23. Blackwell, Oxford.

[96] Griffin A S, Pemberton J M, Brotherton P N M, McIlrath G, Gaynor D, Kansky R, O'Riain J, Clutton-Brock T H (2003) A genetic analysis of breeding success in the cooperative meerkat (*Suricata suricatta*). Behavioural Ecology 14:472-480.

[97] Griffiths S W, Armstrong J D, Metcalfe N B (2003) The cost of aggregation: Juvenile salmon avoid sharing winter refuges with siblings. Behavioural Ecology 14(5):202-206.

[98] Grünbaum D (2012) The logic of ecological patchiness. Interface Focus 2:150-155.

[99] Halley J M (1996) Ecology, evolution and $1/f$ noise. Trends in ecology and evolution 11(1):33-37.

[100] Halley J M, Inchausti P (2004) The increasing importance of $1/f$-noises as models of ecological variability. Fluctuation and Noise Letters 4(2):R1-R26.

[101] Halley J M, Kunin W E (1999) Extinction risk and the $1/f$ family of noise models. Theoretical Population Biology 56:215-230.

[102] Hansen T F, Stenseth N C, Henttonen H, Tast J (1998) Interspecific and intraspecific competition as causes of direct and delayed density dependence in a fluctuating vole population. Proc National Acad Sci USA 96(3):986-991

[103] Hansen T F, Stenseth N C, Henttonen H, Tast J (1998) Interspecific and intraspecific competition as causes of direct and delayed density dependence in a fluctuating vole population. Proceedings of the National Academy of Sciences of the United States of America 96(3):986-991.

[104] Hassell M P, Lawton J H, May R M (1976) Patterns of dynamical behaviour in single species populations. Journal of Animal Ecology 45:471-486.

[105] Hastie G D, Wilson B, Wilson L J, Parsons K M, Thompson P M (2004) Functional mechanisms underlying cetacean distribution patterns: hotspots for bottlenose dolphins are linked to foraging. Marine Biology 144(2):397-403.

[106] Hastings A (1983) Age dependent predation is not a simple process. I. Continuous time models. Theoretical Population Biology 23:347-362.

[107] Hastings A (1984) Delays in recruitment at different trophic levels: effects on stability. J Math Biol 21(1):35-44.

[108] Hastings A, Harisson S, McCann K (1997) Unexpected spatial patterns in an insect outbreak match a predator diffusion model. Proc. R. Soc. Lond. B 264:1837–1840.

[109] Hayek A E (1999) Pathology and epizootiology of *Entomophaga maimaiga* infections in forest *Lepidoptera*. Microbiology and Molecular Biology Reviews: 814-835.

[110] Hayek A E, Glare T R, O'Callaghan M (eds)(2009) Use of microbes for control and eradication of invasive arthropods. Springer.

[111] Hengeveld R (1989) Dynamics of biological invasion. Chapman and Hall, London.

[112] Heywood V H (1989) Patterns, extents and modes of invasions by terrestrial plants. In Biological Invasions: A global perspective SCOPE 37, pp. 31-55. Wiley, New-York.

[113] Hicks H, Blackshaw R P (2008) Differential responses of three Agriotes click beetle species to pheromone traps. Agric. For. Ent. 10:443-448.

[114] Holling C S (1959a) The components of predation as revealed by a study of small mammal predation of the European pine sawfly. Canadian Entomologist 91:293-320.

[115] Holling C S (1959b) Some characteristics of simple types of predation and parasitism. Canadian Entomologist 91:385-398.

[116] Holling C S (1965) The functional response of predators to prey density and its role in mimicry and population regulation. Memoirs of the Entomological Society of Canada 45:1–60.

[117] Holling C S (1966) The functional response of invertebrate predators to prey density. Memoirs of the Entomological Society of Canada 48:1–86.

[118] Holmes E E (1993) Are diffusion models too simple? A comparison with telegraph models of invasion. American Naturalist 142:779-795.

[119] Holt R D (1983) Optimal foraging and the form of the predator isocline. Amer Nat 122:521-541.

[120] Hooge F N, Bobbert P A (1997) On the correlation function of $1/f$ noise. Physica B 239:223-230.

[121] Hoy M A (1976) Establishment of gypsy moth parasitoids in North America: an evaluation of possible reasons for establishment or non-establishment. Perspectives in Forest Entomology (eds J F Anderson and H K Kaya): 215-232. Academic, New York.

[122] Huang W (1998) Global dynamics for a reaction-diffusion equation with time delay.

[123] Hutchinson G E (1948) Circular causal systems in ecology. Annals of the New York Academy of Science 50:221-246.

[124] Inchausti P, Halley J M (2002) The long-term ecological variability and spectral colour of animal populations. Evol. Ecol. Res. 4:1033-1048.

[125] Invasive Species Specialist Group (2008) 100 of the world's worst invasive species. `http://www.issg.org/worst100_species.html`

[126] Jankovic M, Petrovskii S (2013) Gypsy moth invasion in North America: A simulation study of the spatial pattern and the rate of spread. Ecological Complexity 14:132-144.

[127] Jankovic M, Petrovskii S (2014) Are time delays always destabilizing? Revisiting the role of time delays and the Allee effect. Theor Ecol, in press, DOI 10.1007/s12080-014-0222-z.

[128] Jansen V A A, Mashanova A, Petrovskii S V (2012) Model selection and animal movement: Comment on "Levy walks evolve through interaction between movement and environmental complexity." Science 335:918.

[129] Johnson D M, Liebhold A M, Tobin P C, Bjørnstad O N (2006) Allee effects and pulsed invasion by the gypsy moth. Nature 444:361-363.

[130] Johnson J B (1925) The Schottky effect in low frequency circuits. Phys. Rev. 26:71-85.

[131] Jones C G, Ostfeld R S, Richard M P, Schauber E M, Wolff J O (1998) Chain reactions linking acorns to gypsy moth outbreaks and lyme disease risk. Science 279: 1023-1026.

[132] Kaitala V, Ranta E (1996) Red/blue chaotic power spectra. Nature 381:198-199.

[133] Kakutani S, Marcus L (1958) On the non-linear difference-differential equation $y\prime(t) = [A - By(t - \tau)]y(t)$. In Contribution to the theory of nonlinear oscillations, pp 1-18. Princeton University Press.

[134] Kareiva P M (1983) Local movement in herbivorous insects: applying a passive diffusion model to mark-recapture field experiments. Oecologia 57(3):322-327.

[135] Kareiva P, Mullen A, Southwood R (1990) Population dynamics in spatially complex environments: theory and data (and discussion). Phil. Trans. R. Soc. Lond. B 330(1257):175-190.

[136] Kareiva P, Odell G (1987) Swarms of predators exhibit "preytaxis" if individual predators use area-restricted search. American Naturalist 130(2):233-270.

[137] Kasdin N J (1995) Discrete simulation of colored noise and stochastic-processes and $1/f^\alpha$ power-law noise generation. Proc. IEEE 83:802-827.

[138] Keller R P, Lodge D M (2007) Species invasions from commerce in live aquatic organisms: problems and possible solutions. BbioScience 57:428-436.

[139] Kenis M, Vaamonde C L (1998) Classical biological control of the gypsy moth, *Lymantria dispar* (*L.*), in North America: prospects and new strategies. Population Dynamics, Impacts, and Integrated Management of Forest Defoliating Insects (eds M L McManus and A M Liebhold). USDA Forest Service General Technical Report NE-247:213-221.

[140] Kermack W O, McKendrick G A (1927) A contribution to the mathematical theory of epidemics. Proceedings of the Royal Society of London, Series A 115:700-721.

[141] Keshner M S (1979) Renewal process and diffusion models of $1/f$ noise. PhD thesis.

[142] Keshner M S (1982) $1/f$ noise. Proc. IEEE 70:212-218.

[143] Kitabayashi N, Kusunoki Y, Gunji Y P (2002) Active behaviour and $1/f$ noise in shell-changing behaviour of the hermit crabs. Rivista di Biologia 95(2):327-336.

[144] Klausmeier C A (1999) Regular and irregular patterns in semiarid vegetation. Science 284:1826-1828.

[145] Klemmendson J O, Smith J G (1964) Cheatgrass (*Bromus tectorum L.*). The Botanical Review 30:226-262.

[146] Koenig W D, Dickinson J L (2004) Ecology and evolution of cooperative breeding in birds. Cambridge University Press.

[147] Kolar C S, Lodge D M (2001) Progress in invasion biology: predicting invaders. Trends in Ecology and Evolution 16:199-204.

[148] Kolmogorov A, Petrovsky N, Piscunov N S (1937) A study of the equation of diffusion with an increase in the quantity of matter, and its application to a biological problem. Moscow University Bulletin of Mathematics 1:1-25.

[149] Kot M (1992) Discrete-time travelling waves: ecological examples. Journal of Mathematical Biology 30:413-436.

[150] Kot M (2001) Elements of mathematical ecology. Cambridge University Press, Cambridge.

[151] Kot M, Lewis M A, Van den Driessche P (1996) Dispersal data and spread of invading organisms. Ecology 77:2027-2042.

[152] Kot M, Schaffer W M (1986) Discrete-time growth-dispersal models. Mathematical Biosciences 80:109-136.

[153] Kramer A M, Dennis B, Liebhold A M, Drake J M (2009) The evidence for Allee effects. Population Ecology 51:341-354.

[154] Kramer K L (2010) Cooperative breeding and its significance to the demographic success of humans. Annual Review of Anthropology 39:417-436.

[155] Krebs C J (1996) Population cycles revisited. Journal of Mammalogy 77(1):8-24.

[156] Krebs C J and Myers J (1974) Population cycles in small mammals. Advances in Ecological Research 8:267-399.

[157] Kuang Y (1993) Delay differential equations with applications in population dynamics. Academic Press, New York.

[158] Lautenschlager R A, Podgwaite J D, Watson D E (1980) Natural occurrence of the nucleopolyhedrosis virus of the gypsy moth, *Lymantria dispar*(*Lep: Lymantriidae*) in wild birds and mammals. Entomophaga 25(3):261-267.

[159] Lawton J (1988) More time means more variation. Nature 334:563.

[160] Lee C T, Hoopes M F, Diehl J, Gilliland W, Huxel G, Leaver E V, McCann K, Umbanhowar J, Mogilner AC(2001) Non-local concepts and models in biology. Journal of Theoretical Biology 210:201-219.

[161] Leonard D E (1974) Recent developments in ecology and control of the gypsy moth. Annual Review of Entomology 19:197-229.

[162] Leuschner W A, Young J A, Ravlin F W (1996) Potential benefits of slowing the gypsy moth's spread. Southern Journal of Applied Forestry 20(2):65-73.

[163] Levin S (1994) Patchiness in marine and terrestrial systems: from individuals to populations. Phil. Trans. R. Soc. Lond. B 343:99-103.

[164] Levin S A, Segel L A (1976) Hypothesis for origin of planktonic patchiness. Nature 259.

[165] Levins R (1969) Some demographic and genetic consequences of environmental heterogeneity for biological control. Bull Entomol Soc Am 15:237-240.

[166] Lewis M A, Kareiva P (1993) Allee dynamics and the spread of invading organisms. Theoretical Population Biology 43:141-158.

[167] Lewis M A, van den Driessche P. (1993). Waves of extinction from sterile insect release. Mathematical Bioscience 116:221-247.

[168] Li W T, Yan X P, Zhang C H (2008) Stability and Hopf bifurcation for a delayed cooperation diffusion system with Dirichlet boundary conditions. Chaos, Solitons and Fractals 38:227-237.

[169] Liebhold A M, Bascompte J (2003) The Allee effect, stochastic dynamics and the eradication of alien species. Ecology Letters 6:133-140.

[170] Liebhold A M, Elkinton J S, Miller D R, Wang Y S (1989) Estimating oak leaf area index and gypsy moth, *Lymantria dispar* (*L.*)(*Lepidoptera: Lymantriidae*), defoliation using canopy photographs. Environmental Entomology 17:560-566.

[171] Liebhold A M, Elkinton J, Williams D, Muzika R M (2000) What causes outbreaks of the gypsy moth in North America? Population Ecology 42:257-266.

[172] Liebhold A M, Elmes G A, Hawerson J A, Quimby J (1994) Landscape characterization of forest susceptibility to gypsy moth defoliation. Forest Science 40:18-29.

[173] Liebhold A M, Halverson J A, Elmes G A (1992) Gypsy moth invasion in North America: A quantitive analysis. Journal of Biogeography 19(5):513-520.

[174] Liebhold A M, McCullough D G, Blackburn L M, Frankel S J, von Holle B, Aukema J E (2013) A highly aggregated geographical distribution of forest pest invasions in the USA. Diversity Distrib 19(9):1208-16.

[175] Liebhold A M, Tobin P C (2006) Growth of newly established alien populations: comparison of North American gypsy moth colonies with invasion theory. Population Ecology 48:253-262.

[176] Liebhold A M, Tobin P C (2010) Exploiting the Achilles heels of pest invasions: Allee effects, stratified dispersal and management of forest insect establishment and spread. New Zealand Journal of Forestry 40:25-33.

[177] Lindroth R L, Klein K A, Hemming J D C, Feuker A M (1997) Variation in temperature and dietary nitrogen affect performance of the gypsy moth (Lymantria dispar L.). Physiological Entomology 22:55-64.

[178] Liz E, Pinto M, Robledo G, Trofimchuk S, Tkachenko V (2003) Wright type delay differential equations with negative Schwarzian. Discrete and Continuous Dynamical Systems 9:309-321.

[179] Lloyd C, Tasker M L, Partridge K (1991) The status of seabirds in Britain and Ireland. T & AD Poyser, London.

[180] Lockwood D R, Lockwood J A (1997) Evidence of self-organised criticality in insect populations. Complexity 2(4):49-58.

[181] Lockwood J L, Hoopes M F, Marchetti M P (2013) Invasion ecology. Wiley-Blackwell.

[182] Lodge D M (1993) Biological invasions: lessons for ecology. Trends in Ecology and Evolution 8:133-137.

[183] Lonsdale W M (1993) Rates of spread of an invading species: Mimosa pigra in northern Australia. Jjournal of Ecology 81:53-521.

[184] Lundberg P, Ranta E, Ripa J, Kaitala V (2000) Population variability in space and time. TREE 15(11): 460-464.

[185] Malchow H, Petrovskii S V (2002) Dynamical stabilisation of an unstable equilibrium in chemical and biological systems. Mathematical and Computer Modelling 36:307-319.

[186] Malchow H, Petrovskii S V, Venturino E (2008) Spatiotemporal patterns in ecology and epidemiology: Theory, Models and Siulation. Chapman & Hall/CRC.

[187] Maloney K, Baressi J, Schneeberger N F (2010) Reducing damage and slowing the spread. National Gypsy Moth Management Program, USDA Forest Service Special Initiative Brief. Available at `http://www.na.fs.fed.us/ra/specialinitiatives/gm/gysp_moth_featured_brief11.pdf`.

[188] Martin A P (2003). Phytoplankton patchiness: the role of lateral stirring and mixing. Progress in Oceanography 57:125-174.

[189] Mason C J, McManus M L (1981) Larval dispersal of the gypsy moth. The gypsy moth: research toward integrated pest management (ed by C C Doane and M L McManus). USDA Forest Service Technical Bulletin 1584:161-202.

[190] Mather J A (1982) Factors affecting the spatial distribution of natural populations of octopus *Joubini Robson*. Animal Behaviour 30(4):1166-1170.

[191] May R M (1972) Limit cycles in predator-prey communities. Science 177:900-902.

[192] May R M (1975) Stability and complexity in Model Ecosystems. Princeton University Press. Princeton, second edition.

[193] Maynard Smith J (1974) Models in Ecology. Cambridge University Press.

[194] Mayo J H, Straka T J, Leonard D S (2003) The cost of slowing the spread of the gypsy moth (*Lepidoptera: Lymantriidae*). Journal of Economic Entomology 96(5):1448-1454.

[195] McArdle B (1989) Bird population densities. Nature 338:627-628.

[196] McFadden M W, McManus M E (1991) An insect out of control? The potential for spread and establishment of the gypsy moth in new forest areas in the United States. Forest Insect Guilds: Patterns of Interaction with Host Trees (eds Y N Baranchikov, W J Mattson, F P Hain, T L Payne). USDA Forest Service General Technical Report NE-153: 172-186.

[197] Medvinsky A B, Petrovskii S V, Tikhonova I A, Malchow H, Li B L (2002) Spatiotemporal complexity of plankton and fish dynamics. SIAM Review 44:311-370.

[198] Merdan H, Duman O, Akin Ö, Çelik C (2009) Allee effects on population dynamics in continuous (overlapping) case. Chaos, Solitons and Fractals 39:1994-2001.

[199] Merdan H, Gümüş Ö (2012) Stability analysis of a general discrete-time population model involving delay and Allee effects. Applied Mathematics and Computation 219:1821-1832.

[200] Mimura M, Tohma M (2014) Dynamic coexistence in a three-species competition diffusion system: Ecological Complexity, in press `http://dx.doi.org/10.1016/j.ecocom.2014.05.004`.

[201] Miramontes O, Rohani P (1998) Intrinsically generated coloured noise in laboratory insect populations. Proceedings of the Royal Society London B 265:785-792.

[202] Mistro D C, Rodrigues L A D, Petrovskii S V (2012) Spatiotemporal complexity of biological invasion in a space- and time-discrete predator-prey system with the strong Allee effect. Ecological Complexity 9:16-32.

[203] Mitchell I, Newton S, Ratcliffe N, Dunn T E (2004) Seabird populations of Britain and Ireland. T& AD Poyser, London.

[204] Mooney H A (2005) Invasive alien species: the nature of the problem. In: Invasive Alien Species: A New Synthesis, pp.1-15. Island Press, Washington, DC.

[205] Mooney H A, Mack R N, McNeely J A, Neville L E, Schei P J, Waage J K (eds) (2005) Invasive alien species: a new synthesis. Island Press, Washington DC.

[206] Morozov A Y, Petrovskii S V, Li B-L (2006) Spatiotemporal complexity of the patchy invasion in a predatorâĂŞprey system with the Allee effect. J. Theor. Biol. 238:18-35.

[207] Morozov A, Petrovskii S V (2013) Feeding on multiple sources: towards a universal parameterization of the functional response of a generalist predator allowing for switching. PLoS One 8(9): e74586.

[208] Morozov A, Petrovskii S, Li B L (2004). Bifurcations and chaos in a predator-prey system with the Allee effect. Proceedings of Royal Society of London 271:1407-1414.

[209] Morozov A, Petrovskii S, Li B L (2006) Spatiotemporal complexity of patchy invasion in a predator-prey system with the Allee effect. Journal of Theoretical Biology 238:18-35.

[210] Murray J D (2002) Mathematical Biology I: an introduction. Springer.

[211] Naidoo R, Lechowicz M J (2001) Effects of gypsy moth on radial growth of deciduous trees. Forest Science 47(3):338-348.

[212] Nakamura K, Hasan N, Abbas I H, Godfray C J, Bonsall M B (2004) Generation cycles in Indonesian lady beetle populations may occur as a result of cannibalism. Proceedings: Biological Sciences 271(6):S501-S504

[213] Nakaoka S, Wang W, Takeuchi Y (2009) Effect of parental care and aggregation on population dynamics. Journal of Theoretical Biology 260:161-171.

[214] Nature Conservancy (2014) Impacts of invasive species: invading our lands and waters. `http://www.nature.org/ourinitiatives/habitats/forests/explore/invasives-101.xml`.

[215] Neubert M G, Caswell H (2000) Demography and dispersal: Calculation and sensitivity analysis of invasion speed for structured populations. Ecology 81(6):1613-1628.

[216] Novak S J, Mack R N (2001) Tracing plant introduction and spread into naturalized ranges: genetic evidence from *Bromus tectorum* (cheatgrass). BioScience 51:114-122.

[217] Nunney L (1985) Short time delays in population models: a role enhancing stability. Ecology 66(6):1849-1858.

[218] Odell T M, Mastro V C (1980) Crepuscular activity of gypsy moth adults (*Lymantria dispar*). Environmental Entomology 9:613-617.

[219] Okubo A (1986) Dynamical aspects of animal grouping: swarms, schools, flocks and herds. Adv. Biophys. 22:1-94.

[220] Okubo A, Levin S (2001) Diffusion and Ecological Problems: Modern Perspectives. Springer, Berlin.

[221] Park T (1932) Studies in population physiology: the relation of numbers to initial population growth in the flour beetle *Tribolium confusum* Duval. Ecology 13:172-181.

[222] Parker I M, Simberloff D, Lonsdale W M, Goodell K, Wonham M, Kareiva P M, Williamson W H, Von Holle B, Moyle P B, Byers J E, Goldwasser L (1999) Impact: toward a framework for understanding the ecological effects of invaders. Biological Invasions 1:3-19.

[223] Pashby B S, Cudworth J (1962) The fulmar "wreck" of 1962. Brit. Birds 62:97-109.

[224] Petchey O (2000) Environmental colour affects aspects of single-species population dynamics. Proceedings Royal Society London B 267:747-756.

[225] Petrovskii S V, Bearup D, Ahmed D A, Blackshaw R (2012) Estimating insect population density from trap counts. Ecological Complexity 10:69-82.

[226] Petrovskii S V, Li B L (2006) Exactly solvable models of biological invasions. Chapman & Hall, CRC Press.

[227] Petrovskii S V, Li B L, Malchow H (2003) Quantification of the spatial aspect of chaotic dynamics in biological and chemical systems. Bulletin of Mathematical Biology 65:425-446.

[228] Petrovskii S V, Malchow H (1999) A minimal model of pattern formation in a prey-predator system. Mathematical and Computer Modelling 29(8):49-63.

[229] Petrovskii S V, Malchow H (2000) Critical phenomena in plankton communities: KISS model revisited. Nonlinear Analysis: Real World Applications 1:37-51.

[230] Petrovskii S V, Malchow H (2001) Wave of chaos: new mechanism of pattern formation in spatio-temporal population dynamics. Theoretical Population Biology 59: 157-174.

[231] Petrovskii S V, Malchow H, Hilker F M, Venturino E (2005a) Patterns of patchy spread in deterministic and stochastic models of biological invasion and biological control. Biological Invasions 7:771-793.

[232] Petrovskii S V, Morozov A Y, Li B L (2005b) Regimes of biological invasion in a prey predator system with the Allee effect. Bulletin of Mathematical Biology 67:637-661.

[233] Petrovskii S V, Morozov A Y, Venturino E (2002) Allee effect makes possible patchy invasion in a predator−prey system. Ecology Letters 5:345-352.

[234] Petrovskii S, Blackshaw R, Li B L (2008) Consequences of the Allee effect and intraspecific competition on population persistence under adverse environmental conditions. Bulletin of Mathematical Biology 70(2):412-437.

[235] Petrovskii S, Kawasaki K, Takasu F, Shigesada N (2001) Diffusive waves, dynamical stabilization and spatio-temporal chaos in a community of three competitive species. Jpn. J. Ind. Appl. Math. 18:459–481.

[236] Phillips R A, Petersen M K, Lilliendahl K, Solumundsson J, Hamer K C, Camphuysen C J, Zonfrillo B (1999) Diet of northern fulmar, *Fulmarus glacialis*: reliance on commercial fisheries? Marine Biology 135:159-170.

[237] Pilarska D, McManus M, Pilarski P, Georgiev G, Mirchev P, Linde A (2006) Monitoring the establishment and prevalence of the fungal entomopathogen *Entomophaga maimaiga* in two *Lymantria dispar* (*L.*) populations in Bulgaria. Journal of Pest Science 79:63-67.

[238] Pimentel D (ed.) (2002) Biological invasions: Economic and environmental costs of alien platn, animal and microbe species. CRC Press.

[239] Pimm S L, Redfearn A (1988) The variability of population densities. Nature 334:613-614.

[240] Potter D A, Held D W (2002) Biology and Management of the Japanese beetle. Annu.Rev.Entomol.47:175-205.

[241] Powell T M, Richerson P J, Dillon T M, Agee B A, Dozier B J, Godden D A, Myrup L O (1975)

[242] Ranta E, Vaitala K, Lindstrom J, Linden H (1995) Synchrony in population dynamics. Proc. R. Soc. Lond. B 262(1364):113-115.

[243] Real L A, Brown J H (eds.) (1991) Foundations of ecology. Classic papers with commentaries. University of Chicago Press, USA.

[244] Reardon R C, Podgwaite J D, Zerillo R (2009) Gypchek - bioinsecticide for the gypsy moth. The Forest Health Technology Enterprise Team Handbook.

[245] Reeson A F, Wilson K, Cory J S, Hankard P, Weeks J M, Goulson D, Hails R S (2000) Effects of phenotypic plasticity on pathogen transmission in the field in a Lepidoptera-NPV system. Oecologia 124:373-380.

[246] Renshaw E (1991) Modelling Biological Populations in Space and Time. Cambridge University Press, Cambridge UK.

[247] Richardson D M (2011) Invasion science: the roads travelled and the roads ahead. In: Fifty years of Invasion Ecology: The Legacy of Charles Elton, pp. 397-407. Wiley-Blackwell, Oxford, UK.

[248] Richardson D M, Pyšek P (2008) Fifty years of invasion ecology: the legacy of Charles Elton. Diversity and Distributions 14:161-168.

[249] Rietkerk M, Dekker S C, de Ruiter P C, van de Koppel J (2004) Self-organized patchiness and catastrophic shifts in ecosystems. Science 305:1926-1929.

[250] Rietkerk M, van de Koppel J (2007) Regular pattern formation in real ecosystems. Trends in Ecology and Evolution 23(3):169-175.

[251] Ritchie M E (2010) Scale, heterogeneity and the structure and diversity of ecological communities. Princeton, NJ: Princeton University Press.

[252] Robinet C, Lance D R, Thorpe K W, Onufrieva K S, Tobin P C, Liebhold A M (2008) Dispersion in time and space affect mating success and Allee effects in invading gypsy moth populations. Journal of Animal Ecology 77:966-973.

[253] Rosenzweig M L (1971) Paradox of enrichment: Destabilization of exploitation ecosystems in ecological time. Science 171:385-387.

[254] Rossiter M C (1991) Environmentally-based maternal effects: A hidden force in insect population dynamics. Oecologia 87(2):288-294.

[255] Royama T (1981) Fundamental concepts and methodology for the analysis of animal population dynamics, with particular reference to univoltine species. Ecological Monographs 51:473-493.

[256] Ruan S G (1995) The effect of delays on stability and persistence in plankton models. Nonlinear Analysis – Theory, Methods & Applications 24:575-585.

[257] Ruokalainen L, Linden A, Kaitala V, Fowler M S(2009) Ecological and evolutionary dynamics under coloured environmental variation. Trends in ecology and evolution 24(10):555-563.

[258] Sakai A K, Allendorf F W, Holt J S, Lodge D M, Molofsky J, With K A, Baughman S, Cabin R J, Cohen J E, Ellstrand N C, McCauley D E, O'Neil P, Parker I M, Thompson J N, Weller S G (2001) The population biology of invasive species. Annual Review Of Ecology And Systematics 32:305-332.

[259] Salomonsen F (1965) Geographic variation in the Fulmar (*Fulmarus glacialis*) and zones of the marine environment in the North Atlantic. Auk 85:327-355.

[260] Schaffer W M (1984) Stretching and folding in lynx fur returns: evidence for a strange attractor in nature? American Naturalist 124(6):798-820.

[261] Scheuring I (1999) Allee effect increases the dynamical stability of populations. Journal of Theoretical Biology 199:407-414.

[262] Segel L A, Jackson J L (1972) Dissipative structure: an explanation and an ecological example. J. Theor. Biol. 37:545-559.

[263] Shapiro M (1981) In vivo production at Otis Air base, Massachusetts. "The Gypsy Moth: Research Toward Integrated Pest Management" (eds C.C. Doane and M.L. McManus): 464-467. United States Department of Agriculture, Washington D.C. 1981.

[264] Sharov A A, Leonard D, Liebhold A M, Roberts E A, Dickerson W (2002) "Slow the Spread": A national program to contain the gypsy moth. Journal of Forestry 100(5): 30-36(7).

[265] Sharov A A, Liebhold A M (1998) Model of slowing the spread of gypsy moth (*Lepidoptera: Lymantriidae*) with a barrier zone. Ecological Applications 8(4):1170-1179.

[266] Sharov A A, Liebhold A M, Ravlin F W (1995a) Prediction of gypsy-moth (*Lepidoptera, Lymantriidae*) mating success from pheromone trap counts. Environmental Entomology 24(5):1239-1244.

[267] Sharov A A, Liebhold A M, Roberts E A (1997) Correlation of counts of gypsy moths (*Lepidoptera: Lymantriidae*) in pheromone traps with landscape characteristics. Forest Science 43 (3):483-490.

[268] Sherratt J A (1994) Irregular wakes in reaction-diffusion waves. Physica D 70:370-382.

[269] Sherratt J A (2001) Periodic travelling waves in cyclic predator-prey systems. Ecol. Lett. 4:30-37.

[270] Sherratt J A (2013) Pattern solutions of the Klausmeier model for banded vegetation in semi-arid environments V: the transition from patterns to desert. SIAM J. Appl. Math. 73, 1347-1367.

[271] Sherratt J A, Eagan B T, Lewis M A (1997) Oscillations and chaos behind predator-prey invasion: mathematical artefact or ecological reality? Philosophical Transactions of the Royal Society B 352:21-38.

[272] Sherratt J A, Lewis M A, Fowler A (1995) Ecological chaos in the wake of invasion. Proceedings of the National Academy of Sciences of the United States of America 92:2524-2528.

[273] Sherratt J A, Smith M J (2008) Periodic travelling waves in cyclic populations: field studies and reaction-diffusion models. J R Soc Interface 5:483-505.

[274] Shigesada N, Kawasaki K (1997) Biological Invasions: Theory and Practice. Oxford University Press, Oxford.

[275] Shigesada N, Kawasaki K, Takeda Y (1995) Modelling stratified diffusion in biological invasions. American Naturalist 146:229-251.

[276] Skellam J G (1951) Random dispersal in theoretical populations. Biometrika 38:196-218.

[277] Skellam J G (1973) The formulation and interpretation of mathematical models of diffusionary processes in population biology. In the Mathematical Theory of the Dynamics of Biological Populations, pp. 63-85. New York: Academic Press.

[278] Smith G D (1965) Numerical solution of partial differential equations. Oxford University Press.

[279] Smith G D (1978) Numerical solution of partial differential equations: finite difference methods. Oxford University Press.

[280] Smith M J, White A, Lambin X, Sheratt J A, Begon M (2006) Delayed-density dependent season length alone can lead to rodent population cycles. The American Naturalist 167(5):695-704.

[281] Smitley D R, Bauer L S, Hayek A E, Sapio F J, Humber R A (1995) Introduction and establishment of *Entomophaga maimaiga*, a fungal pathogen of gypsy moth (*Lepidoptera: Lymantriidae*) in Michigan. Environmental Entomology 24(6):1685-1695.

[282] Snowdon C T, Pickhard J J (1999) Family feuds: Severe aggression among cooperatively breeding cotton top tamarins. International Journal of Primatology 20(5):651-663.

[283] So J W H, Wu J, Zou W (2001) Structured population on two patches: modeling dispersal and delay. Journal of Mathematical Biology 43:37-51.

[284] Solomon N G, French J A (1997) Cooperative breeding in mammals. Cambridge University Press.

[285] Spear R J (2005) The great gypsy moth war: the history of the first campaign in Massachusetts to eradicate the gypsy moth, 1890-1901. University of Massachusetts Press, Amherst.

[286] Steele J H (1985) A comparison of terrestrial and marine ecological systems. Nature 313:355-358.

[287] Stephens P A, Sutherland W J, Freckleton R P (1999) What is the Allee effect? Oikos 87(1):185-190.

[288] Storch D, Gaston K J, Cepak J (2002) Pink landscapes: $1/f$ spectra of spatial environmental variability and bird community composition. Proc. R. Soc. Lond. Ser. B-Biol. Sci. 269:1791-1796.

[289] Su Y, Wei J, Shi J (2009) Hopf bifurcations in a reaction diffusion population model with delay effect. Journal of Differential Equations 247:1156-1184.

[290] Sugihara G (1995) From out of the blue. Nature 378:559-560.

[291] Summers J N (1922) Effect of low temperature on the hatching of gypsy moth eggs. US Department of Agriculture Bulletin 1080.

[292] Szendro P, Vincze G, Szasz A (2001) Pink- noise behaviour of biosystems. European Biophysics Journal 30(3):227-231.

[293] Tamburello L, Bulleri F, Bertocci I, Maggi E, Benedetti-Cecchi L (2013) Reddened seascapes: experimentally induced shifts in 1/f spectra of spatial variability in rocky intertidal assemblages. Ecology 94(5):1102-1111.

[294] Taylor C M, Hastings A (2005) Allee effects in biological invasions. Ecology letters 8:895-908.

[295] Thompson P M (2006) Identifying drivers of change; did fisheries play a role in the spread of North Atlantic fulmar? In: Management of marine ecosystems: monitoring change in upper trophic levels. Cambridge University Press.

[296] Thompson P M, Ollason J C (2001) Lagged effects of ocean climate change on fulmar population dynamics. Nature 413:417-420.

[297] Tobin P C, Blackburn L M (2008) Long-distance dispersal of the gypsy moth (*Lepidoptera: Lymantriidae*) facilitated its initial invasion of Wisconsin. Environmental Entomology 37(1):87-93.

[298] Tobin P C, Liebhold A M (2011) Gypsy moth. Encyclopedia of Biological Invasions (eds D. Simberloff and M. Rejmanek), pp. 298-304 University of California Press, Berkeley.

[299] Tobin P C, Liebhold A M, Roberts E A (2007a) Comparison of methods for estimating the spread of a non-indigenous species. Journal of Biogeography 34:305-312.

[300] Tobin P C, Robinet C, Johnson D M, Whitmire S L, Bjørnstad O N, Liebhold A M (2009) The role of Allee effects in gypsy moth(*Lymantria dispar L.*) invasions. Population Ecology 51:373-384.

[301] Tobin P C, Sharov A A, Liebhold A M, Leonard D S, Roberts E A, Learn M R (2004) Management of the gypsy moth through a Decision Algorithm under the STS project. American Entomologist 50(4):200-209.

[302] Tobin P C, Whitmire S L, Johnson D M, Bjørnstad O N, Liebhold A M (2007b) Invasion speed is affected by geographical variation in the strength of Allee effects. Ecology Letters 10:36-43.

[303] Turchin P (1988) Quantitative Analysis of Movement: Measuring and Modeling Population Redistribution in Animals and Plants. Sunderland, MA: Sinauer.

[304] Turchin P (1990) Rarity of density dependence or population regulation with lags? Nature 344:660-663.

[305] Turchin P (1999) Population regulation: A synthetic view. Oikos 84(1):153-159.

[306] Turchin P (2003) Complex population dynamics: A theoretical/empirical synthesis. Princeton University Press.

[307] Turchin P, Taylor A D (1992) Complex dynamics in ecological time series. Ecology 73(1):289-305.

[308] Turchin P, Taylor A D, Reeve J D (1999) Dynamical role of predators in population cycles of a forest insect: an experimental test. Science 285(5430):1068-1071.

[309] Turing A M (1952) The chemical basis of morphogenesis. Philosophical Transactions of the Royal Society of London, Series B, Biological Sciences 237:37-72.

[310] U.S. Congress, Office of Technology Assessment (1993) Harmful Non-Indigenous Species in the United States. OTA-F-565, U.S. Government Printing Office, Washington DC.

[311] Van de Koppel J, Gascoigne J C, Theraulaz G, Rietkerk M, Mooij W M, Herman P M J (2008) Experimental evidence for spatial self-organisation and its emergent effects in mussel bed ecosystems. Science 322(5902):739-742.

[312] Van den Bosch F, Hengeveld R, Metz J A J (1992) Analysing the velocity of animal range expansion. Journal of Biogeography 19:135-150.

[313] Van Kooten T, De Roos A M, Persson L (2005) Bistability and an Allee effect as emergent consequences of stage-specific predation. Journal of Theoretical Biology 237:67-74.

[314] Van Leeuwen E, Brännström Å, Jansen V A, Dieckmann U, Rossberg A G (2013) A generalized functional response for predators that switch between multiple prey species. J Theor Biol 328: 89–98.

[315] Vasseur D A, McCann K A (2007) The impact of environmental variability on ecological systems. Volume 2-The Peter Yodzis Fundamental Ecology Series. Springer, Dordrecht.

[316] Vasseur D A, Yodzis P (2004) The color of environmental noise. Ecology 85(4):1146-1152.

[317] Vercken E, Kramer A M, Tobin P C, Drake J M (2011) Critical patch size generated by Allee effect in gypsy moth, Lymantria dispar (L.). Ecology Letters 14:179-186.

[318] Verhulst P F (1845) Recherches mathematiques sur la loi d'accroissement de la population. Nouv. m 'em. de l'Academie Royale des Sci. et Belles-Lettres de Bruxelles 18:1-41.

[319] Vezina A, Peterman R M (1985) Tests of the role of a nuclear polyhedrosis virus in the population dynamics of its host, douglas-fir tussock moth, Orgyia pseudotsata (Lepidoptera: Lymantriidae). Oecologia 67:260-266.

[320] Vitousek P M, D'Antonio C M, Loope L L, Westbrooks R (1996) Biological invasions as global environmental change. American Scientist 84:468-478.

[321] Volpert V, Petrovskii S V (2009) Reaction-diffusion waves in biology. Physics of Life Reviews 6:267-310.

[322] Wallace B (1966) On the dispersal of *Drosophila*. American Naturalist 100:551-563.

[323] Walsh R K, Bradley C, Apperson C S, Gould F (2012) An experimental field study of delayed density dependence in natural populations of Aedes albopictus. PLoS ONE 7(4): e35959. doi:10.1371/journal.pone.0035959.

[324] Wanatabe S, Utida S, Yosida T (1952) Dispersion of insect and change of distribution type in its process: experimental studies on the dispersion of insects. Res. Popul. Ecol. 1:94-108.

[325] Watanabe S (2005) Multi-Lorentzian model and $1/f$ noise spectra. Journal of the Korean Physical Society 46(3):646-650.

[326] Webb J R, Cosby B J, Deviney F A, Eshleman K N, Galloway J N (1995) Change in the acid-base status of an Appalachian mountain catchment following forest defoliation by the gypsy moth. Water, Air, and Soil Pollution 85:535-540.

[327] White A, Begon M, Bowers R (1996) Red/blue chaotic power spectra. Nature 381:198.

[328] Whitmire S L, Tobin P C (2006) Persistence of invading gypsy moth populations in the United States. Oecologia 147:230-237.

[329] Wilder J W, Christie I, Colbert J J (1995) Modelling of two-dimensional spatial effects on the spread on forest pests and their management. Ecological Modelling 82(3):287-298.

[330] Wiley H R, Rabenold K N (1984) The evolution of cooperative breeding by delayed reciprocity and queuing for favourable social positions. Evolution 38(3):609-621.

[331] Williams D W, Liebhold A M (1995) Detection of delayed density dependence: effects of autocorrelation in an exogenous factor. Ecology 76:1005-1008.

[332] Williamson M H (1996) Biological invasions. Chapman & Hall.

[333] Williamson M H (1999) Invasions. Ecography 22:5-12.

[334] Witter J A, Stoyenoff J L, Sapio F (1992) Impacts of the gypsy moth in Michigan. Michigan Academician 25:67-90.

[335] Wynne-Edwards V C (1962) Animal dispersal in relation to social behaviour. Oliver and Boyd, Edinburgh, UK.

[336] Yamanaka T, Tatsuki S, Shimada M (2003) An individual-based model for sex-pheromone-oriented flight patterns of male moths in a local area. Ecological Modelling 161:35-51.

[337] Yoshida K (1982) The Hopf bifurcation and its stability for semilinear diffusion equations with time delay arising in ecology. Hiroshima Mathematical Journal 12:321-348.

[338] Young A J, Carlson A A, Monfort S L, Russell A F, Bennett N C, Clutton-Brock T H (2006) Stress and the suppression of subordinate reproduction in cooperatively breeding meerkats. Proceedings of the National Academy of Sciences of the United States of America 103(32):12005-12010.

[339] Zouhar K (2003) Bromus tectorum. In: Fire Effects Information System. U.S. Department of Agriculture, Forest Service, Rocky Mountain Research Station, Fire Sciences Laboratory.